Targeting Protein Quality Control Pathways in Spinal and Bulbar Muscular Atrophy

by

Adrienne M. Wang

A dissertation submitted in partial fulfillment
of the requirements for the degree of
Doctor of Philosophy
(Neuroscience)
in The University of Michigan
2012

Doctoral Committee:

Associate Professor Andrew P. Lieberman
Professor Roger L. Albin
Professor Henry L. Paulson
Professor Emeritus William B. Pratt
Assistant Professor Jason E. Gestwicki

To my parents, Peter and Sylvia Wang, who instilled in me a love of learning and life.

Thank you.

Acknowledgements

This thesis is representative of the work and support of so many people who have contributed to my personal and professional development, thank you.

In particular, thank you to members of the Lieberman lab and the Collins lab; Nahid Dadgar and Satya Reddy for taking care of us all technically and emotionally, Chris Pacheco for being a friend I could look up to professionally, Matt Elrick for being a friend I could march through the trenches with, and Jason Chua for being a friend I could dump my projects on. Thank you to all members of the Collins lab for welcoming me and helping me learn a whole new model, especially Susan Klinedinst, whose support and teaching was invaluable. I thank the Neuroscience program, and especially Valerie Smith, who facilitates so much, for everyone.

Thank you to my friends in Ann Arbor, particularly, Cynthia Schoen, Louise Hecker, MaryGrace Lauver, Elizabeth Gibbs, and especially Ian Whiteford, who has been such a source of encouragement and fun – you all helped make this home for me.

I would like to thank my thesis committee, Bill Pratt, Jason Gestwicki, Hank Paulson and Roger Albin for your continued advice and counsel.

A very special thank you to my mentor, Andy Lieberman - I always say that joining your lab was the best decision I've made, and I will forever be grateful to you for your guidance, leadership and support. You demonstrated how to pursue science and life with focus, collaboration, integrity and levity. It has been an honor to work with you.

Finally, a huge thank you goes to my family, my brothers and sisters (Tim, Kirsten, Michelle and Chris) and especially my parents, to whom this is dedicated, for your limitless encouragement, support, and love.

Table of Contents

List of figures

Abstract

Spinal and bulbar muscular atrophy (SBMA) is a progressive neurodegenerative disease caused by a CAG/glutamine (polyQ) expansion in the androgen receptor (AR). Like many other age-dependent neurodegenerative diseases, SBMA is characterized by the buildup of misfolded proteins into nuclear aggregates and neurodegeneration. The mutant protein disrupts several cellular pathways, and decreasing levels of disease causing protein may circumvent several of the downstream pathological processes. Here we investigate the effects of manipulating protein quality control pathways in cell and animal models of SBMA, identifying novel therapeutic targets and advancing our understanding of molecular chaperones and their role in protein triage.

Cells degrade proteins through two main pathways, autophagy and the ubiquitin proteasome pathway. Autophagy degrades cytosolic proteins in bulk, and increased autophagy has been shown to be beneficial in some models of protein aggregation diseases. Our results however, show that activating autophagy increases muscle wasting, while inhibiting autophagy significantly increases the lifespan and size of muscle fibers in a mouse model of SBMA. Our findings are surprising, and suggest that activation of autophagy in SBMA may exacerbate disease progression.

The Hsp90/Hsp70-based chaperone machinery regulates the stabilization and degradation of Hsp90 clients through the proteasome, and presents an alternative

therapeutic target to modulate proteostasis. Little is known however, about how this machinery functions to triage misfolded proteins, and few modulators of Hsp70 exist. Here we advance our understanding of chaperone machinery function, and present novel strategies to target Hsp70's substrate affinity. We demonstrate that inhibiting Hsp70 function leads to accumulation of toxic AR, while increasing Hsp70 substrate affinity through overexpression of the co-chaperone Hip, or through treatment with a newly identified small molecule allosteric activator, promotes client protein ubiquitination and polyQ AR clearance. Both genetic and pharmacologic approaches to increase Hsp70 activity rescue disease phenotype in a *Drosophila* model of SBMA. Our results reveal a new therapeutic strategy of targeting Hsp70 to treat SBMA and perhaps other neurodegenerative diseases, while providing insights into the role of the chaperone machinery in protein quality control.

Chapter 1

Introduction

A diverse group of neurodegenerative diseases that affect the aging population are characterized by accumulations of abnormally processed or mutant proteins that misfold and aggregate. Among these are nine genetic disorders caused by expansions of a trinucleotide CAG repeat within the coding regions of disease-causing genes (**Table 1.1**). As CAG codes for glutamine, this group of diseases is referred to as polyglutamine repeat diseases (polyQ diseases).

In these nine disorders, the polyQ expansion occurs within unrelated genes and affects different neuronal subtypes, yet these polyQ diseases share several clinical and pathological features [1]. Disease onset occurs most often in middle age despite lifelong expression of mutant protein, and exhibits an inverse correlation with CAG repeat length. The longer the glutamine expansion, the earlier the patient becomes symptomatic, and the more acute the disease progression. These expanded polyglutamine repeats unfortunately are also highly unstable, making them prone to genetic anticipation in which instability leads to an increase in length with each successive generation. The expanded repeat is inherited in an autosomal dominant manner in all polyglutamine diseases except spinal

bulbar muscular atrophy (SBMA), which is X-linked, suggesting that pathology is due in part to a toxic gain of function [1].

Table 1.1 Polyglutamine Diseases

Disease		Protein	Normal repeat length	Pathogenic repeat length	Brain region/neurons affected
SBMA	Spinal Bulbar Muscular Atrophy	androgen receptor	6-36	38-62	Lower motor neurons and dorsal root ganglion
HD	Huntington's disease	huntingtin	11-34	40-121	Striatum and cortex
DRPLA	Dentatorubral-pallidoluysian atrophy	atrophin-1	7-34	49-88	Globus pallidus, dentate-rubral and subthalamic nucleus
SCA 1	Spinocerebellar ataxia 1	ataxin-1	6-39	40-82	Purkinje cells, dentate nucleus and brainstem
SCA 2	Spinocerebellar ataxia 2	ataxin-2	15-24	32-200	Cerebellum, pontine nuclei, substantia nigra
SCA 3 (MJD)	Spinocerebellar ataxia 3/Machado-Joseph disesae	ataxin-3	13-36	61-84	Substantia nigra, globus pallidus, pontine nucleus, cerebellar cortex
SCA 6	Spinocerebellar ataxia 6	P/Q-type calcium channel subunit α1A	4-20	20-29	Cerebellum, brainstem
SCA 7	Spinocerebellar ataxia 7	ataxin-7	4-35	37-306	Photoreceptor and bipolar cells, cerebellum, brainstem
SCA 17	Spinocerebellar ataxia 17	TATA-box-binding protein	25-42	47-63	Gliosis and Purkinje cell loss

The unstable polyglutamine expansion can adopt an abnormal β-sheet conformation leading to the formation of insoluble aggregates, and these polyglutamine diseases are characterized by the accumulation of nuclear and/or cytoplasmic protein inclusions. In SBMA, these inclusions are seen in the remaining motor neurons of patient

spinal cords, and are composed of the mutant AR protein, as well as heat shock proteins (Hsps) and ubiquitin [2]. There is considerable debate in the field whether aggregates are toxic or protective, or whether their presence simply reflects the end stage of accumulation, with the toxic species being the precursors to aggregates such as oligomers or proteolyzed monomer [3-6]. Regardless, the presence of aggregates in SBMA patients and mouse models is associated with the late stages of disease pathogenesis, and implies that the accumulation of misfolded toxic proteins may be a key step in degeneration.

SBMA Pathology

SBMA is a progressive neuromuscular disorder that affects only men, and is characterized by proximal limb and bulbar muscular weakness, atrophy and fasiculations [7]. Symptom onset is typically between 30-60 years of age, but muscle weakness is often preceded by muscle cramping and tremor. The clinical features of SBMA correlate with loss of lower motor neurons in the brainstem and spinal cord, and with marked myopathic and neurogenic changes in skeletal muscle [8]. Patients may also exhibit partial androgen insensitivity such as gynecomastia, testicular atrophy and decreased fertility [9]. Disease progression is slow, but many patients eventually require assistance to walk, and risk for aspiration pneumonia increases as bulbar paralysis develops. Currently, very few treatment options exist for SBMA patients, the most promising of which are testosterone blockade therapies [10-12].

The endogenous function of the androgen receptor has been well characterized, making it an ideal context in which to study the effects of a toxic polyQ tract. In SBMA, the toxic glutamine tract expansion occurs in the first exon of the androgen receptor (AR) [13]. The repeat length found in the normal population is 9-36 glutamines, with an

expansion to a length between 38 and 62 glutamines in SBMA patients. In addition to the glutamine tract in the N-terminal transactivation domain, the AR contains a nuclear localization sequence, and a central DNA binding domain (DBD) linked to the C-terminal ligand binding domain (LBD) by a hinge region. (**Figure 1.1**) Without ligand, the nuclear localization signal is masked, and the AR is localized to the cytoplasm where it is held in a high affinity ligand binding state by molecular chaperones. Binding of testosterone to the ligand binding domain exposes a nuclear localization signal within the hinge region of the AR, allowing for the binding of importin-α and the subsequent trafficking and import of the AR into the nucleus [14]. Once in the nucleus, ligand-bound AR dimerizes and binds to androgen responsive elements (AREs), triggering transcription or repression of androgen dependent genes [15,16].

Figure 1.1 Androgen receptor domain structure

The AR protein consists of 3 functional domains: the N-terminal transactivation domain containing the glutamine tract, the DNA-binding domain (DBD), and the ligand binding domain (LBD). The nuclear localization signal (NLS) is found within the hinge region that links the DBD and the LBD. (modified from Katsuno et al, 2004)

In the presence of an abnormally expanded glutamine tract, the AR suffers from both a partial loss of endogenous function as well as a toxic gain of function. Expansion of the polyglutamine tract mildly suppresses transcriptional activities of the AR [17-19]. This loss of function likely contributes to the partial testosterone insensitivity seen in SBMA

patients. However, patients with other types of loss of function mutations in the *AR* gene and mouse models with similar loss of function mutations in the AR show androgen insensitivity and testicular feminization, without the motor impairment observed in SBMA [20]. Evidence for a toxic gain of function by the pathogenic AR is robust. Several SBMA mouse models have been created in which transgenic expression of the aberrant AR leads to hormone and glutamine length dependent muscular atrophy and motor dysfunction in the continued presence of the wild type protein [21-24]. Similarly, exogenous expression of the mutant AR in transformed cell lines and primary neurons leads to altered cellular processes and cell death [25,26]. Taken together, these data indicate that the polyglutamine tract expansion in the AR leads to both a toxic gain of function and a partial loss of normal function, and suggest that toxic effects of the mutant protein are the main drivers of disease pathogenesis.

Mechanisms of Toxicity

The mutant protein in SBMA, as in other polyglutamine disorders, disrupts multiple cellular pathways, and toxicity is likely due to the cumulative effects of altering a diverse array of downstream cellular processes (summarized in Figure 1.2). A brief summary of the data implicating disruption of these pathways in SBMA follows:

Transcriptional Dysregulation

Several polyglutamine diseases require nuclear localization of the mutant protein and exhibit altered transcription prior to phenotypic onset [27,28]. A SCA1 mouse model in which the polyQ Ataxin-1 is cytoplasmically retained shows neither the characteristic ataxia nor Purkinje cell loss, while allowing nuclear transport, but prohibiting nuclear aggregation in the same model leads to pathogenesis, establishing nuclear events as a

requirement for polyglutamine toxicity [29]. Similarly, cytoplasmic retention of the AR rescues the disease in an SBMA mouse, while nuclear localization of an unliganded AR in cell models is insufficient to cause the toxicity seen in the presence of ligand [30]. The endogenous function of the AR as a nuclear transcription factor lends weight to the idea that transcriptional dysregulation underlyies disease pathogenesis in SBMA. Ligand binding, nuclear translocation and DNA binding have all been shown to be requirements in SBMA toxicity [30-32].

The mutant AR abnormally interacts with transcriptional co-regulators, and has been shown to alter transcription in both fly and cellular models of SBMA [18,19,26,31,33]. Several of these co-regulators are transcription factors that modify the acetylation state of the histones that package and compact nuclear DNA, thus modifying the accessibility of DNA to the transcriptional machinery. Further, the acetylation state of the AR itself has been suggested to regulate the subcellular localization and misfolding of the receptor [34] as well as interaction with co-regulators [35]. One of these co-regulators, CREB-binding protein (CBP), is a histone acetyltransferase and an important co-activator. CBP is functionally sequestered in the nuclear inclusions seen in cell culture, animal models and tissue derived from SBMA patients, resulting in downregulation of CBP mediated transcription [36]. Overexpression of CBP rescues polyQ AR mediated toxicity in cell and drosophila models restoring normal transcription and histone acetylation levels [36,37]. Similarly, inhibiting histone deacetylases has also been shown to decrease the toxicity of a truncated fragment of the expanded AR [38], further implicating transcriptional dysregulation as one pathogenic mechanism in SBMA.

Post-transcriptional changes in gene expression also affect protein expression and can produce dysfunction in much the same way as altered transcription. Toxic forms of RNA have been implicated in other repeat expansion diseases, such as myotonic dystrophy, where they alter RNA splicing by affecting expression of splicing factors and/or by sequestering RNA binding proteins [39]. Aberrant RNA processing can have widespread effects on many transcripts, and can amplify existing transcriptional dysregulation. RNA missplicing has also been shown to contribute to SBMA pathogenesis in a knock-in mouse, where changes in RNA binding protein expression and mRNA splicing have been observed [40].

Mitochondrial Dysfunction

Mitochondrial dysfunction has also been implicated in polyQ disease pathogenesis. In vitro and in vivo models of SBMA show altered expression of peroxisome proliferator-activated receptor gamma coactivator-1 (PGC-1), a transcription factor that governs mitochondrial biogenesis and function. Mitochondria in cells expressing pathogenic polyQ AR are lower in number and exhibit decreased mitochondrial membrane potential. This occurs in conjunction with higher levels of reactive oxygen species (ROS) [41]. Mitochondrial abnormalities are also detectable in the leukocytes of SBMA patient samples, highlighting the role of mitochondrial bioenergetics in polyglutamine disease [42].

Axonal Trafficking

Neurons, and especially motorneurons, with their long axonal projections, are highly reliant upon fast axonal transport to shuttle nutrients and molecular signals between the nucleus and the cell periphery, and defects in axonal transport have been

reported in several neurodegenerative and polyglutamine diseases [43-45]. Furthermore, specific disruption of this pathway by dynactin mutations causes an inherited form of motor neuron disease [46]. Controversy exists as to the extent of axonal trafficking defects in SBMA models. Axonal trafficking defects caused by the polyQ AR occur in isolated squid axons, where impaired fast transport occurs secondary to activation of JNK signaling [44,47] Defects have also been documented in several, but not all, SBMA mouse models that have been studied. Dynactin 1 is a regulator of retrograde axonal transport, and is expressed at lower levels in SBMA transgenic mice that show perturbed axonal trafficking [48]. Early deficits in retrograde transport also occur in both SBMA knock-in mice and a myogenic mouse model that overexpresses wild type AR exclusively in muscle [49]. In contrast, YAC transgenic SBMA mice show no change in retrograde transport or dynactin levels [50] suggesting that these defects may not be necessary for the occurrence of a disease phenotype.

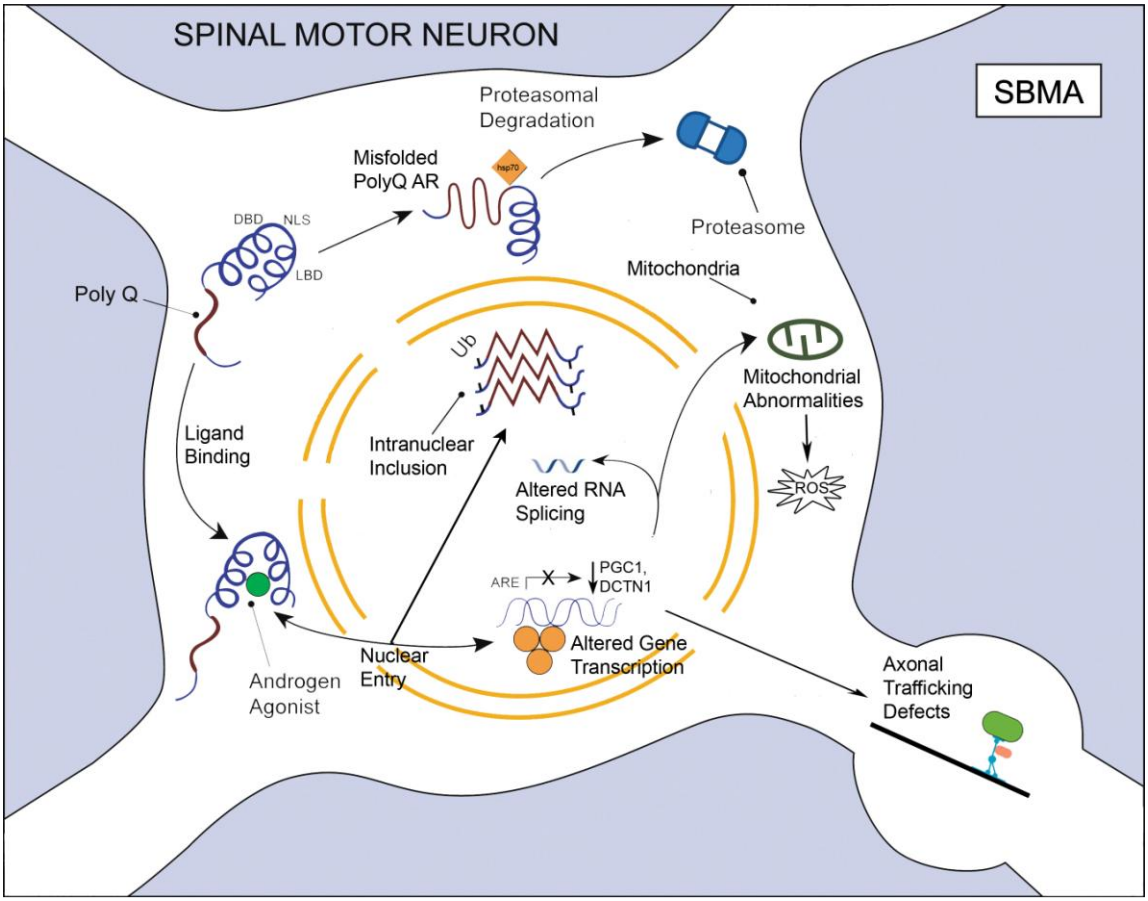

Figure 1.2 Mechanisms of Toxicity in SBMA

PolyQ AR affects many cellular processes, both nuclear and cytoplasmic. (Modified from Ross, Neuron, 2002). Proteasomal degradation is shown occurring in the cytoplasm, but also occurs within the nucleus. (DBD) DNA binding domain, (NLS) nuclear localization sequence, (ARE) androgen responsive elements, (ROS) reactive oxygen species.

With such a diverse array of cellular processes affected by the presence of the mutant AR, therapeutic treatments targeting individual pathways are likely to be unsuccessful. The common upstream factor in all the toxic mechanisms is the activation of the abnormal AR. Therefore, diminishing levels of the misfolded protein could abrogate multiple downstream effects. Perhaps the most promising route to achieving this is to enhance the cell's natural protein quality control pathways. This machinery contains

several distinct and interacting components, including molecular chaperones, the ubiquitin-proteasome system and autophagy.

Protein Degradation

The two main protein degradation pathways in eukaryotic cells are the ubiquitin-proteasome system (UPS) and autophagy. Both of these degradation pathways serve to modulate protein homeostasis and have been identified as potential therapeutic targets in neurodegenerative diseases. The UPS degrades damaged or misfolded proteins in both the cytoplasm and nucleus, while autophagy is responsible for bulk degradation of long-lived proteins and organelles in the cytosol.

The Ubiquitin Proteasome System

The ubiquitin proteasome system (UPS) governs the selective and tightly regulated process of degrading soluble cytosolic and nuclear proteins into short peptide chains. By selectively degrading short lived and misfolded or damaged proteins, the UPS is able to govern localized protein concentrations allowing for regulation of cell cycle and growth regulators, signal transduction, metabolic enzymes and general housekeeping functions [51]. Degradation of a protein through the UPS requires 2 steps; the covalent attachment of multiple ubiquitin molecules, and the degradation of the ubiquitinated protein by the proteasome.

Ubiquitination of the target protein is achieved in a stepwise process. In the first ATP-dependent step, an E1 ubiquitin activating enzyme activates the ubiquitin molecule and forms a transient E1-S~ubiquitin intermediate prior to recognition by an E2 ubiquitin conjugating enzyme. The E2 ubiquitin conjugating enzyme then transfers the ubiquitin

from the transient E1-S~ubiquitin intermediate to a residue within the E2 enzyme forming another transient thioester intermediate. Finally, the ubiquitin molecule is transferred by an E3 ubiquitin ligase to a lysine residue on the targeted substrate [52]. The E3 ubiquitin ligase is what confers specificity to the reaction, binding to the target molecule while recruiting the E2-Ub molecule for covalent binding to a lysine residue on the substrate. This process repeats itself, allowing for sequential addition of ubiquitins upon the initial ubiquitin. Once a protein incurs a chain longer than four ubiquitins, it is targeted to the 26S proteasome for degradation [53].

The 26S proteasome is a multi-subunit, multi-catalytic protease found in both the nucleus and cytoplasm. It is comprised of a 20S core catalytic complex flanked by two 19S regulatory components forming a barrel shaped structure (20S) with a lid (19S). In a highly energy dependent manner, the 19S subunit functions to identify and bind polyubiquitinated proteins, open the pore of the 20S proteasome, unfold the substrate, remove the ubiquitin chain and finally feed the unfolded target protein into the 20S pore. Once inside the 20S proteasome, the protein is degraded into oligopeptides ranging from 4-25 amino acids which are then released from the 20S proteasome for reuse [54].

Steroid hormone receptor degradation occurs through the proteasome, and harnessing the cell's innate degradation pathways to decrease levels of polyQ AR is a promising therapeutic strategy. Components of the UPS, as well as the molecular chaperones Hsp70 and Hsp40, are found in the nuclear aggregates of SBMA models and patients, indicating the recognition of the misfolded protein and cellular attempt at degradation [2,23,55]. Accumulation of UPS components in aggregates has also been implicated in proteasome inhibition, where sequestration of the components in inclusions

would lead to downregulation of proteasomal degradation [56]. Importantly for therapeutic purposes, the activity of the UPS in an SBMA model mouse is preserved and even upregulated in late stages of disease [57]. As discussed below, manipulating the expression or function of certain molecular chaperones and chaperone-dependent ubiquitin ligases ameliorates the disease phenotype in SBMA mice, consistent with the notion that clearance of the polyQ AR through the UPS is critically important to the disease.

Autophagy

Autophagy, or "self eating", is a process in which a cell is able to engulf contents of cytoplasm and deliver them to the lysosome for degradation and recycling [58]. Several forms of autophagy have been identified, demonstrating more selective degradation pathways than originally thought. Microautophagy is a process in which the lysosome itself takes up small portions of the cytoplasm through invaginations in the lysosomal compartment [59]. Chaperone mediated autophagy allows for selective uptake of proteins containing a KFERQ motif. Hsp70 recognizes this same domain, and allows for the targeting to the lysosome via the lysosomal integral membrane protein LAMP-2A [60]. Macroautophagy is the mechanism by which cells are able to engulf large portions of cytosol within double membrane vesicles that fuse to late endosomes or lysosomes for degradation [58]. From here on, macroautophagy will be the subtype discussed in this dissertation and will be referred to as autophagy.

Activation of autophagy involves tightly regulated stepwise induction of a double membraneous autophagic vesicle that grows to engulf cytoplasmic components the proteasome cannot degrade, such as mitochondria and protein aggregates, as well as long-lived proteins. This mechanism consists of several discrete steps executed by autophagy

related (Atg) proteins, that are analogous to the cascade required to attach ubiquitin to target proteins. Once the autophagosome is completed, it fuses with lysosomes where the contents of the autophagosome are enzymatically broken down for reuse by the cell [61].

Upstream of the formation of the autophagic vesicle, autophagy is regulated primarily by two proteins, the mammalian target of rapamycin (mTOR) and Beclin-1. mTOR negatively regulates autophagy and is responsive to cellular signals indicating the energy and nutrient status of the cell. In periods of excess energy, mTOR inhibits autophagy; nutrient deprivation leads to a release of this inhibition, allowing for autophagy induction and an increase in nutrients via this recycling pathway. Beclin-1 is required for both autophagosome formation and autophagic flux [62]. It associates with the class III phosphatidylinositol-3-kinase (PI3K) complex to generate PI(3)P, a lipid component of the autophagosome membrane [63]. Beclin-1 also binds to the anti-apoptotic bcl-2 family of proteins. This binding inhibits the induction of autophagy by sequestering Beclin-1 away from the PI3K complex. Thus, activation of autophagy by Beclin-1 can be initiated by transcriptional regulation or by disruption of binding to bcl-2 by phosphorylation of either binding partner [64]. In chapter 3 of this dissertation, we will explore the role of macroautophagy in SBMA pathogenesis.

Molecular Chaperones

Hsp90

In the absence of ligand, the AR resides in the cytoplasm where it forms a multi-protein heterocomplex, bound to heat shock proteins, co-chaperones, and tetratricopeptide repeat (TPR)-containing proteins [65]. The Hsps are molecular chaperones

that bind to, and stabilize the AR in a high-affinity state primed for ligand binding [66]. The interaction of Hsp90 with the AR, and the regulation of AR proteostasis by Hsp90, makes it an Hsp90 "client" protein, and puts the AR in a class with many other steroid hormone receptors and signaling molecules. Much of what is known about the action of Hsp90 on its client proteins has come from work on other signaling molecules that are Hsp90 clients, such as the glucocorticoid receptor (GR) and neuronal nitric oxide synthase (nNOS) [65].

Hsp90 is an abundant molecular chaperone that controls the maturation, function, and turnover of its client proteins. Binding of Hsp90 to its client protein is preceded by the binding of Hsp70 to hydrophobic residues found on partially unfolded client proteins. Once Hsp70 has primed the steroid binding cleft, Hsp90 binds and stabilizes the binding cleft in an open conformation with high affinity for ligand [67]. Both Hsp70 and Hsp90 have intrinsic ATPase activity that is required in the stepwise assembly of the chaperone machinery. The binding affinity of these molecular chaperones to their protein substrates is mediated by their nucleotide binding state, with the ATP-bound form being the low affinity state and the ADP-bound form being the high affinity state [68] Once ligand binds to the accessible ligand binding cleft of the primed AR, interaction with Hsp90 is required to help traffic the client protein to the site of its action, the nucleus [34,69,70].

Hsp90 inhibitors, which target the ATPase activity of Hsp90, have been shown to have beneficial effects in several models of SBMA. 17-AAG or geldanamycin, both Hsp90 inhibitors, ameliorate disease pathology in cell culture and mouse models of SBMA [57,71]. These drugs promote degradation of the mutant AR protein through the ubiquitin-proteasome system by inhibiting Hsp90's ATP-dependent progression toward

the stabilized heterocomplex. They decrease accumulation of aggregated mutant receptor by enhancing its degradation and ameliorate the motor phenotype of SBMA mice [57,72]. These drugs also serve to induce a stress response, which upregulates the levels of several heat shock proteins, including the inducible form of Hsp70 [73]. The beneficial effects of Hsp90 inhibition however, are independent of the heat shock response, as AR112Q expressing mouse embryonic fibroblasts (MEFs) deficient in HSF-1 (the Hsp90-regulated transcription factor required to induce a heat shock response) still clear6 polyQ AR after treatment with Hsp90 inhibitors, even in the absence of a stress response [69].

Hsp70

While Hsp90 binds to and stabilizes client proteins in their native conformation, Hsp70 binds to hydrophobic residues exposed by partially unfolded or misfolded proteins in non-native conformations, and targets them for degradation by the ubiquitin proteasome system. In fact, Hsp70 is required for both ubiquitination and the subsequent degradation of ubiquitinated proteins [74]. The best studied chaperone-dependent ubiquitin E3 ligase is the CHIP (carboxy terminus of Hsp70-interacting protein). CHIP interacts with Hsp70 through its amino-terminal TPR domain and with E2 ubiquitin conjugating enzymes through a carboxy-terminal U-box domain [75]. In this manner, it is thought that CHIP is able to initiate the ubiquitination and promote the degradation of proteins that have been identified as unfolded or misfolded by Hsp70. (**Figure 1.3**) CHIP is also associated with nuclear inclusions characteristic of polyglutamine disease, including SBMA [76], and overexpression of CHIP has been shown to rescue both a Drosophila model of SCA1[77] and a mouse model of SBMA [78]. Notably, although CHIP plays an

important role in client protein degradation, other chaperone-dependent ligases, such as Parkin, can function redundantly with CHIP to promote client protein degradation [76].

Like Hsp90 inhibition, Hsp70 over-expression has been shown to have beneficial effects in a variety of neurodegenerative diseases including the polyglutamine diseases. Hsp70, in conjunction with its co-chaperone Hsp40, inhibits aggregation of the truncated huntingtin protein (Htt) in both *in vitro* and cellular and yeast models of polyglutamine aggregation [79]. Overexpression studies in disease models have also indicated that these particular chaperones may be promising therapeutic targets. Hsp70 suppresses both apoptosis and aggregation in neurons expressing a truncated form of the AR with an expanded polyQ tract [80]. Further, when Hsp70 is overexpressed in a mouse model of SBMA, there is decreased aggregated and soluble AR, indicating that increased levels of Hsp70 promote degradation of the AR. Importantly, these mice also showed improved survival and motor phenotype when compared to SBMA mice that were not overexpressing Hsp70 [81].

These data have led to our working model of chaperone machinery function. In this model, Hsp70 and Hsp90 operate in opposing manners upon client proteins (**Figure 1.3**). Association with Hsp90, or overexpression of p23, allows for the stable formation of the complete heterocomplex [69] and stabilization of the client protein in its native conformation. In contrast, inhibition of Hsp90 disrupts the complex and allows for substrate bound Hsp70 to recruit chaperone-dependent ubiquitin ligases to target the client protein for degradation through the proteasome. In this model, increasing the affinity of Hsp70 for misfolded substrates could serve to increase the degradation of

Hsp90 client proteins like the polyQ AR. This model will be probed in chapters 3 and 4 of this dissertation.

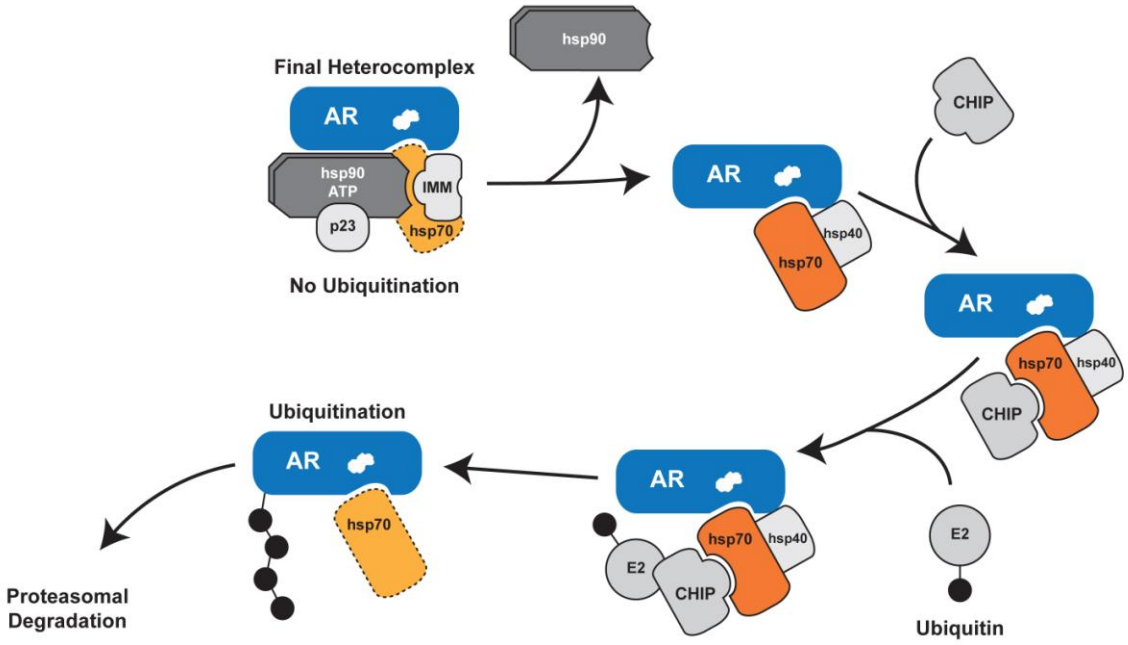

Figure 1.3 Model of the Hsp90-based chaperone machinery and regulation of polyQ AR degradation.

Hsp90 forms a heterocomplex to stabilize the polyQ AR, enable ligand binding and guide intracellular localization (top left). Dissociation of Hsp90, as after treatment with an Hsp90 inhibitor, permits polyQ AR unfolding. Substrate-bound Hsp70 then recruits chaperone dependent ligases such as CHIP to promote degradation through the proteasome. (AR) Androgen receptor, (IMM) Immunophilin binding protein, (E2) E2 ubiquitin conjugating enzyme, (CHIP) carboxy terminus of Hsp70-interacting protein.

Modulating Hsp70

Hsp70 interacts with several co-factors or co-chaperones in the course of recognizing, binding and targeting misfolded proteins to the proteasome. These co-factors serve to modulate Hsp70 activity and substrate binding affinity. In particular, Hsp40 is a well characterized family of Hsp70 co-chaperones that affect substrate binding by enhancing Hsp70s ATPase activity [82]. Experimental modulation of Hsp70 activity has

proven difficult, and small molecules specifically targeting Hsp70 have been identified only recently [83-85]. Due to this, much of the evidence probing Hsp70 as a modulator of neurodegeneration has come from overexpression studies. In chapter 3, we characterize methylene blue as a small molecule inhibitor of Hsp70, and show its utility in probing Hsp70-dependent roles in the quality control of the Hsp90 client proteins nNOS and the polyQ AR.

Hsp70-Interacting Protein

One way to modulate Hsp70 activity in a more physiologically relevant manner is by altering its nucleotide binding state through interaction with its endogenous co-regulators. Hip (hsc70-interacting protein) is a co-chaperone that interacts with the ATPase domain of Hsp70/ Hsc70 and stabilizes it in its ADP bound state [86]. Hip and BAG-1 (Bcl-2-associated gene product-1), a nucleotide exchange factor, compete for binding to separate sites on the ATPase domain of Hsp70, and both have been recovered in small amounts from Hsp90-hop-Hsp70 complexes [87,88]. This suggests that their association may be indicative of two subtypes of heterocomplex assembly, with BAG-1 association promoting ATP-bound Hsp70 and Hip association stabilizing ADP-bound Hsp70. As ADP-bound Hsp70 binds substrates with high affinity, our model of chaperone machinery function predicts that Hip overexpression will be beneficial in SBMA models. Consistent with this idea, Hip expression in yeast enhances the Hsp70-dependent maturation of the GR [89], and Howarth et al showed that overexpression of Hip, especially in conjunction with Hsp70, decreased aggregates formed by an expanded polyglutamine tract in mouse neuroblastoma cells [90]. Importantly, Hip also decreases the formation of fibrils by another Hsp90 client protein, α-synuclein, the protein that

aggregates in Parkinson disease (PD). Knock down of Hip in a C. elegans model of PD leads to an increase in inclusion formation, and reduced expression of HIP is found in serum from PD patients [91,92]. The extent to which Hip may be a therapeutic target in SBMA is unknown, and will be investigated in chapter 4.

Research Objectives

Despite advances in understanding the etiology of numerous neurodegenerative diseases, efficacious therapies still remain elusive. Harnessing cells' protein quality control pathways to degrade toxic proteins is an attractive therapeutic target and may serve to halt disease progression upstream of several pathological features of protein aggregation diseases. The work presented in this dissertation probes the role of two different protein quality control pathways in modulating disease pathogenesis. The first objective is to determine the extent to which autophagy modulates the SBMA phenotype through Beclin-1. This work, presented in chapter 2, demonstrates that, contrary to our expectations, upregulating autophagy may not be therapeutically beneficial. Our data show that genetically impairing autophagy by Beclin-1 haploinsufficiency increases lifespan and muscle fiber size in a mouse model of SBMA. The second objective of this dissertation is to elucidate the mechanism by which modulation of Hsp70's nucleotide binding domain promotes degradation of the polyQ AR protein (**Figure 1.3**). In chapter 3, I show that pharmacologically inhibiting Hsp70's intrinsic ATPase activity in our cellular model of SBMA increases aggregation of the expanded full-length receptor. Building upon this data, in chapter 4 I show that stabilizing Hsp70 in its ADP-bound state by both pharmacological and genetic manipulation serves to decrease the amount of aggregated AR in cellular and Drosophila models. Further, these pharmacologic and

genetic manipulations rescue the SBMA phenotype in Drosophila. Taken together, these data indicates that targeting Hsp70's activity may be a successful therapeutic strategy in SBMA.

Chapter 2

Macroautophagy is regulated by the UPR-mediator CHOP and accentuates the phenotype of SBMA mice

Abstract

Altered protein homeostasis underlies degenerative diseases triggered by misfolded proteins, including spinal and bulbar muscular atrophy (SBMA), a neuromuscular disorder caused by a CAG/glutamine expansion in the androgen receptor. Here we show that the unfolded protein response (UPR), an ER protein quality control pathway, is induced in skeletal muscle from SBMA patients, AR113Q knock-in male mice and surgically denervated wild type mice. To probe the consequence of UPR induction, we deleted CHOP (C/EBP homologous protein), a transcription factor induced following ER stress. CHOP deficiency accentuated atrophy in both AR113Q and surgically denervated muscle through activation of macroautophagy, a lysosomal protein quality control pathway. Conversely, impaired autophagy due to Beclin-1 haploinsufficiency decreased muscle wasting and extended lifespan of AR113Q males, producing a significant and unexpected amelioration of the disease phenotype. Our findings highlight critical cross-talk between the UPR and macroautophagy, and indicate that autophagy activation accentuates aspects of the SBMA phenotype.

Introduction

Many adult onset neurodegenerative disorders are characterized by the accumulation of abnormally folded proteins that self-associate into soluble oligomeric species or coalesce into insoluble protein aggregates. Among these disorders are ones caused by expansions of CAG/glutamine tracts[1,93]. Spinal and bulbar muscular atrophy (SBMA), a member of this group, is a progressive neuromuscular disorder caused by an expanded glutamine tract near the amino terminus of the androgen receptor (AR) [94]. This mutation leads to hormone-dependent AR unfolding, and to the predominant loss of lower motor neurons in the brainstem and spinal cord of affected males. Clinical onset occurs in adolescence to adulthood and is characterized initially by muscle cramps and elevated serum creatine kinase [10,95]. These myopathic features commonly precede muscle weakness, which inevitably develops as the disease progresses and is most severe in the proximal limb and bulbar muscles. Late in the course of disease, the pathologic features of SBMA include loss of motor neurons in the brainstem and spinal cord and the occurrence of myopathic and neurogenic changes in skeletal muscle [7,8].

Studies in mouse models have defined several general principles that guide our understanding of SBMA pathogenesis. Transgenic over-expression of the expanded glutamine AR leads to disease, consistent with the notion that toxicity is predominantly mediated through a gain-of-function mechanism [22,32]. This toxicity is androgen-dependent in mice and in SBMA patients, an observation that led to recent clinical trials with anti-androgens [11,12,96]. To model SBMA in mice, our laboratory used gene targeting to exchange 1340 bp of mouse *Ar* exon 1 with human sequence containing 21 or 113 CAG repeats [97,98]. Mice expressing the expanded glutamine AR (AR113Q) develop

androgen-dependent neuromuscular and systemic pathology that models SBMA [98,99], whereas AR21Q males are similar to wild type littermates [97,98]. In AR113Q mice, denervation and muscle pathology occur early in life, prior to detectable motor neuron loss, indicating that neuronal dysfunction or distal axonal degeneration and myopathy are early disease manifestations. The notion that pathology arising in muscle contributes to disease is consistent with findings in transgenic mice in which over-expression of the wild type AR in skeletal muscle leads to hormone-dependent myopathy and motor axon loss [100], and with data showing a rescue of the disease phenotype in SBMA transgenic mice by over-expressing IGF-1 in skeletal muscle [101]. Taken together, these observations focused our attention on the role of skeletal muscle in disease pathogenesis.

The cellular pathways by which the expanded glutamine AR mediates toxicity are complex and incompletely understood, with evidence in several model systems showing disruption of gene expression [17-19,26,33,36], alterations in RNA splicing [40], impairments in axonal transport [43,44,48] and defects in mitochondrial function [41]. Toxicity likely results from the cumulative effects of altering a diverse array of cellular processes, indicating that potential treatments targeting a single downstream pathway are likely to be unsuccessful. These findings prompted us to concentrate instead on understanding the proximal mechanisms that regulate degradation of the mutant protein. Work in cellular and mouse models has established that degradation and aggregation of the polyglutamine AR are regulated by the Hsp90-based chaperone machinery [69,71], and that manipulating the expression or function of Hsp70-dependent E3 ubiquitin ligases markedly affects AR turnover through the ubiquitin-proteasome pathway [76,78,85].

In addition to the chaperone machinery, other pathways regulating protein quality control have been implicated in SBMA pathogenesis. Here we explored the role of the unfolded protein response (UPR), an integrated signal transduction pathway that transmits information about protein folding within the ER lumen to the nucleus and cytosol to regulate protein synthesis and folding and to influence cell survival[102,103]. Prior studies showed that amino-terminal fragments of the polyglutamine AR activate the UPR *in vitro* [104], but little is known about the role of this pathway in more complex models of disease. We now show that the UPR is activated in skeletal muscle from SBMA patients and AR113Q mice. Moreover, genetic disruption of the ER stress response by deletion of the gene encoding the transcription factor C/EBP homologous protein (CHOP), a mediator of the UPR [102], accentuates skeletal muscle atrophy in AR113Q mice. Further, we show that enhanced muscle wasting in the setting of CHOP deficiency is due to increased macroautophagy (hereafter referred to as autophagy), a lysosomal protein quality control pathway implicated in the pathogenesis of polyglutamine and motor neuron diseases. In contrast, diminished autophagy due to Beclin-1 haploinsufficiency decreased muscle wasting and extended the lifespan of AR113Q males, unexpectedly ameliorating the disease phenotype. Our findings highlight cross-talk between the UPR and autophagy, and demonstrate that increased autophagy promotes atrophy of SBMA muscle.

Results

The UPR is activated in SBMA muscle.

To determine whether the ER stress response is activated in SBMA we obtained skeletal muscle from patients and male controls. Gene expression analysis by qPCR

demonstrated that SBMA muscle contained significantly higher levels of several mRNAs that are induced in response to ER stress (**Figure 2.1A**) [102,103]. These encoded the ER chaperone immunoglobulin binding protein (BiP), the transcription factors activating transcription factor-4 (ATF4) and its target CHOP, and the ER folding enzyme protein disulfide isomerase (PDI). Further, increased splicing of mRNA encoding X-box binding protein-1 (XBP1) was detected (**Figure 2.1B**), indicating that activation of the proximal UPR sensor inositol-requiring protein-1 (IRE1) had occurred.

Analysis of proximal hind limb muscle from adult AR113Q male mice similarly demonstrated the induction of mRNAs encoding BiP, ATF4, CHOP and PDI (**Figure 2.1C**). This was associated with increased expression of BiP and PDI proteins, as demonstrated by western blot (**Figure 2.1D**). As the neuromuscular phenotype of these mice is both hormone and glutamine-length dependent [98], we sought to determine whether the occurrence of ER stress was similarly regulated. Surgical castration at 5 – 6 wks ameliorated the induction of these transcripts in adult AR113Q males, demonstrating that UPR activation was responsive to levels of circulating androgens (**Figure 2.1C**). Further, direct comparison with mice generated using the same gene targeting strategy but with only 21 CAG repeats in the *Ar* gene [97] confirmed that UPR activation was dependent upon the presence of an expanded glutamine tract (**Figure 2.1E**). In contrast, we did not detect induction of ER stress-induced mRNAs such as BiP and CHOP in spinal cords of AR113Q males (**Figure 2.1F**), nor did we detect increased expression of BiP or PDI proteins in spinal motor neurons (not shown). We conclude that the UPR is activated in skeletal muscle from SBMA patients and knock-in mice.

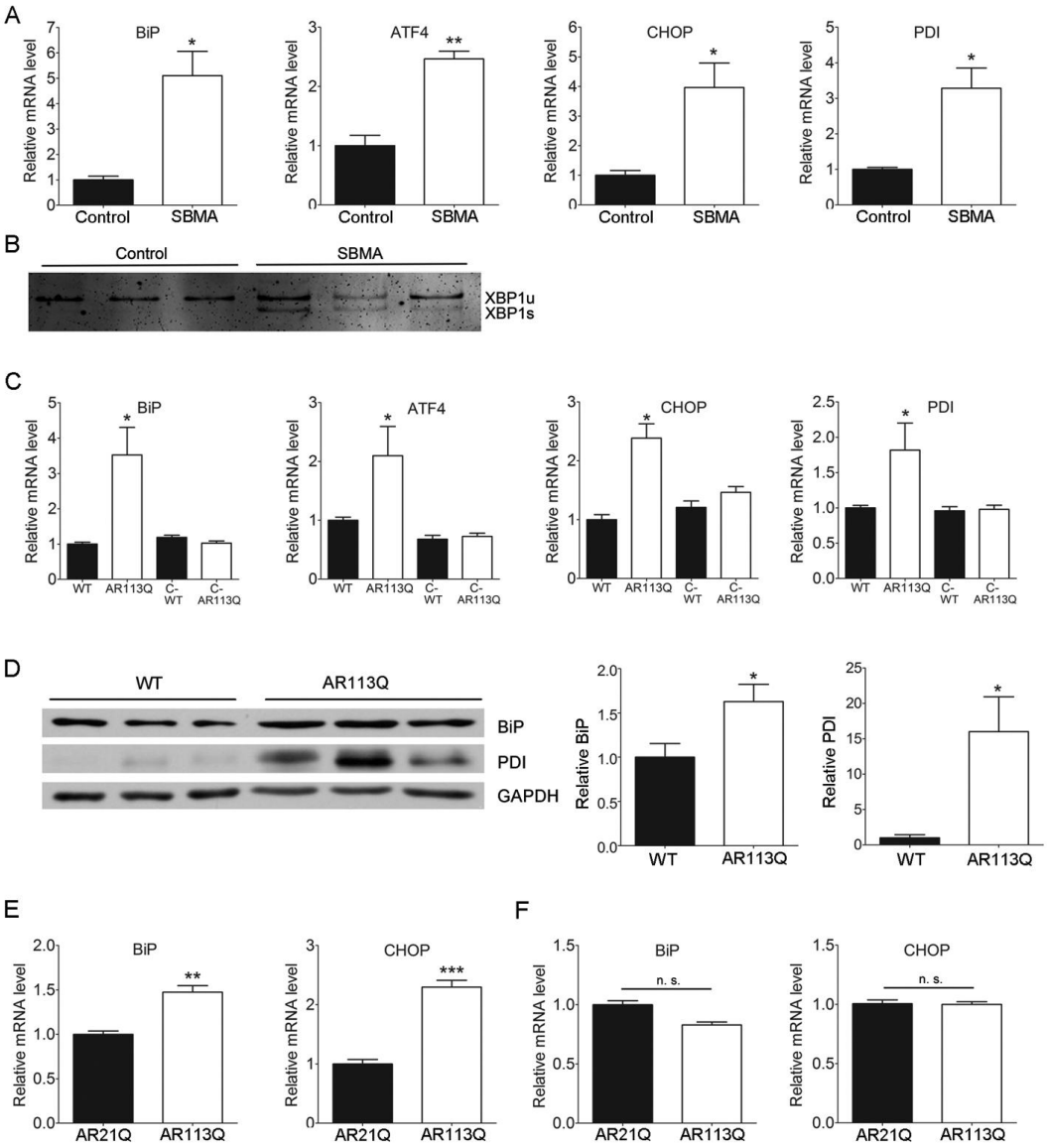

Figure 2.1 The UPR is activated in SBMA muscle.

(A) Relative mRNA expression in skeletal muscle from SBMA patients (white bars, *n*=3) and controls (black bars, *n*=3) (mean +/- SEM). * p<0.05, ** p<0.01 by Student's *t* test. **(B)** Splicing of XBP1 mRNA was assessed by RT-PCR. Products from unspliced (XBP1u) and spliced (XBP1s) transcripts were resolved on a nondenaturing polyacrylamide gel and stained with SYBR green. **(C)** Relative mRNA expression in proximal hind limb muscle (mean +/- SEM). Mice evaluated were littermate WT (*n*=6), AR113Q (*n*=6), castrated WT (C-WT, *n*=6) and castrated AR113Q males (C-AR113Q, *n*=5) on a mixed C57BL/6J-129 genetic background. *p<0.05 by ANOVA. **(D)** Western blot of BiP and PDI expression in proximal hind limb muscle. Right panels show quantification of signal relative to loading control (mean +/- SEM). * p<0.05 by Student's *t* test. **(E)** Relative mRNA expression in proximal hind limb muscle of AR21Q (*n*=5) and AR113Q (*n*=3) males backcrossed to C57BL/6J. ** p<0.01, ***p<0.001 by Student's *t* test. **(F)** Relative mRNA expression in spinal cord of AR21Q (*n*=5) and AR113Q (*n*=3) males (mean +/- SEM). n. s. = not significant by Student's *t* test. Experiments performed by Zhigang Yu.

CHOP deletion increases AR113Q muscle atrophy and activates autophagy.

As the UPR plays a central role in protein homeostasis in the ER and influences survival in a cellular model of SBMA [104], we sought to determine its role in disease pathogenesis *in vivo*. To accomplish this, we generated AR113Q males deficient in CHOP, a regulator of cell survival during ER stress that we found to be up-regulated in SBMA muscle. CHOP null mice exhibit impaired programmed cell death following pharmacological induction of ER stress [105]. Further, CHOP deficiency accentuates the phenotype of Pelizaeus-Merzbacher Disease mice [106] yet rescues the motor deficits of Charcot-Marie-Tooth 1B mice [107], demonstrating that deletion of this transcription factor is an informative approach to probing the role of the UPR in model systems. Notably, CHOP null mice do not display neuromuscular pathology, thereby enabling us to assess the outcome of genetic disruption of the UPR on the SBMA phenotype.

CHOP deficiency markedly affected AR113Q muscle, the site of UPR activation, by accentuating skeletal muscle atrophy (**Figure 2.2A, B**). This unexpected effect on muscle fiber size yielded a significant shift in the distribution of fibers towards a smaller cross sectional area, resulting in a mean fiber size that was ~1/3 smaller than that measured in AR113Q males. In contrast, CHOP null males expressing the wild type AR had muscle fibers that were similarly sized to age matched wild type males (**Figure 2.2C**). Although CHOP deficiency did not alter AR113Q total body mass or survival (not shown), our data show that disruption of the UPR by CHOP deletion increased muscle wasting in AR113Q male mice.

To determine the mechanism by which CHOP deficiency increased skeletal muscle atrophy, we initially considered the possibility that motor neuron degeneration

was more severe in AR113Q mice deficient in CHOP, resulting in enhanced neurogenic atrophy. However, we found no evidence of increased motor neuron loss in the spinal cords of these double mutants (not shown). Furthermore, skeletal muscle expression of mRNAs induced following denervation [108], including those encoding myogenin and MyoD, was similar in AR113Q and AR113Q, CHOP null males (Data not shown). These findings suggested that enhanced muscle atrophy in animals deficient in CHOP was not mediated by increased motor neuron loss, but rather reflected augmented activation of a pathway that mediates muscle wasting. To directly test this notion, we first examined the expression of muscle RING-finger protein 1 (MuRF1) and Atrogin1/Muscle Atrophy F-box (MAFbx) (**Figure 2.3A**), two E3 ubiquitin ligases that are induced in atrophying skeletal muscle and mediate enhanced protein degradation through the proteasome[109]. While modest induction of MuRF1 mRNA was observed in AR113Q muscle, its expression was not further increased by CHOP deficiency. No significant change in MAFbx expression was detected. Additionally, CHOP deficiency did not alter expression of the 20S proteasome subunit in skeletal muscle (Data not shown). We conclude that enhanced atrophy of hind limb muscle in AR113Q, CHOP null mice was not associated with a significant induction of E3 ligases that promote muscle protein degradation through the ubiquitin-proteasome pathway.

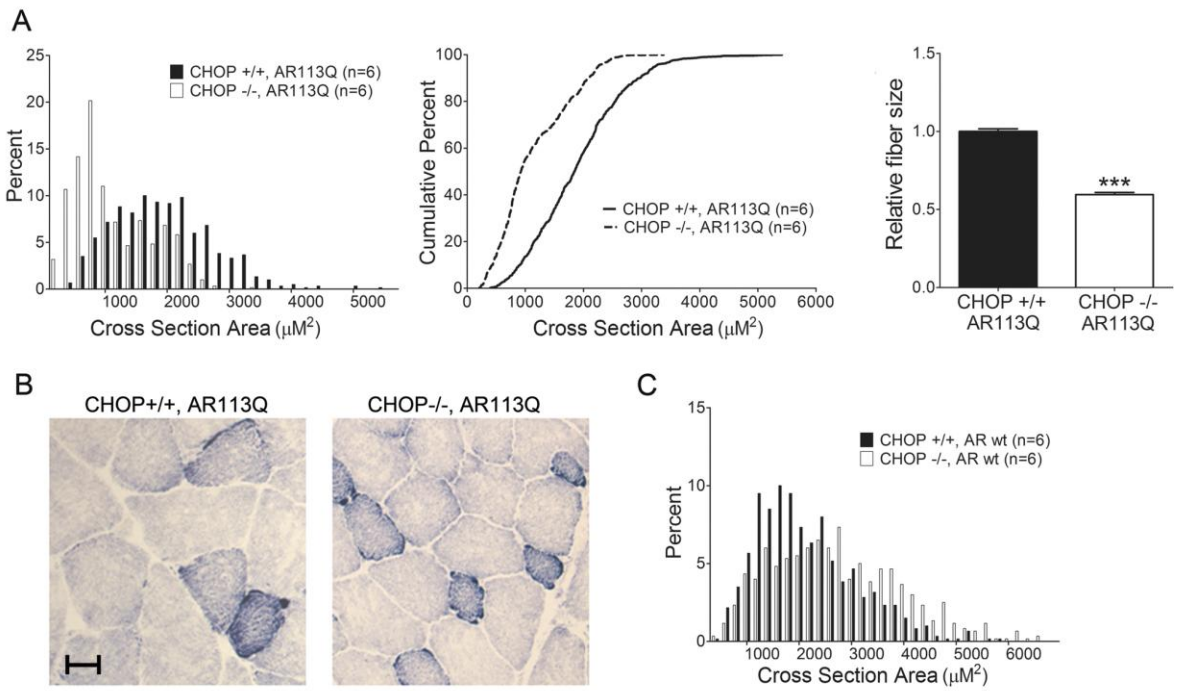

Figure 2.2 CHOP deletion accentuates muscle atrophy in AR113Q mice.

(A) Muscle fiber size (100 fibers/mouse) was quantified from proximal hind limb muscle of AR113Q (black) or AR113Q, CHOP -/- mice (white) at 12 wks. Left panel shows fiber size distribution, middle panel shows cumulative percent of fibers as a function of fiber area, and right panel shows relative fiber cross sectional area (mean +/- SEM). Left, middle panels, $p<0.0001$ by Mann-Whitney test. Right panel, $p<0.001$ by Student's *t* test. **(B)** Representative image of muscle fibers following NADH stain. Bar = 20 μM. **(C)** Distribution of proximal hind limb muscle fiber size from wt (black) and CHOP -/- (white) mice at 12 wks. Difference not significant by Mann-Whitney test. Experiments performed by Zhigang Yu.

These findings prompted us to consider the possibility that another protein degradation pathway underlies the increased atrophy triggered by CHOP deficiency. As recent studies demonstrate that autophagy contributes to skeletal muscle wasting [110], we next examined the activity of the autophagic pathway following disruption of the UPR. Western blot demonstrated a ~3-fold increase in the autophagosome marker LC3-II (microtubule-associated protein 1, light chain 3-II) in skeletal muscle from AR113Q, CHOP null mice (**Figure 2.3B**). No accumulation of p62 was detected (**Figure 2.3B**) consistent with the notion that flux through the autophagic pathway was intact following

disruption of the UPR. Consistent with the notion that CHOP deficiency induced autophagy in AR113Q muscle, we detected increased expression of mRNAs encoding the autophagy regulators Atg5, Atg9B, LC3B and UVRAG (**Figure 2.3C**). Notably, induction of autophagy was not associated with altered levels of AR protein (**Figure 2.3D**) or the appearance of AR immunoreactive intranuclear inclusions in skeletal muscle nuclei (**Figure 2.3E**). These observations are consistent with a prior report demonstrating that the androgen receptor largely escapes autophagic degradation following its translocation into the nucleus [30], and indicate that enhanced muscle atrophy in CHOP null mice is independent of changes in AR protein levels. CHOP deficiency did not alter phosphorylation of eukaryotic translation initiation factor 2 alpha (eIF2 alpha) or splicing of XBP1 mRNA (**Figure 2.3F**), signals generated by the proximal UPR sensors protein kinase RNA-like ER kinase (PERK) and IRE1 that have been linked to the regulation of autophagy[111,112]. In contrast, we observed a modest, but significant increase in the phosphorylation of c-Jun N-terminal kinases (JNK) (**Figure 2.3F**), suggesting that signaling through JNK may contribute to enhanced activation of autophagy in AR113Q, CHOP null muscle, as observed in other systems[113].

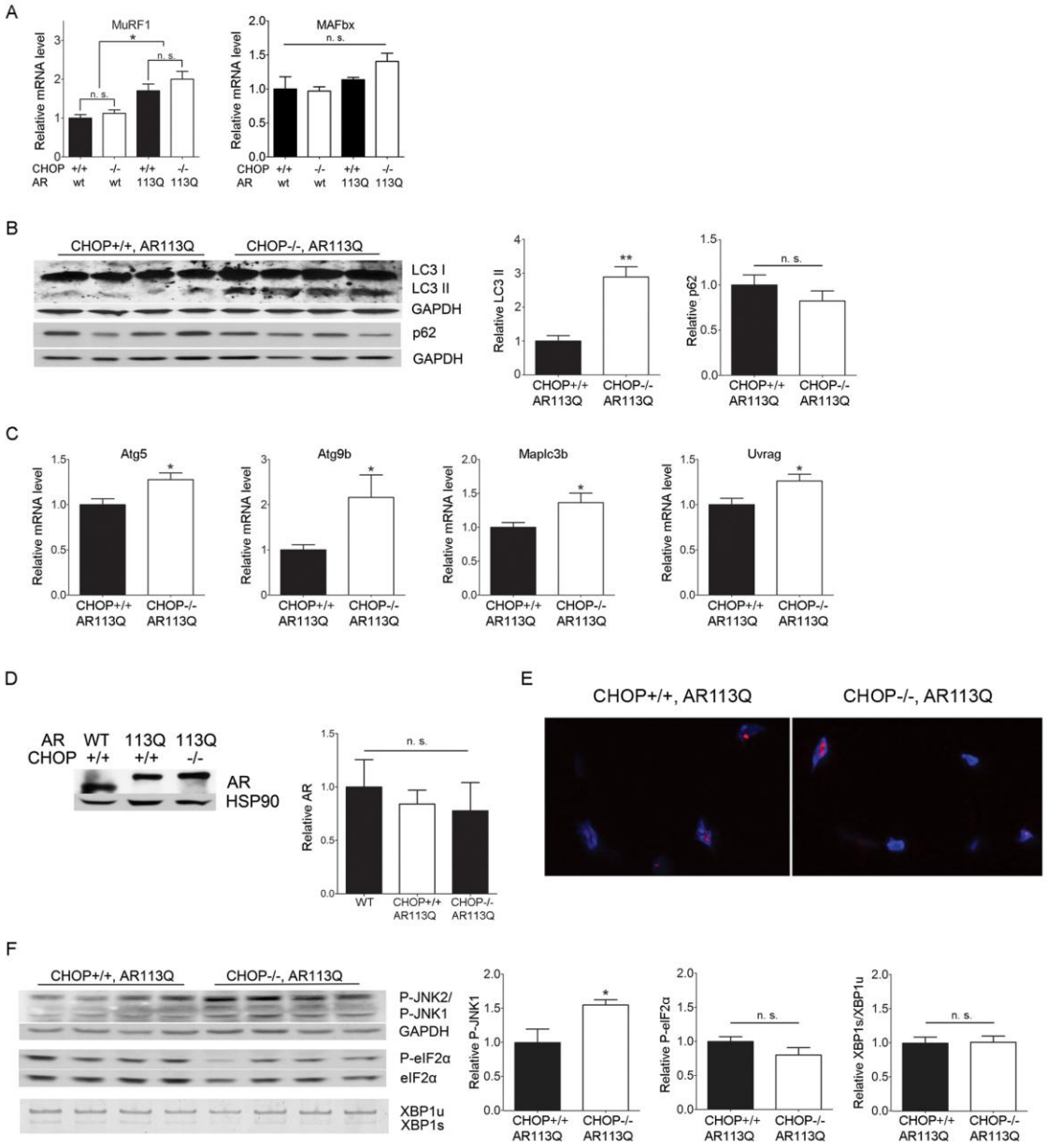

Figure 2.3 Autophagy is increased in AR113Q, CHOP -/- muscle.

(A) Relative expression of MurRF1 and MAFbx mRNAs in proximal hind limb muscle of 12 wk mice (*n*=5-6/genotype). *p<0.05 by ANOVA, n. s. = not significant. **(B)** LC3 and p62 expression in proximal hind limb muscle of 12 wk mice was assessed by western blot. Right panels show quantification of signal relative to GAPDH. **p<0.01 by Student's *t* test. **(C)** Relative expression of mRNAs encoding autophagy regulators in proximal hind limb muscle. *p<0.05 by Student's *t* test.**(D**) Androgen receptor protein expression in skeletal muscle of 12 wk mice. Hsp90 serves as a loading control. Right panel shows quantification of relative signal intensity (*n*=3/genotype). **(E)** Proximal hind limb muscles stained for the androgen receptor (in red) exhibit intranuclear inclusions. Nuclei are stained by DAPI (in blue). **(F)** P-JNK and P-eIF2 alpha expression (top, middle) and XBP1 mRNA splicing (bottom) in proximal hind limb muscle of 12 wk mice. Right panels show quantification of signal relative to loading control. **p<0.01 by Student's *t* test. n. s. = not significant. Experiments performed by Zhigang Yu.

CHOP deficiency increases autophagy-induced atrophy of denervated muscle.

Our observation of robust UPR activation in AR113Q skeletal muscle raised the possibility that muscle denervation induces ER stress, and that disruption of the UPR by CHOP deficiency enhances wasting by altering the cellular response to ER stress. To first test whether denervation is sufficient to activate the UPR in skeletal muscle, wild type male mice underwent unilateral sciatic nerve transection, and denervated and intact gastrocnemius muscles were harvested at 3 or 7 days post surgery. Denervation significantly increased phosphorylation of eIF2 alpha and splicing of XBP1 mRNA (**Figure 2.4A**) indicating that activation of the proximal UPR sensors PERK and IRE1 had occurred. Further, gene expression analysis by qPCR demonstrated a significant induction of BiP and CHOP mRNAs in denervated muscle, while ATF4 mRNA levels exhibited a similar trend that failed to reach statistical significance (**Figure 2.4B**). We conclude that denervation activated the UPR in skeletal muscle.

These results encouraged us to use this system to further explore the relationship between the UPR and autophagy, and to test the notion that CHOP deficiency enhances muscle wasting through the induction of autophagy. Surgical denervation of male mice expressing the wild type AR demonstrated that CHOP deficiency significantly increased activity of the autophagic pathway, similar to our findings in AR113Q muscle. Denervated CHOP null muscle harvested 7 days post surgery contained ~2.5 fold more LC3-II than did wild type muscle (**Figure 2.4C**). p62 did not accumulate in CHOP deficient muscle, indicating that flux through the autophagic pathway was intact. CHOP deficiency also accentuated skeletal muscle atrophy following denervation, producing a significant decrease in mean fiber size (**Figure 2.4D**). Our findings demonstrate that

CHOP deficiency enhances autophagy and increases muscle wasting following denervation.

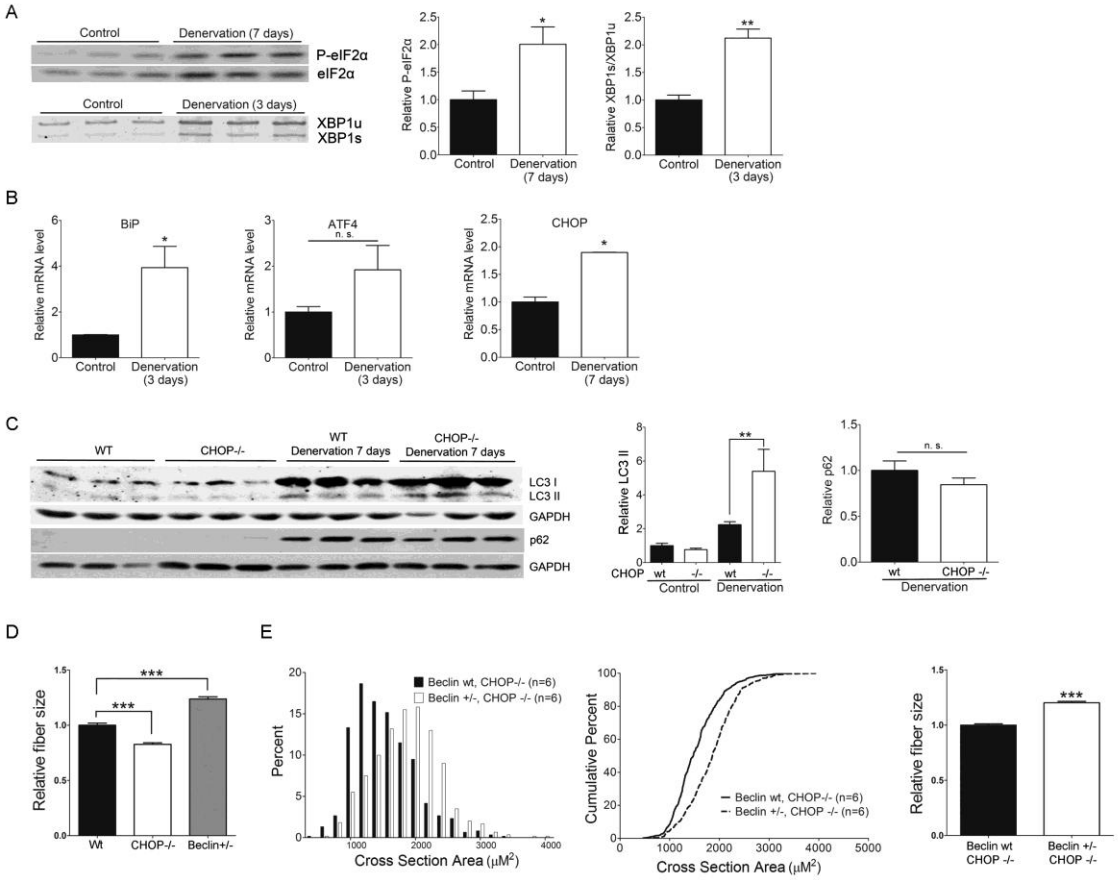

Figure 2.4 CHOP deficiency increases denervation-induced atrophy through autophagy.

Denervated gastrocnemius muscles or contralateral intact controls were harvested at the indicated times following unilateral sciatic nerve transection in 6 wk male mice. **(A)** Western blot shows enhanced eIF2 alpha phosphorylation (top) and RT-PCR demonstrates increased XBP1 mRNA splicing (bottom) in denervated muscle. Right panels show relative quantification of signal intensity. *p<0.05 by Student's *t* test. **(B)** Relative expression of BiP, ATF4 and CHOP mRNA (*n*=3). *p<0.05 by Student's *t* test **(C)** Following surgical denervation of wild type or CHOP-/- mice, LC3 and p62 expression was assessed by western blot. Right panels show quantification of signal relative to GAPDH. ***p<0.001 by ANOVA, n. s. = not significant. **(D)** Muscle fiber size (100 fibers/mouse) was quantified from wild type (black, *n*=5), CHOP -/- (white, *n*=3) and Beclin-1 +/- (grey, *n*=3) mice 7 days post sciatic nerve transection. Shown is relative fiber cross sectional area (mean +/- SEM). ***p<0.001 by ANOVA.**(E)** Muscle fiber size (100 fibers/mouse) was quantified from CHOP -/- (black, *n*=6) or CHOP -/-, Beclin-1 +/- mice (white, *n*=6) 7 days post sciatic nerve transection. Left panel shows fiber size distribution, middle panel shows cumulative percent of fibers as a function of fiber area, and right panel shows relative fiber cross sectional area (mean +/- SEM). Left, middle panels, p<0.0001 by Mann-Whitney test. Right panel, p<0.001 by Student's *t* test. Experiments performed by Zhigang Yu.

To confirm that autophagy contributes to muscle atrophy following surgical denervation, we transected the sciatic nerve of Beclin-1 haploinsufficient male mice [114]. Beclin-1 (encoded by *Becn1)* is a critical regulator of autophagy that binds class III phosphoinositide 3-kinase and is both required for the initiation of autophagosome formation and contributes to autophagosome maturation [115]. Mice haploinsufficient for Beclin-1 form fewer autophagosomes in skeletal muscle [116] and therefore allowed us to probe the role of autophagy in the response of muscle to sciatic nerve transection. Muscle haploinsufficient for Beclin-1 exhibited significantly increased mean fiber size compared to either wild type or CHOP null muscle following surgical denervation (**Figure 2.4D**) supporting a role for autophagy in muscle wasting. To directly test the notion that CHOP deficiency enhanced muscle wasting by activating autophagy, we generated CHOP null mice haploinsufficient for Beclin-1 (**Figure 2.4E**). Following denervation, these mice exhibited significantly less atrophy than CHOP null males, demonstrating that the effects of CHOP deficiency on muscle wasting were mediated through autophagy.

Beclin-1 haploinsufficiency attenuates the phenotype of AR113Q males.

Our finding that enhanced autophagy triggered by CHOP deficiency promoted muscle wasting in AR113Q mice prompted us to determine the consequences of limiting autophagy on the SBMA phenotype. To accomplish this, we generated AR113Q males haploinsufficient for Beclin-1. Similar to effects following surgical denervation, Beclin-1 haploinsufficiency significantly increased AR113Q muscle fiber size, although in this case the effect was less robust (**Figure 2.5A**). Limiting activity of the autophagic pathway did not alter levels of either the wild type or polyglutamine AR protein (**Figure**

2.5B), consistent with the notion that other protein quality control pathways, such as the proteasome, degrade the receptor once localized to the nucleus.

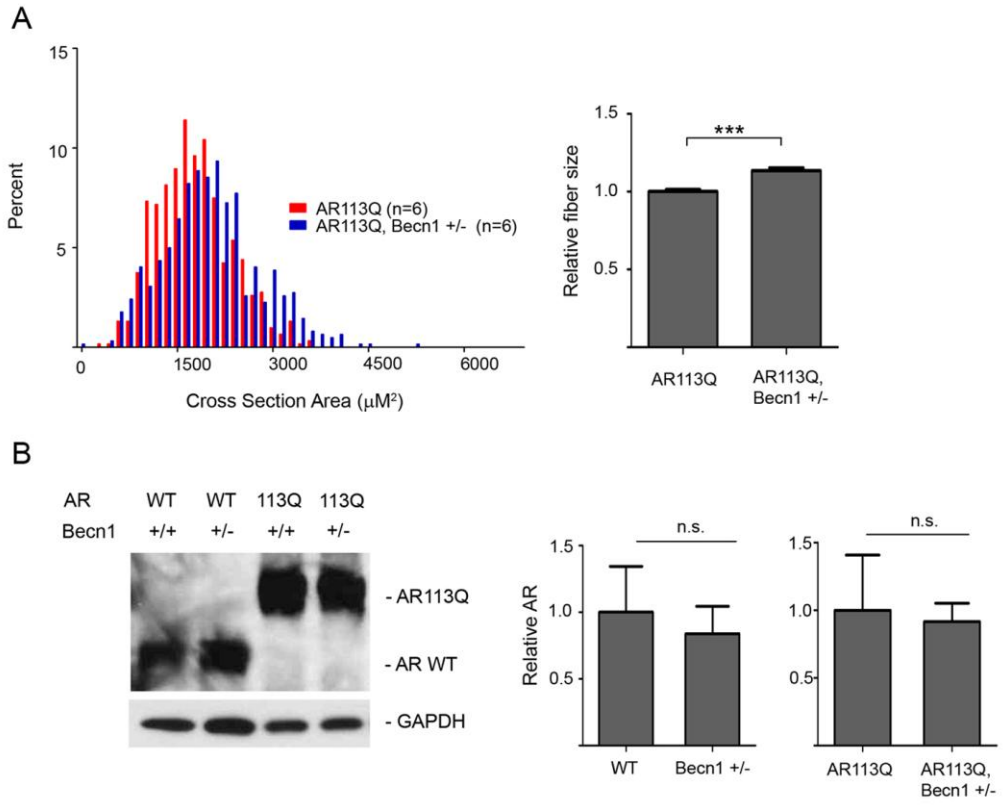

Figure 2.5 Effects of Beclin-1 haploinsufficiency on AR113Q muscle.

(A) Muscle fiber size (100 fibers/mouse) was quantified from proximal hind limb muscle of AR113Q (red, *n*=6) or AR113Q, Beclin-1 +/- (blue, *n*=6) mice at 16 wks. Left panel shows fiber size distribution, and right panel shows relative fiber cross sectional area (mean +/- SEM). Left panel, p<0.0001 by Mann-Whitney test. Right panel, p<0.0001 by Student's *t* test. **(B)** AR expression in skeletal muscle of 16 wk mice was assessed by western blot. GAPDH controls for loading. Right panel shows quantification of signal relative to GAPDH (mean +/- SEM). Differences not significant (n. s.).

Despite the limited changes in AR113Q muscle, Beclin-1 haploinsufficiency had a striking effect on survival. The lifespan of AR113Q males haploinsufficient for Beclin-1 was extended on average by ~10 wks compared to AR113Q, Beclin-1 wild type littermates (**Figure 2.6A**). AR113Q males exhibited a mean survival of 21.6 wks;

Beclin-1 haploinsufficiency extended mean lifespan by ~44% to 31.1 wks. Lifespan extension was not associated with rescue to wild type levels of body mass or motor performance as measured by grip strength (**Figure 2.6B, C**). However, AR113Q males haploinsufficient for Beclin-1 aged over 20 weeks maintained motor function while AR113Q, Beclin-1 wild type littermates exhibited a marked drop-off (**Figure 2.6C**). Consistent with the notion that the effects of Beclin-1 haploinsufficiency on motor function were most manifest in older mice, we found no change in the age of disease onset (defined as the point at which grip strength was 5% less than controls) due to Beclin-1 haploinsufficiency (**Figure 2.6D**). Our data indicate that Beclin-1 haploinsufficiency significantly extended the duration of disease by prolonging survival and maintaining motor function of SBMA mice.

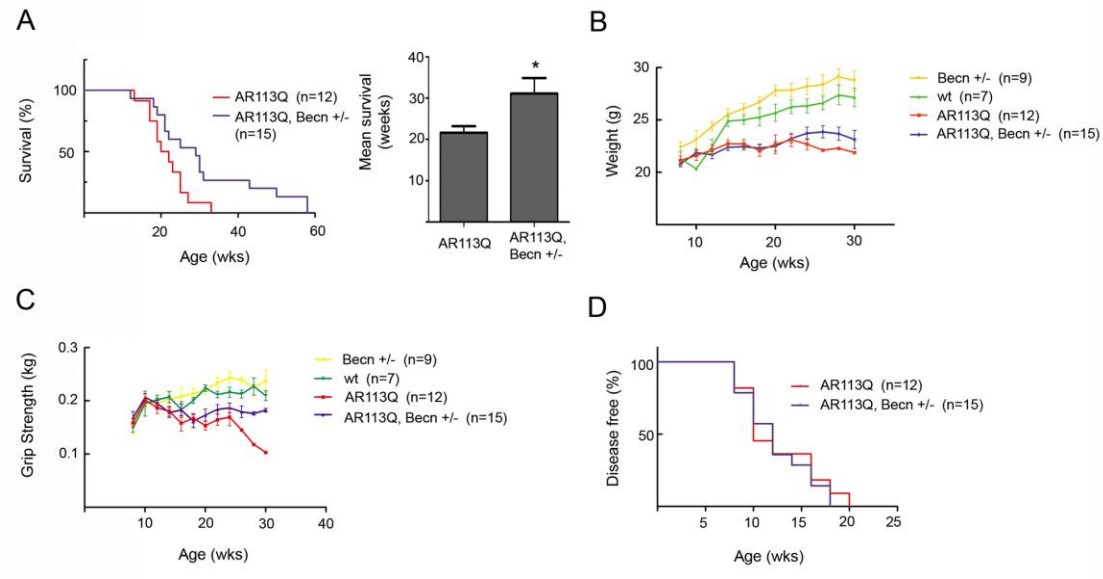

Figure 2.6 Beclin-1 haploinsufficiency extends lifespan in AR113Q males.

(A) Left panel, Kaplan-Meyer survival curve of AR113Q males. (red line, *n*=12) and AR113Q *p<0.05 by log-rank analysis. Right panel, mean survival +/- SEM. *p<0.05 by Student's *t*-test. **(B,C)** Body weight (panel B) and grip strength (panel C) at different ages for wild type (wt, green line, *n*=7), Beclin-1 +/- (yellow line *n*=9), AR113Q (red line, *n*=12), and AR113Q, Beclin-1 +/- (blue line, *n*=15) male mice. **(D)** Age of disease onset as measured by a decrease of 5% or more in forelimb grip strength (not significant by log rank analysis).

Discussion

The accumulation of misfolded, mutant proteins is a common basis for adult onset neurodegenerative diseases including those caused by CAG/glutamine tract expansions [1,93], and pathways controlling protein homeostasis are central to the cellular response to these stressors. Here we investigated the role of the UPR, a regulator of ER protein quality control [102,103], in the pathogenesis of SBMA, a neuromuscular disease caused by a glutamine tract expansion in the AR. Our findings demonstrate the occurrence of ER stress in skeletal muscle from SBMA patients, AR113Q mice, and wild type mice following surgical denervation. To identify the functional consequence of this response, we generated AR113Q mice deficient in the UPR-mediator CHOP, a transcription factor

induced downstream of ATF4 following ER stress. We show that CHOP deletion accentuates muscle atrophy in both AR113Q mice and in surgically denervated wild type males. Notably, in both cases, enhanced muscle wasting due to CHOP deficiency is mediated by increased autophagy, a lysosomal protein quality control pathway that has emerged as a central regulator of proteostasis in several protein aggregation neurodegenerative diseases. While CHOP deficiency activates autophagy and enhances muscle wasting in SBMA mice, limiting autophagy by Beclin-1 haploinsufficiency diminishes muscle atrophy, maintains motor function in aged animals and markedly extends lifespan. Our data highlight the central role of the UPR in remodeling the activity of the protein quality control machinery, and indicate that robust activation of autophagy accentuates the muscle atrophy of SBMA.

Activation of the UPR has been reported previously in yeast and mammalian cell culture models of polyglutamine disease [104,117,118], and the induction of ER stress responsive transcripts has been noted in Huntington disease mice [119]. The findings reported here extend these observations, demonstrating that the ER stress response is triggered in skeletal muscle from both SBMA patients and knock-in mice. Further, we define new aspects of the functional link between the UPR and autophagy. Several mechanisms by which the UPR regulates autophagy have been proposed based on studies in mammalian models, but a role for CHOP has not been identified previously. Data from a cellular model of polyglutamine disease indicate that phosphorylation of eIF2 alpha by PERK mediates the induction of LC3-II [112], while a recent study in cellular and mouse models of superoxide dismutase 1 (SOD1)-linked ALS show that XBP1 deletion activates autophagy [111]. As CHOP deficiency altered neither phosphorylation of eIF2

alpha nor splicing of XBP1 in AR113Q mice, we suggest that the effects identified here occur through a distinct mechanism. JNK, a downstream target of IRE1[120], can also stimulate LC3-II formation [113], and the occurrence of increased JNK phosphorylation in AR113Q, CHOP null muscle raises the possibility that this signaling pathway contributes to autophagy activation.

The functional consequences of altered autophagy in SBMA mice were unexpected and suggest that limiting activity of this pathway is beneficial for certain aspects of the disease phenotype. As the polyglutamine AR resides in the nucleus in the presence of ligand and largely escapes degradation through this pathway[30], we found that soluble and aggregated species of the mutant AR do not change when mice are deficient in CHOP or haploinsufficient for Beclin-1. We suggest that this reflects predominant degradation of the AR by the proteasome, a protein quality control pathway active in the nucleus. The extension of AR113Q lifespan by Beclin-1 haploinsufficiency contrasts with findings in Drosophila showing that disruption of autophagy exacerbates degeneration when the polyglutamine AR is expressed in the eye [121]. This difference may reflect variations in the extent to which autophagy is disrupted, as Beclin-1 haploinsufficiency decreases autophagosome number but does not completely block this pathway. Additionally, small molecule activators of autophagy reportedly promote survival of cultured motor neurons expressing the polyglutamine AR[30], raising the possibility that the findings described here in AR113Q mice reflect predominant effects outside the CNS, such as in skeletal muscle. While activation of autophagy following UPR disruption exacerbates atrophy of SBMA muscle in mice, recent studies in SOD1 models of ALS show that autophagy induction following XBP1 deletion ameliorates the

disease phenotype[111]. Mutant SOD1, a cytosolic protein, is a target for autophagic degradation and stimulating this pathway clears aggregates of the mutant protein.

Of the clinical symptoms experienced by SBMA patients, muscle wasting is a substantial contributor to morbidity. Here we show that activation of autophagy significantly enhances atrophy of surgically denervated and AR113Q muscle. In contrast, limiting autophagy prolongs lifespan and maintains motor function in SBMA mice. While the effects of Beclin-1 haploinsufficiency are relatively mild in AR113Q muscle, lifespan extension is striking, and likely reflects benefits of limited autophagy in cell types other than muscle fibers, perhaps including effects on metabolism. Defining the targets affected by Beclin-1 haploinsufficiency that mediate lifespan extension remains an important goal for future work. Notably, strategies to modulate the activity of the autophagic pathway have attracted considerable attention as studies in several polyglutamine disease models have documented degradation of cytoplasmic protein aggregates through autophagy[122]. Efforts are now underway to identify small molecules that activate the autophagic pathway in hopes of ameliorating the phenotypes of these diseases [123,124]. Our data suggest that autophagy activators are unlikely to be effective therapeutics for the subset of protein aggregation disorders where nuclear localization of the mutant protein is required for toxicity. Furthermore, in SBMA, the effects of disease on muscle may be accentuated by activation of autophagy. We suggest that alternative approaches to stimulate other components of the protein quality control machinery, such as the Hsp90-based chaperone machinery, are more likely to yield clinical benefits in SBMA and related protein aggregation disorders.

Materials and Methods

Mice

Derivation of mice with targeted *Ar* alleles containing 21 or 113 CAG repeats in exon 1 was described previously[98,99]. Briefly, mice were generated by recombining a portion of human exon 1 encompassing amino acids 31–484 with the mouse *Ar* gene in CJ7 embryonic stem cells. Male chimeras were mated with C57BL/6J females, and females heterozygous for the targeted *Ar* allele were backcrossed to C57BL/6J to generate mice used in this study. Surgical castration of 5-6 wk old males was as previously described [98]. Unless otherwise specified, skeletal muscles were harvested from adult AR113Q male mice at 3 – 5 months, except from castrated AR113Q males, in which case animals were 18 months of age. CHOP deficient mice (B6.129S-Ddit3^{tm1Dron}/J) [105] were purchased from the Jackson Laboratory and backcrossed to C57BL/6J ten or more generations. Mice with a *Becn1* null allele were previously reported [114] and backcrossed to C57BL/6J ten or more generations. All procedures involving mice were approved by the University of Michigan Committee on Use and Care of Animals, in accord with the NIH Guidelines for the Care and Use of Experimental Animals.

Sciatic nerve transaction

7 wk old C57BL/6J, CHOP deficient or *Becn1* haploinsufficient male mice congenic to C57BL6/J were used for studies of denervated muscle. Under deep inhaled anesthesia with 2% isoflurane, the right sciatic nerve was exposed at the thigh just below the sciatic notch. Both the proximal and distal sides were ligated with monocryl 4-0 suture, and about 2 mm of sciatic nerve was cut between the ligations to prevent axonal regeneration. At 3 and 7 days after surgery, the right gastrocnemius and tibialis anterior muscle were

dissected and frozen for histology or RNA and protein analysis. The contralateral side was used as control.

Human Skeletal Muscle Samples

Anonymized SBMA muscle and control biopsy samples were obtained from the University of Michigan Medical School in accordance with IRB procedures and in a manner that assured patient privacy. Additionally, anonymized skeletal muscle was harvested from SBMA patients at autopsy, as approved by the ethics committee of the Nagoya University Graduate School of Medicine and in accordance with the Declaration of Helsinki (Hong Kong Amendment).

Muscle fiber size quantification

Muscle was frozen in isopentane chilled by liquid nitrogen, cut in cross section at a thickness of 5 μm and stained by H&E. Digital images were captured using a Zeiss Axioplan 2 imaging system. The area of each muscle fiber was defined using Adobe Photoshop CS4 or ImageJ, and the pixel number was converted to μm^2 according to scale. 100 adjacent fibers from each section were measured.

RNA analysis

Total RNA isolated from tissues with Trizol (Invitrogen, Carlsbad, CA) served as a template for cDNA synthesis using the high capacity cDNA archive kit from Applied Biosystems (Foster City, CA). Gene-specific primers and FAM labeled probes (Human: BiP, Hs99999174_m1; CHOP, Hs99999172_m1; ATF4, Hs00909568_g1; PDI, Hs00168586_m1; Mouse: BiP, Mm00517691_m1; CHOP, Mm00492097_m1; ATF4, Mm00515324_m1; PDI: Mm01243184_m1; MAFbx, Mm00499518_m1; MuRF1, Mm01185221_m1; α-acetylcholine receptor, Mm00431627_m1; Myod1,

Mm00440387_m1; Myog, Mm00446194_m1; Atg5, Mm00504340_m1; Atg9b, Mm01157883_g1; Maplc3b, Mm00782868_sH; Uvrag, Mm00724370_m1) were purchased from Applied Biosystems. TaqMan assays were performed in duplicate using 5 ng aliquots of cDNA on an ABI 7500 Real Time PCR system. Relative expression levels were calculated comparing with the expression of 18S rRNA. Semi-quantitative RT-PCR analysis of Xbp1 RNA splicing was performed using primers (mouse: 5'-GAACCAGGAGTTAAGAAC-3' and 5'-AGGCAACAGTGTCAGAGT-3'; human: 5'-GAATGAGTGAGCTGGAACAG-3' and 5'-GAGTCAATACCGCCAGAATC-3') to amplify 10 ng of cDNA through 22 cycles. One tenth of the total PCR products were resolved on 15% nondenaturing polyacrylamide gels and stained with SYBR Green 1 (Invitrogen, Eugene, OR) after electrophoresis. Bands were visualized on a Typhoon Trio+ scanner (Amersham Biosciences, Pistcataway, NJ) and analyzed with AlphaImager 2200 software (Alpha Innotech Corporation, San Leandro, CA).

Protein expression analysis

Muscle tissue was homogenized in RIPA buffer containing complete protease inhibitor cocktail (Roche, Indianapolis, IN) and phosphatase inhibitor (Thermo scientific, Rockford, IL) using a motor homogenizer (TH115, OMNI International, Marietta, GA). Sample lysates were incubated on a rotator at 4^{o} C for 1 hour and the pre-cleared by centrifugation at 15,000 *g* for 15 minutes at 4° C. Samples were resolved by 7 or 10% SDS-PAGE and transferred to nitrocellulose membranes (Bio-Rad, Hercules, CA). Blots were probed with primary antibodies and proteins were visualized by chemiluminescence (Thermo Scientific, Rockford, IL). The AR (N-20), HSP90 and eIF2α antibodies were from Santa Cruz Biotechnology (Santa Cruz, CA), phospho-eIF2α (Ser51) and phospho-

JNK antibodies were from Cell Signaling Technology (Danvers, MA), LC3B antibody was from Novus Biologicals (Littleton, CO), GAPDH, BiP and PDI antibodies were from AbCam (Cambridge, MA), 20S proteasome antibody was from Calbiochem (Gibbstown, NJ) and p62 antibody was from American Research Products (Belmont, MA). Western blot quantification was performed using ImageJ.

Muscle histochemistry and immunofluorescence

Frozen muscle tissue was sectioned at 5 μm with a cryostat and stained with H&E or NADH. For immunofluorescence, 5 μM frozen sections were stained with an antibody against AR and an Alexa Fluor 594 conjugated secondary antibody (Invitrogen). Confocal images were captured with a Zeiss LSM 510 microscope and a water immersion lens (×63).

Grip strength analysis

The grip strength meter (Columbus Instruments) was positioned horizontally and mice were lowered toward the apparatus. Mice were allowed to grasp the smooth metal triangular pull bar with their fore limbs only, and then were pulled backward in the horizontal plane. The force applied to the bar at the moment the grasp was released was recorded as the peak tension (kg). The test was repeated 5 consecutive times within the same session, and the highest value from the 5 trials was recorded as the grip strength for that animal.

Statistics

Statistical significance was assessed by two-tailed Student's *t*-test or by ANOVA with the Newman-Keuls multiple comparison test. The distribution of muscle fiber size was

analyzed by Mann-Whitney test. All statistics was performed by the Prism 5 (GraphPad Software, San Diego, CA). *P* values less than 0.05 were considered significant.

Acknowledgements

This work was supported by grants from the National Institutes of Health (R01 NS055746 to AP Lieberman, R01 NS060123 to Z Yu, and P50 CA69568 to DM Robins) and from the Department of Defense (DOD17-02-1-0099 to DM Robins).

This work was originally published as: Yu, Z., Wang, A.M., Adachi, H., Katsuno, M., Sobue, G., Yue, Z., Robins, D.M., Lieberman, A.P. **Macroautophagy is regulated by the UPR-mediator CHOP and accentuates the phenotype of SBMA mice** *PLoS Genet* **7**, (2011) with ZY and AW as co-first authors. ZY contributed figures 1-4 and AW contributed figures 5 and 6.

Chapter 3

Inhibition of Hsp70 by Methylene Blue Affects Signaling Protein Function and Ubiquitination and Modulates Polyglutamine Protein Degradation

Abstract

The Hsp90/Hsp70-based chaperone machinery regulates the activity and degradation of many signaling proteins. Cycling with Hsp90 stabilizes client proteins, whereas Hsp70 interacts with chaperone-dependent E3 ubiquitin ligases to promote protein degradation. To probe these actions, small molecule inhibitors of Hsp70 would be extremely useful, however few have been identified. Here we test the effects of methylene blue, a recently described inhibitor of Hsp70 ATPase activity, in three well-established systems of increasing complexity. First, we demonstrate that methylene blue inhibits the ability of the purified Hsp90/Hsp70-based chaperone machinery to enable ligand binding by the glucocorticoid receptor and show that this effect is due to specific inhibition of Hsp70. Next, we establish that ubiquitination of neuronal nitric oxide synthase by the native ubiquitinating system of reticulocyte lysate is dependent upon both Hsp70 and the E3 ubiquitin ligase CHIP and is blocked by methylene blue. Finally, we demonstrate that methylene blue impairs degradation of the polyglutamine expanded androgen receptor, an Hsp90 client mutated in spinal and bulbar muscular atrophy. In

contrast, degradation of an amino-terminal fragment of the receptor, which lacks the ligand-binding domain and therefore is not a client of the Hsp90/Hsp70-based chaperone machinery, is enhanced through homeostatic induction of autophagy that occurs when Hsp70-dependent proteasomal degradation is inhibited by methylene blue. Our data demonstrate the utility of methylene blue in defining Hsp70-dependent functions and reveal divergent effects on polyglutamine protein degradation depending on whether the substrate is an Hsp90 client.

Introduction

The Hsp90/Hsp70-based chaperone machinery that regulates a wide variety of Hsp90 'client' proteins (reviewed in [67]) is also a part of the cellular defense against unfolded proteins [125]. In this machinery, Hsp90 and Hsp70 have opposing effects on client protein stability. Hsp90 stabilizes client proteins, and, when their cycling with Hsp90 is blocked by specific Hsp90 inhibitors, like geldanamycin and radicicol, the client proteins undergo rapid degradation through the ubiquitin/proteasome pathway [126]. In contrast, Hsp70, along with its cochaperone Hsp40, is required for the degradation of many proteins [74,127].

Similar opposing roles of Hsp90 and Hsp70 are seen with signaling proteins that are canonical Hsp90 client proteins such as the glucocorticoid receptor (GR) and with signaling proteins that undergo dynamic cycling with Hsp90 such as neuronal nitric oxide synthase (nNOS) [128]. Opposing roles of Hsp90 and Hsp70 also regulate protein turnover in some of the polyglutamine expansion disorders. This group of neurodegenerative diseases is characterized by the accumulation of aberrant proteins, and includes Huntington disease (HD), spinal and bulbar muscular atrophy (SBMA), and several

autosomal-dominant spinocerebellar ataxias (e.g. SCA1, SCA3). Some of the mutant proteins that misfold and aggregate in these diseases, including huntingtin [129] in HD and the androgen receptor in SBMA [69], form heterocomplexes with Hsp90 and Hsp70. Inhibition of Hsp90 by geldanamycin prevents aggregation of these proteins in animal models of HD [130] and SBMA [71]. Because Hsp90 binding to heat shock factor 1 (HSF1) maintains this transcription factor in an inactive state and treatment of cells with geldanamycin induces an HSF1-dependent stress response [131,132], it is often proposed that geldanamycin alleviates the phenotype and accumulation of misfolded proteins in neurodegenerative disease models by inducing a stress response [73,130,133]. This explanation however, cannot be correct because geldanamycin promotes proteasomal degradation of the polyglutamine expanded androgen receptor (polyQ AR) in *Hsf1*$^{-/-}$ cells that cannot mount a stress response [69]. Further, overexpression of Hsp70 or Hsp40 decreases polyglutamine protein levels and improves viability in cellular models of HD [134] and SBMA [135], and overexpression ameliorates polyglutamine disease phenotypes in *Drosophila* and mouse models of neurodegenerative disease ([81,136,137], reviewed in [133]). These observations raise the possibility that Hsp70 plays a critical role in diminishing polyglutamine toxicity when Hsp90 function is inhibited.

There is considerable evidence that Hsp70 promotes degradation of the polyglutamine expanded proteins by promoting ubiquitination mediated by chaperone-dependent E3 ubiquitin ligases. The most studied of these is CHIP (carboxy terminus of Hsc70-interacting protein), a 35-kDa U-box E3 ubiquitin ligase [138]. CHIP binds to Hsc/Hsp70 through its amino-terminal tetratricopeptide repeat (TPR) domain [75,139], and it binds to the UBCH5 family of E2 ubiquitin conjugating enzymes through a carboxy-

terminal U-box [140]. Parkin is another E3 ligase [141] that is targeted to substrate by Hsp70 [142]. For some proteins, such as the GR, only CHIP promotes degradation, whereas for others, such as nNOS, CHIP and parkin are functionally redundant in promoting degradation [76]. Overexpression of either CHIP or parkin increases ubiquitination of polyglutamine-expanded ataxin-3 and reduces its cellular toxicity in a manner that is promoted by Hsp70 [134,142]. Interest has focused on CHIP because it is found in aggregates of huntington, androgen receptor, ataxin-1 and ataxin-3 [34,77,134,143], and CHIP overexpression suppresses aggregation and protein levels in cellular disease models [77,134,143]. The notion that CHIP is a critical mediator of the neuronal response to misfolded proteins is buttressed by the observations that overexpression of CHIP in a *Drosophila* model of SCA1 [77] and a mouse model of SBMA [78] suppresses toxicity, and that HD transgenic mice haploinsufficient for CHIP display an accelerated disease phenotype [143].

Most of what is known about Hsp70's role in the degradation of polyglutamine-expanded proteins comes from Hsp70 overexpression experiments. To enhance mechanistic understanding of Hsp70-dependent processes in general, it would be useful to have small molecule inhibitors of Hsp70, analogous to geldanamycin in probing Hsp90-dependent effects. To this end, the Gestwicki laboratory employed a high-throughput chemical screen to identify compounds that inhibit Hsp70 ATPase activity. An inhibitor identified in the compound library was methylene blue, which was shown to interact with purified Hsp70 by NMR spectroscopy [84]. Methylene blue reduced tau levels in both cellular and animal models of tauopathy [84], although it was not established that this effect was due to an effect of methylene blue on Hsp70. Methylene blue has been

demonstrated to affect multiple systems, most notably cGMP signaling; thus, its action is not directed against Hsp70 as a single target.

Our goal here is to determine the usefulness of methylene blue as a research tool for probing Hsp70-dependent effects in three well-established systems of increasing complexity, from the purified Hsp90/Hsp70-based chaperone machinery, to an ubiquitinating system from reticulocyte lysate, to inhibition of polyQ AR degradation in cells. We first show that methylene blue inhibits the generation of steroid binding activity of the glucocorticoid receptor, an established physiological action of Hsp70 [67]. Activation of GR steroid binding activity by purified chaperones requires Hsp70 [144], and we show that the methylene blue inhibition of activation is specific for the Hsp70 component of the Hsp90/Hsp70-based, multiprotein chaperone machinery. We then use methylene blue as a tool to probe the pathway regulating ubiquitination of neuronal nitric oxide synthase. Using the canonical system that was originally used to resolve the components of the ubiquitin-protein ligase pathway [52], we show that nNOS ubiquitination by the DE52-retained fraction of rabbit reticulocyte lysate is Hsp70-dependent. Methylene blue inhibits nNOS ubiquitination, and the blocked ubiquitination is overcome by addition of purified Hsp70. Additionally, nNOS ubiquitination is inhibited by anti-CHIP serum. This suggests that Hsp70-directed CHIP E3 ligase activity is responsible for nNOS ubiquitination in this system. Finally, we examine the effects of methylene blue in cells on the degradation of the polyQ AR with 112 glutamines (AR112Q) and a truncated amino-terminal fragment of the androgen receptor containing the expanded polyglutamine tract (trAR112Q). We show that inhibition of Hsp70 by methylene blue impairs AR112Q degradation and enhances ligand-dependent aggregation. In contrast to

effects on the full-length androgen receptor, we show enhanced degradation of an amino-terminal fragment of the expanded glutamine androgen receptor in the presence of methylene blue, and that this is mediated by homeostatic induction of macroautophagy.

Results

Methylene Blue Inhibits Hsp70 Action on the GR

To bind steroid with high affinity the GR must be assembled into a heterocomplex with Hsp90 [67]. These heterocomplexes are assembled by a multichaperone machinery present in lysates of all eukaryotic cells. **Fig. 3.1A** shows that incubation of an Hsp90-free GR immunopellet with rabbit reticulocyte lysate generates GR•Hsp90 heterocomplexes that bind steroid, and both formation of heterocomplexes and generation of steroid binding activity are reduced when the Hsp90 inhibitor geldanamycin is present. Methylene blue also inhibits the generation of steroid binding activity by reticulocyte lysate in a concentration dependent manner (**Fig. 3.1B**). The formation of GR•Hsp90 heterocomplexes by reticulocyte lysate requires Hsp70 [67], and our presumption was that if methylene blue is acting as an Hsp70 inhibitor, it might inhibit Hsp70 binding to the GR. However, in the presence of 30 μM methylene blue, which inhibits generation of a majority of the steroid binding activity, the same amount of Hsp70 is bound to the GR as in control incubations without methylene blue (**Fig. 3.1C**). Surprisingly, the methylene blue treated samples also contain the same amount of Hsp90 (**Fig. 3.1C**), distinguishing this effect from the action of the Hsp90 inhibitor geldanamycin.

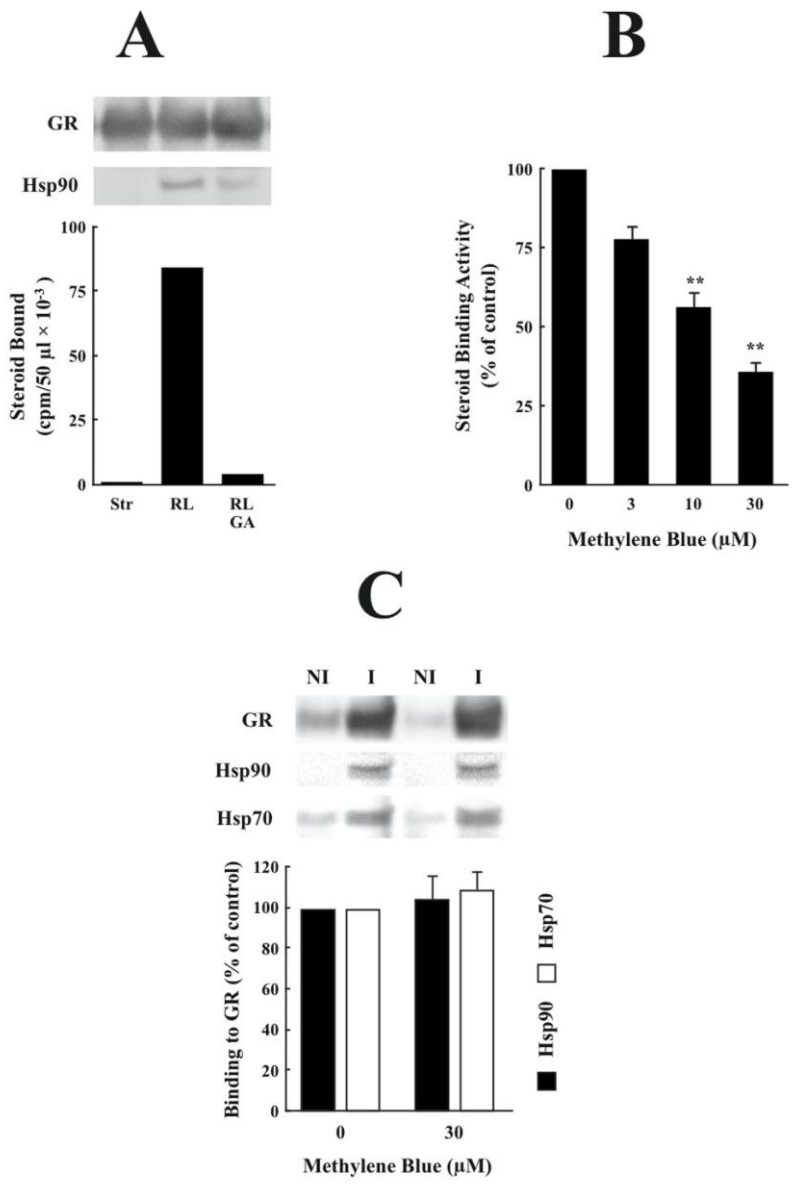

Figure 3.1 Methylene blue inhibits generation of steroid binding activity but not GR•Hsp90 heterocomplex assembly by reticulocyte lysate.

(A) The assay. GR stripped of Hsp90 (Str) was incubated with reticulocyte lysate (RL) in the absence or presence of 10 µM geldanamycin (GA). Immunopellets were washed and Western blotted for GR and Hsp90. Duplicate pellets were incubated with [3H]dexamethasone to assay steroid binding activity. **(B)** Methylene blue inhibits generation of GR steroid binding activity. Stripped GRs were reactivated by reticulocyte lysate in the presence of the indicated concentrations of methylene blue. **Different from control at p<0.01. **(C)** Methylene blue does not inhibit GR•Hsp90 heterocomplex assembly. Stripped nonimmune (NI) or immune (I) GR pellets were incubated with reticulocyte lysate in the absence or presence of 30 µM methylene blue. Immunopellets were washed and Western blotted for GR, Hsp90, and Hsp70. A typical radiogram of a Western blot is shown above the bar graph. GR specific Hsp90 (solid bars) and Hsp70 (open bars) were determined in six separate experiments and are presented in the graph relative to the 0 methylene blue control set at 100%. Experiments performed by Yoshinari Morishima.

To determine if methylene blue inhibition of steroid binding activity is specific to an effect on Hsp70, we examined the effect of methylene blue on generation of steroid binding activity by a purified 5-protein assembly system composed of Hsp90, Hsp70, Hop, Hsp40 and p23 [67]. In this system, both Hsp90 and Hsp70 are required for steroid binding [67,144], and maximal generation of steroid binding activity in this system requires 15 µg Hsp90 and 15 µg Hsp70 in the incubation mixture. In the experiment of **Fig. 3.2A**, the stripped GR was incubated with the 5-protein system containing low amounts (0.5–5 µg) of Hsp70 in the presence or absence of 30 µM methylene blue. As the concentration of Hsp70 is increased, there is more generation of steroid binding activity both in the presence and absence of methylene blue (**Fig. 3.2A**). However, when the percent inhibition of reactivation of GR steroid binding is plotted as a function of the amount of Hsp70, we find that the extent of inhibition decreases as the amount of Hsp70 is increased (**Fig. 3.2B**), supporting the notion that Hsp70 function is inhibited by methylene blue. Consistent with this interpretation is the finding that methylene blue is a more potent inhibitor of steroid binding reactivation at lower Hsp70 concentration (**Fig. 3.2C**). In contrast, when Hsp70 is present in a nonlimiting amount but Hsp90 is limiting, methylene blue has the same potency at each Hsp90 concentration (**Fig. 3.2D**).

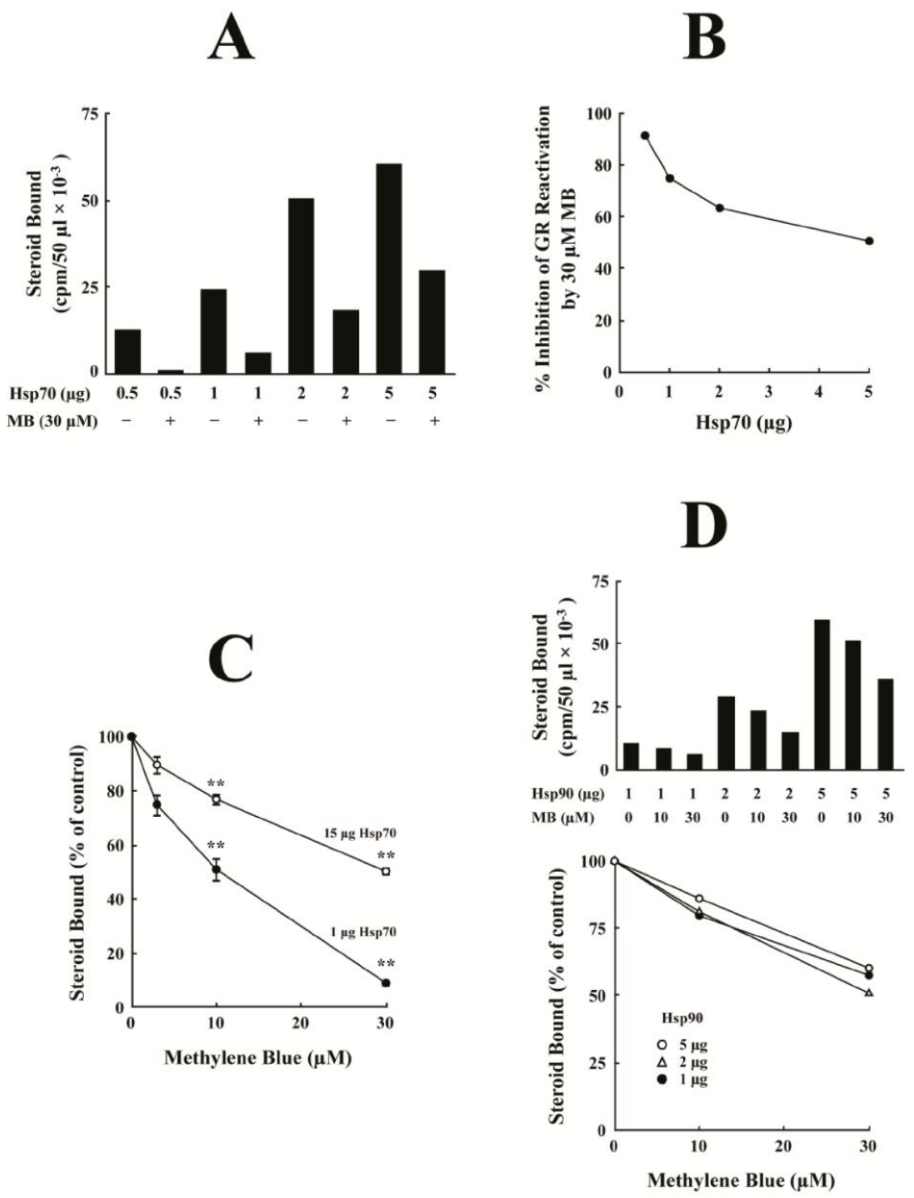

Figure 3.2 Methylene blue inhibition of generation of steroid binding activity by the purified five-protein assembly system varies with the concentration of Hsp70.

(A) Stripped GR immune pellets were incubated with Hsp90, Hop, Hsp40 and p23 in the presence of the indicated concentrations of Hsp70 and in the presence or absence of 30 µM methylene blue. Immune pellets were washed and steroid binding activity was assayed. **(B)** Plot of the data of Panel A as % inhibition of reactivation of steroid binding activity by methylene blue at each concentration of Hsp70. **(C)** Concentration dependency of methylene blue inhibition of GR reactivation in the presence of 1 (●) or 15 (○) µg Hsp70. **Different from control at $p<0.01$. **(D)** Concentration dependency of methylene blue in the presence of 15 µg Hsp70 and limiting amounts of Hsp90. Upper panel presents cpm of steroid bound, and lower panel presents binding as a % of the control without methylene blue. Experiments performed by Yoshinari Moishima.

These data suggest that it is the Hsp70 component of the multiprotein chaperone machinery that is inhibited by methylene blue. Methylene blue does not inhibit Hsp70 binding to the GR (**Fig. 3.1C**), but it may affect Hsp70 function once it has bound to the receptor. The first step in GR•Hsp90 heterocomplex assembly is the ATP-dependent priming of the GR to form a GR•Hsp70 complex that can interact with Hsp90 and Hop. This complex undergoes another ATP-dependent step to yield the high affinity steroid binding form of the receptor [145]. Hsp90 is required to open the steroid binding cleft in the GR, and the amount of steroid binding activity generally reflects the amount of Hsp90 recovered in GR heterocomplexes. Notably, this is not what is seen in **Fig. 3.1C**.

Hop binds independently via an N-terminal tetratricopeptide repeat (TPR) domain to Hsp70 and via a central TPR domain to Hsp90 [146]. This brings the two essential chaperones together into a more efficient machinery for heteroprotein complex assembly [144]. Hsp90 can be present in GR heterocomplexes because it is bound via Hop to receptor-bound Hsp70. This does not require a direct interaction of Hsp90 with the Hsp70-primed receptor to yield steroid binding activity [144]. This is illustrated with the Hsp90 inhibitor geldanamycin in **Fig. 3.3A**. When GR•Hsp90 heterocomplexes are assembled with the 5-protein system containing Hop, a substantial amount of Hsp90 is present in the GR immune pellet formed in the presence of geldanamycin (lane 3). However, when heterocomplexes are assembled without Hop, only a trace amount of Hsp90 is present in the geldanamycin-treated sample (lane 5). To test if this is the case with methylene blue, we incubated stripped GR with the 5-protein system minus Hop in the presence and absence of the inhibitor. As shown in **Figs. 3.3B** and **C**, both in the presence and absence of Hop, steroid binding is inhibited by methylene blue, but the amount of Hsp90 in GR

immunopellets is similar to that in the controls. This suggests that methylene blue does not inhibit Hsp70 promotion of Hsp90 binding to the GR, but it inhibits priming of the receptor by Hsp70 that allows the GR to interact productively with Hsp90 to open the steroid binding cleft.

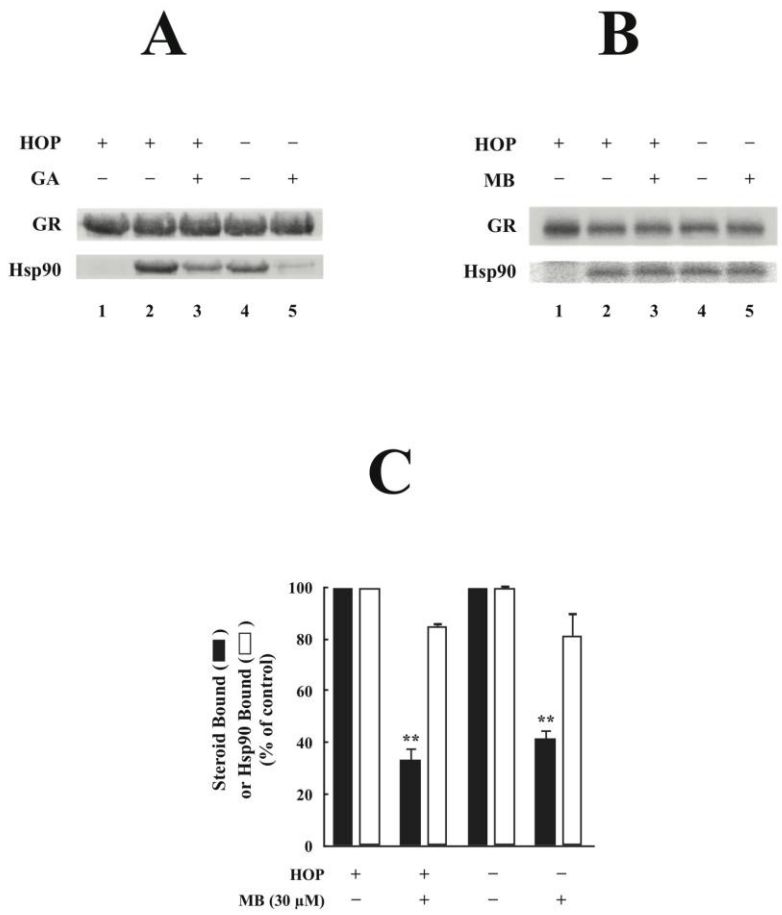

Figure 3.3 Effect of methylene blue on GR•Hsp90 heterocomplex assembly in the presence and absence of Hop.

Stripped GR was incubated in the presence of the 5-protein system containing 15 µg Hsp70 (+Hop) or in the presence of the system minus Hop (–Hop) with or without 10 µM geldanamycin (GA) in **(A)** or 30 µM methylene blue in **(B)**. Immunopellets were washed and immunoblotted for GR and Hsp90. Lane 1, stripped GR; lanes 2–5, stripped GR incubated with chaperone mix for 20 min. The bar graph shows the results of four experiments where duplicate pellets were assayed for steroid binding activity and the relative amount of GR-bound Hsp90 was determined by scanning immunoblots as in **Fig. 3.1C**. GR-bound Hsp90 in methylene blue samples is presented as a % of the untreated controls. **Different from control at $p<0.01$. Experiments performed by Yoshinari Morishima.

Use of Methylene Blue as a Tool to Determine Hsp70 Dependence of nNOS Ubiquitination

Because a good Hsp70 inhibitor has not been available, it has been difficult to establish whether or not ubiquitination events are Hsp70-dependent. It is known, for example, that the reaction of certain inactivators in the heme/substrate binding cleft of nNOS triggers its ubiquitination and degradation [147,148] and that overexpression of either CHIP or parkin promotes nNOS degradation [76,149]. These data suggest that Hsp70 may be involved. Ubiquitination of purified nNOS by a purified ubiquitinating system using CHIP as the E3 ligase is promoted by purified Hsp70 [149,150], but it is not known if nNOS ubiquitination by a physiological ubiquitinating system is Hsp70-dependent. Thus, we used this system to test the effectiveness of methylene blue in detecting the Hsp70 dependence of nNOS ubiquitination.

We have previously reported that nNOS is ubiquitinated in human embryonic kidney cells and in rat brain cytosol [147] and that the ubiquitination is mimicked by incubating purified nNOS with an extract of rabbit reticulocyte lysate, ubiquitin and ATP [147,150]. The extract of reticulocyte lysate contains all material that is retained by a DE52 column, and this DE52-retained fraction is the same as lysate 'fraction II' that has been extensively used to study protein ubiquitination [52]. The DE52-retained fraction contains Hsp70 and its cochaperone Hsp40, as well as the ubiquitinating enzymes, with all of the components being present in the same ratios as exist in reticulocyte lysate [147,151]. To determine if ubiquitination by this system requires Hsp70, nNOS was incubated with the DE52-retained fraction in the presence of increasing concentrations of methylene blue. As shown in **Fig. 3.4A**, methylene blue inhibits nNOS ubiquitination. The concentration of Hsp70 in this ubiquitinating system is ~5% of Hsp70 in the reticulocyte lysate

experiments of **Fig. 3.1**, and therefore, much lower concentrations of methylene blue are effective at inhibiting ubiquitination. Importantly, the inhibition produced by 1 μM methylene blue is largely overcome when purified Hsp70 is added to the incubation mix (**Fig. 3.4A**, lane 7). This indicates that methylene blue is inhibiting the Hsp70-dependent E3 ligase step in ubiquitination and not the E1 or E2 enzymes, which are not Hsp70-dependent. These data suggest that methylene blue may be a useful reagent to detect Hsp70-dependent effects, much as geldanamycin has been useful to probe for Hsp90-dependent effects.

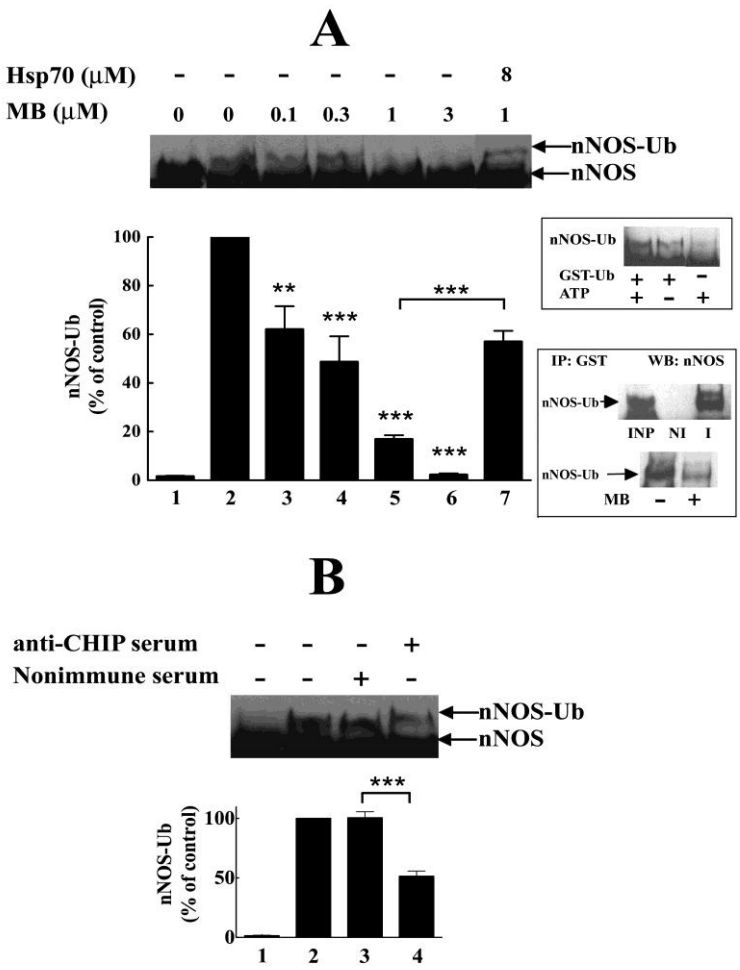

Figure 3.4 nNOS ubiquitination by the DE52-retained fraction of reticulocyte lysate requires Hsp70 and CHIP.

(A) Methylene blue inhibits nNOS ubiquitination. Purified nNOS was incubated 1 h at 37º C with the DE52-retained fraction of reticulocyte lysate, ATP, GST-ubiquitin and the indicated concentrations of methylene blue. In addition 8 μM purified Hsp70 was added to a sample of the DE52-retained fraction containing 1 μM methylene blue. Samples were western blotted by probing with anti-nNOS. Lane 1, incubation time 0; lanes 2–7, incubation time 1 h. For bar graph, the relative amount of monoubiquitinated nNOS (nNOS-Ub) in replicate experiments was determined by scanning and expressed as % of the one hour control without methylene blue. The values are the mean ± S.E. (*n*=3). Asterisks over the columns denote significantly different from control and asterisks over the line denote that condition 7 is significantly different from condition 5. The top inset shows controls without GST-Ub and without added ATP. (Note: the stock, DE52-retained fraction contains 0.5 mM ATP.) The bottom inset (top row) shows an aliquot of input (*INP*) ubiquitinated nNOS of which 50 μl aliquots were immunoadsorbed with nonimmune (*NI*) or α-GST (*I*) IgG and immunoblotted with α-nNOS. The bottom row shows the effect of 3 μM methylene blue on samples immunoadsorbed with α-GST and immunoblotted with α-nNOS. **(B)** CHIP is the major E3 ligase for nNOS ubiquitination. Purified nNOS was incubated with the DE52-retained fraction of reticulocyte lysate as above but in the presence of 1% nonimmune serum or 1% anti-CHIP serum. Lane 1, incubation time 0; lanes 2–4, incubation time 1 h. Experiments performed by Yoshinari Morishima.

Although overexpression of CHIP promotes nNOS degradation [149] and CHIP directs nNOS ubiquitination in a purified ubiquitination system [149,150], it is not known if CHIP is the dominant E3 ligase for nNOS ubiquitination by a physiological ubiquitination system. To assess this, purified nNOS was incubated with the DE52-retained fraction of reticulocyte lysate in the presence of anti-CHIP antibody. As shown in **Fig. 3.4B**, nNOS ubiquitination is markedly reduced in the presence of anti-CHIP serum (lane 4) compared to nonimmune serum (lane 3). Taken together, the data of **Fig. 3.4** suggest that nNOS ubiquitination by this model physiological ubiquitinating system is both Hsp70-dependent and CHIP-dependent, with the ubiquitinating activity being inhibited by methylene blue.

Effect of Methylene Blue on polyQ AR Degradation in Cells.

Because transient overexpression of Hsp70, Hsp40 or CHIP reduces levels of polyQ AR in models of SBMA [76,78,135], it seems clear that the mutant AR can undergo Hsp70/CHIP-dependent proteasomal degradation. However, it is not known whether this is the major pathway or a minor pathway of polyQ AR degradation in the absence of overexpression of major proteins of the degradation pathway. To determine if Hsp70 normally plays a role in polyQ AR degradation, HeLa cells expressing AR112Q were treated first with the AR agonist R1881 to activate the receptor, and then with 10 μM methylene blue to inhibit Hsp70 dependent degradation. As shown in the immunoblot of total cellular AR112Q in **Fig. 3.5A**, methylene blue promotes accumulation of AR112Q both in the absence (lane 3) and presence (lane 4) of R1881. The accumulation of AR is particularly striking in the sample treated with both R1881 and methylene blue where there is also the accumulation of high molecular weight AR112Q oligomers seen with

ligand-dependent aggregation. The quantitation of the methylene blue effect on the full-length AR112Q is shown in **Fig. 3.5B**. The fact that the proteasome inhibitor MG132 produces similar AR112Q accumulation (**Fig. 3.5C**) supports the model that methylene blue is inhibiting Hsp70-dependent degradation by the ubiquitin proteasome pathway.

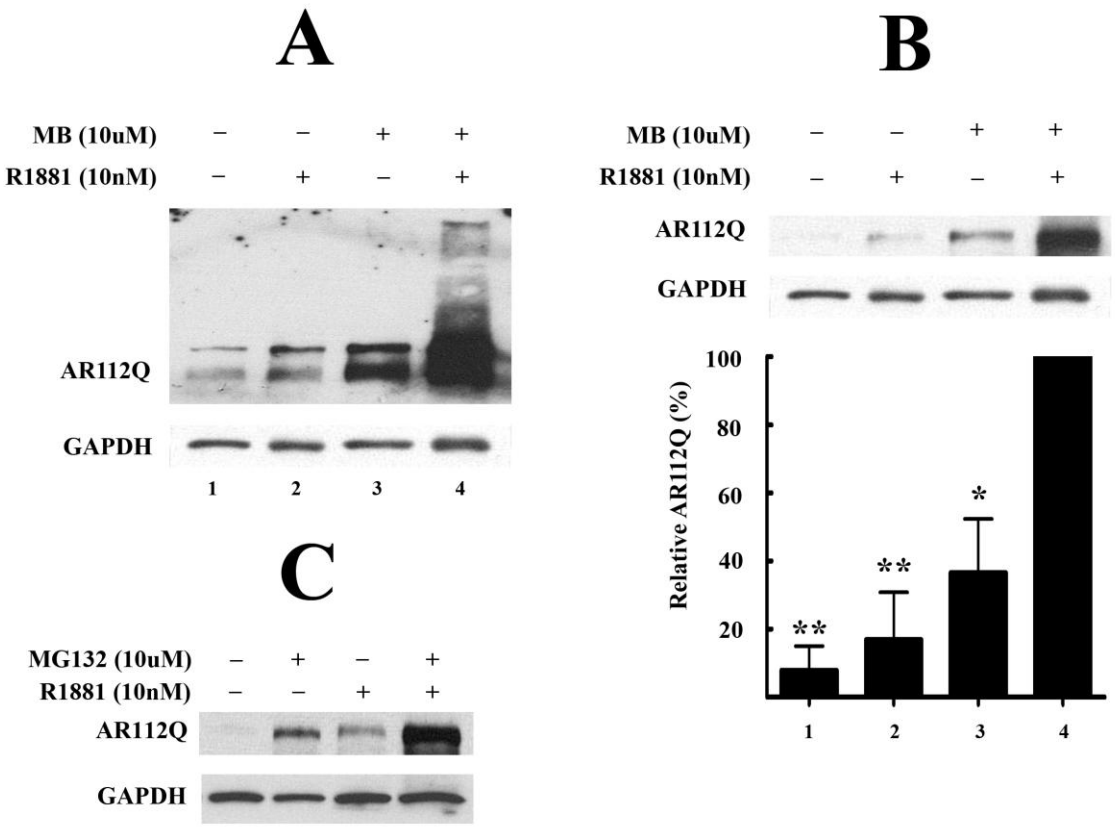

Figure 3.5 Methylene blue inhibits AR112Q degradation in HeLa cells.

(A) HeLa cells expressing AR112Q were incubated at 4 ºC, and treated sequentially with R1881for 30 min and then with 10 µM methylene blue for 30 min. Cells were then incubated at 37 ºC for 8 hr. Protein lysates were collected and analyzed by western blot for AR expression. GAPDH controls for equal loading. **(B)** Shown is a short exposure of the western blot in panel A (top), and quantification of the AR signal (bottom) relative to the amount in cells treated with R1881 plus methylene blue. Data are mean ± SEM. **(C)** Same conditions as above except that 10 µM MG132 was substituted for methylene blue.

While methylene blue inhibited degradation of the full-length androgen receptor, it had opposite effects on amino-terminal fragments of the receptor containing a

glutamine tract flanked by approximately 50 amino acids. These truncated fragments lack the receptor's ligand binding domain and therefore are not clients of the Hsp90/Hsp70-based chaperone machinery. As shown in **Fig. 3.6A**, expression of both trAR16Q and trAR112Q were markedly decreased by methylene blue. This effect was dose dependent (**Fig. 3.6B**) and abrogated glutamine-length dependent cytotoxicity (**Fig. 3.6D**). As similar fragments of mutant huntingtin are preferentially degraded by macroautophagy, we sought to determine whether the protective effect of methylene blue was associated with the induction of this alternative protein degradation pathway. We found that methylene blue increased levels of LC3-II, a marker of autophagosomes (**Fig. 3.6A**), and that the dose-dependence of this induction coincided with diminished trAR112Q levels (**Fig. 3.6B**). We observed a similar induction of LC3-II in cells treated with either methylene blue or MG132 (**Fig. 3.7A**), indicating that inhibition of Hsp70-dependent ubiquitination is as potent an inducer of macroautophagy as blockade of the proteasome. The notion that methylene blue increased autophagic flux is supported by the super-induction of LC3-II in cells treated with both methylene blue and the lysosomal protease inhibitors E64d and pepstatin A (**Fig. 3.7B**) and by the observation that p62 did not accumulate in methylene blue treated cells (**Fig. 3.6A**). Methylene blue also increases LC3-II in cells expressing full-length AR112Q (**Fig. 3.6C**). However the full-length AR is not efficiently degraded by autophagy since ligand-dependent nuclear translocation moves the receptor to a compartment devoid of this degradation pathway. We conclude that inhibition of Hsp70 by methylene blue leads to the compensatory induction of macroautophagy, a pathway that preferentially degrades truncated androgen receptor fragments and thereby diminishes toxicity.

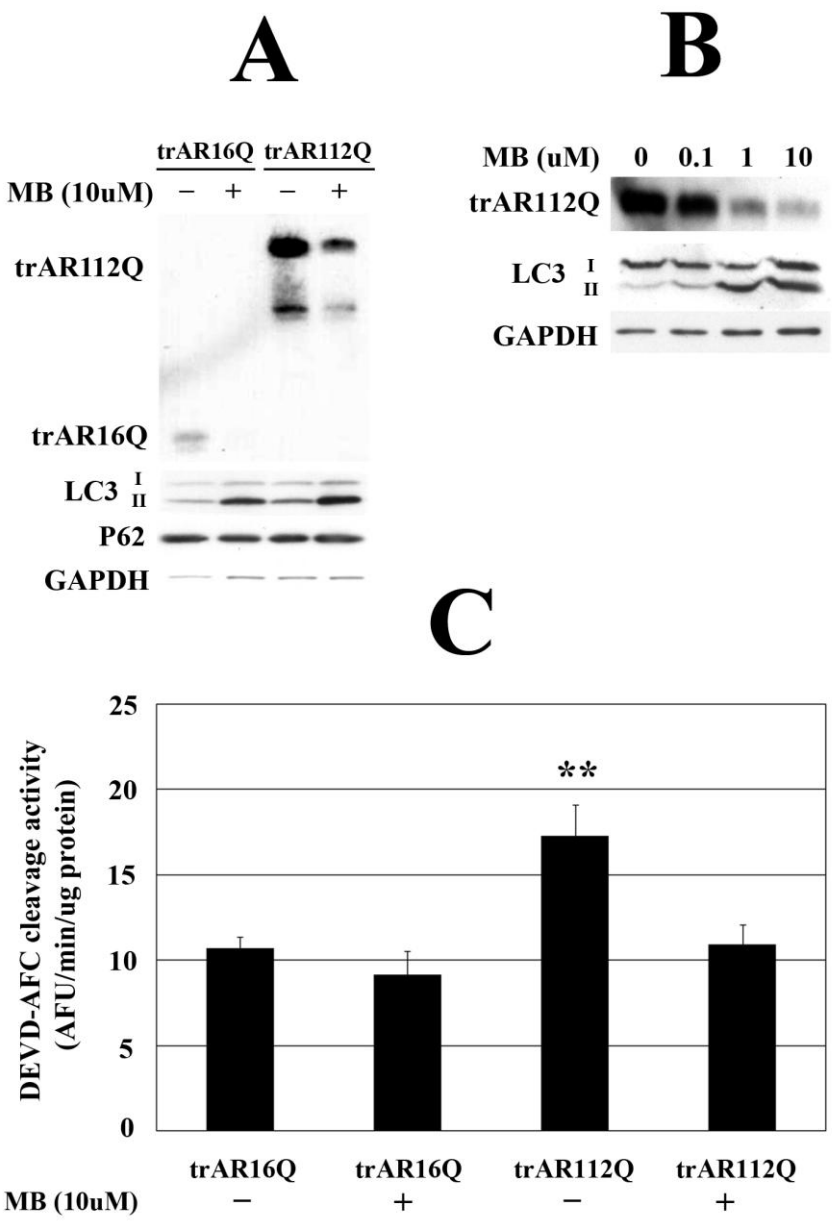

Figure 3.6 Methylene blue enhances degradation of amino-terminal AR fragments and activates autophagy.

HeLa cells expressing trAR16Q or trAR112Q were treated with indicated concentrations of methylene blue or vehicle control for 24 hr. **(A)** Protein lysates were collected and analyzed by western blot for expression of AR, LC3 and p62. GAPDH controls for loading. **(B)** Dose-dependent effects of methylene blue on trAR112Q and LC3 expression were determined by western blot. **(C)** Effect of methylene blue on LC3-II levels in cells expressing full-length AR112Q. **(D)** Caspase activity was determined by measuring cleavage of the fluorescent substrate DEVD-AFC. Data are reported as mean ± SEM. ** Different from all other samples at $p<0.01$.

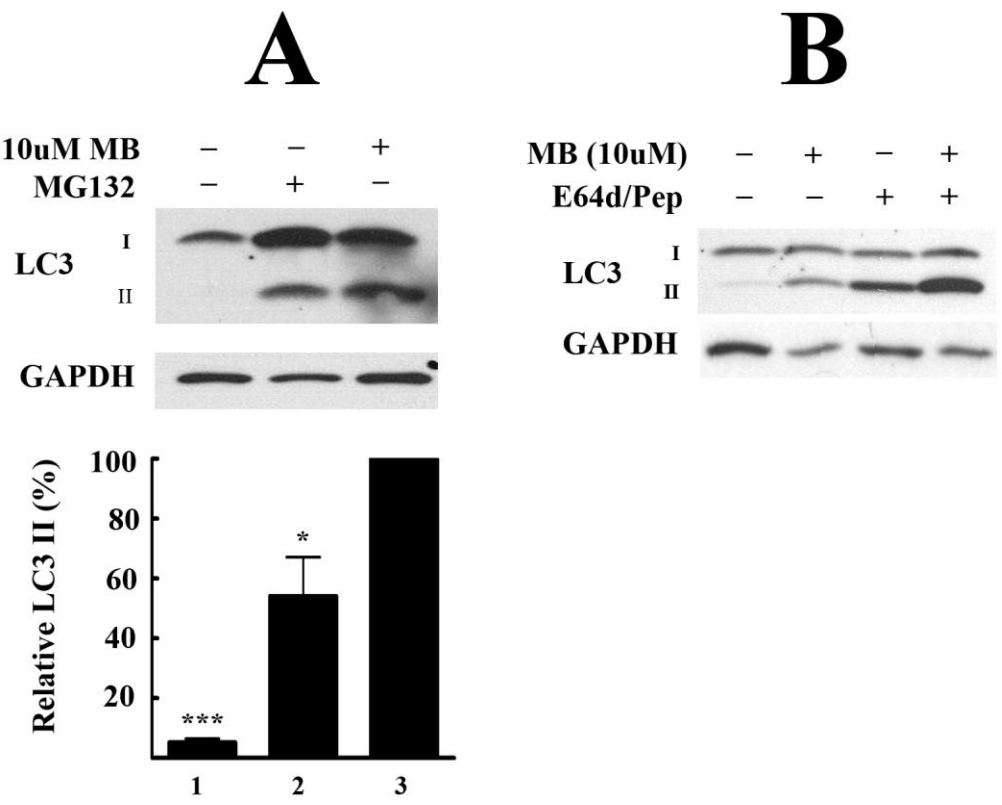

Figure 3.7 Autophagic flux is increased by methylene blue.

(A) HeLa cells were treated with 10 μM methylene blue or MG132 for 24 hr. Protein lysates were collected and analyzed by western blot for expression of LC3 and GAPDH (top). Quantification of LC3-II/GAPDH signal relative to the amount in cells treated with methylene blue (bottom). Data are mean ± SEM. Different from control at (*) $p<0.05$ or (***) $p<0.001$. **(B)** HeLa cells were treated as indicated with 10 μM methylene blue, 10 μg/ml E64d plus pepstatin A, or in combination. LC3 and GAPDH levels were determined by western blot.

Finally, to confirm that cellular effects of methylene blue were mediated by the inhibition of Hsp70, we over-expressed Hsp70 along with full-length AR112Q. Over-expressed Hsp70 inhibited the accumulation of high molecular weight AR112Q oligomers and the induction of LC3-II that occurred following methylene blue treatment (**Fig. 3.8**). These data indicate that methylene blue acts through Hsp70 in cells to target these protein quality control pathways.

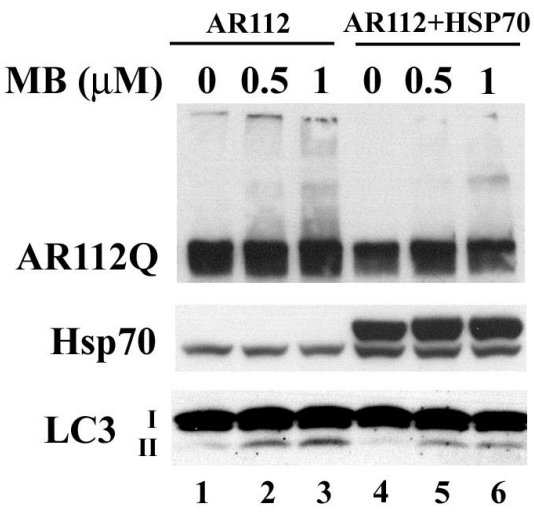

Figure 3.8 Over-expression of Hsp70 diminishes the effects of methylene blue on levels of AR112Q and LC3-II.

Hela cells expressing AR112Q alone (lanes 1-3) or with His-tagged Hsp70 (lanes 4-6) were incubated at 4ºC, and treated sequentially with R1881 for 30 min and then with 0.5 or 1 μM methylene blue for 30 min. Cells were then incubated at 37º C for 8 hr. Protein lysates were collected and analyzed by western blot for AR, Hsp70 and LC3. His-tagged Hsp70 migrates slightly more slowly than the endogenous protein. Endogenous Hsp70 and LC3-I levels serve as loading controls.

Discussion

Several laboratories have been interested in developing small molecule inhibitors of Hsp70 for potential use in the treatment of cancers as well as neurodegenerative diseases characterized by the accumulation of aberrant proteins [83,151-155]. Methylene blue was identified in a screen for compounds that inhibit Hsp70 ATPase activity [84]. Unlike geldanamycin, which binds in the unique nucleotide binding pocket of Hsp90 and produces effects that are quite specific for inhibition of Hsp90 family proteins in eukaryotes [67], methylene blue has multiple cellular and molecular targets, including multiple neurotransmitter systems, ion channels and enzymes (reviewed in [156]). Although modulation of cGMP signaling is often considered its most significant effect, the redox properties of methylene blue are utilized in the treatment of methemoglobinemias and

ifosfamide-induced encephalopathy, and probably account for its use as an antimicrobial agent [156]. Given its multiple molecular targets, methylene blue would seem *a priori* to be an imprecise research tool for probing Hsp70-dependent effects. Yet, we indicate here that this readily available compound can be used in both subcellular and cellular systems for this purpose.

Using an established subcellular system where both Hsp70 and Hsp90 are required components, we show that the generation of steroid binding activity by the GR is inhibited by methylene blue. The effect occurs without inhibition of the binding of either Hsp70 or Hsp90 to the receptor (**Fig. 3.1**). Using the purified five-protein•Hsp90 heterocomplex assembly system, we show that methylene blue inhibition of the activation of steroid binding activity depends upon the concentration of Hsp70 (**Fig. 3.2**). Although steroid binding activity is inhibited in the presence or absence of Hop, there is no depletion of GR-bound Hsp90 under either condition (**Fig. 3.3**). This suggests that the Hsp70 priming of the receptor, which is required for Hsp90-dependent opening of the steroid binding cleft, is inhibited by methylene blue. This priming step requires the ATPase activity of Hsp70 [157], and the ATPase activity is inhibited by methylene blue [84]. Taken together, the GR experiments suggest that methylene blue inhibits an established physiological action of Hsp70 in a cell-free system.

Overexpression of CHIP has been shown to promote proteasomal degradation of a wide variety of normal and aberrant proteins. Although overexpression of CHIP promotes the proteasomal degradation of nNOS [149], there is clear redundancy in E3 ligase action on nNOS [76], and overexpression of one E3 ligase could favor a normally minor pathway of ubiquitination. Thus, it was not previously established that Hsp70-dependent CHIP

activity is the principal physiologic pathway for nNOS ubiquitination. Methylene blue causes virtually complete inhibition of nNOS ubiquitination by the DE52-retained fraction of reticulocyte lysate (**Fig. 3.4A**). This finding suggests that all of the nNOS ubiquitination by the reticulocyte system may be Hsp70-dependent. Similarly, inhibition of ubiquitination by anti-CHIP antibody (**Fig. 3.4B**) suggests that CHIP is a major E3 ligase for nNOS in reticulocytes. Even though methylene blue affects a variety of biochemical process, including a well established inhibition of the NOS enzymes [158,159], these data demonstrate that it can be used as a research tool to identify Hsp70-mediated processes in cell-free systems.

Using this tool, we explore the role of Hsp70 in controlling the proteostasis of the expanded glutamine androgen receptor in a cellular system. The Hsp90/Hsp70-based chaperone machinery binds to the C-terminal domain of the receptor, and like its action on the GR, regulates opening of the steroid-binding cleft to permit ligand binding [67,128]. In this system, Hsp90 functions to prevent androgen receptor unfolding. The extent to which this activity regulates stability of the expanded glutamine androgen receptor was previously demonstrated in *Hsf1*$^{-/-}$ cells that cannot mount a stress response [69]. Treatment of these cells with geldanamycin or radicicol promotes androgen receptor degradation, demonstrating that Hsp90 normally functions to stabilize the receptor. Our data support a model in which ligand-dependent activation of the polyglutamine androgen receptor leads to Hsp70-dependent degradation through the ubiquitin proteasome pathway. Ubiquitination of the androgen receptor may be mediated by CHIP and other Hsp70-dependent E3 ligases that function redundantly [76]. Here we show that methylene blue

prevents degradation of the expanded glutamine androgen receptor and promotes the accumulation of aggregated species in an Hsp70-dependent manner.

The contrasting effects of methylene blue on degradation of trAR112Q are striking. We show that methylene blue promotes degradation of amino-terminal fragments of the receptor, thereby ameliorating glutamine-length dependent toxicity. These androgen receptor fragments include the glutamine tract flanked by approximately 50 amino acids [25] and therefore lack the ligand-binding domain. In the absence of this domain, these proteins are not Hsp90 clients whose stability is regulated by the Hsp90/Hsp70-based chaperone machinery. Truncated fragments of the huntingtin protein are primarily degraded by macroautophagy [122,160], and it is likely that these androgen receptor fragments are handled similarly. We show that methylene blue promotes induction and flux through the autophagic pathway. This homeostatic response likely reflects impairment of Hsp70-dependent degradation through the ubiquitin proteasome pathway. Others have observed similar induction of macroautophagy with genetic mutants that block degradation by the proteasome [121]. These results suggest that degradation of trAR112Q is facilitated by methylene blue due to the compensatory activation of the pathway through which it is normally degraded.

Our findings demonstrate the effectiveness of methylene blue as a chemical tool to study Hsp70-dependent functions in well-established systems. Few other small molecule inhibitors of Hsp70 are available, and their potential use as chemical probes to define Hsp70-mediated effects in models of neurodegenerative diseases and cancer offers great promise. Small molecule inhibitors could be used to define the role of Hsp70 in regulating the function, trafficking and turnover of proteins that are clients of the

Hsp90/Hsp70-based chaperone machinery, and may be used to probe the role of Hsp70 in protein quality control decisions. For example, 2-phenylethynesfulonamide (PES), a recently described inhibitor of Hsp70, is reported to decrease the CHIP-Hsp70 association and alter autophagy, though in this case, autophagic flux may be impaired [83]. In contrast to PES, methylene blue treatment of cells did not decrease the amount of CHIP co-immunoadsorbed with Hsp70 (data not shown), suggesting that the two compounds inhibit Hsp70 by quite different mechanisms. Future studies will help define the experimental and therapeutic utility of this emerging class of small molecules.

Materials and Methods

Materials

HeLa cells were purchased from the American Type Culture Collection. Phenol red-free Dulbecco's modified Eagle's medium was from Invitrogen (Carlsbad, CA), and charcoal-stripped calf serum was from Thermo Scientific Hyclone Products (Thermo Fisher Scientific, Waltham, MA). Untreated rabbit reticulocyte lysate was purchased from Green Hectares (Oregon, WI). [1,2,4,6,7-^{3}H]Dexamethasone (85 Ci/mmol) was from GE Healthcare (Amersham Place, UK), Fugene 6 was from Roche (Indianapolis, IN), and MG132, E64d, pepstatin A, anti-GST IgG and methylene blue (M9140) were from Sigma (St. Louis, MO). ^{125}I-conjugated goat-anti-mouse IgG was obtained from Perkin Elmer Life Sciences (Boston, MA). HRP-tagged goat anti-rabbit IgG was from Millipore (Temecula, CA). The N27F3-4 anti-72/73-kDa Hsp70 monoclonal IgG (anti-Hsp70) and the AC88 monoclonal against Hsp90 were from StressGen Biotechnologies

(Ann Arbor, MI). Affinity-purified IgG against nNOS was from BD Transduction Laboratories (Lexington, KY). The FiGR monoclonal IgG used to immunoadsorb the mouse GR was provided by Dr. Jack Bodwell (Dartmouth Medical School, Lebanon, NH). The BuGR2 monoclonal IgG used to immunoblot the mouse GR and rabbit anti-CHIP antibody were from Affinity Bioreagents (Golden, CO). The AR antibody (N-20) was from Santa Cruz Biotechnology (Santa Cruz, CA), GAPDH antibody from Abcam (Cambridge, MA), LC3 antibody from Novus Biologicals (Littleton, CO), and p62 (C-terminal) antibody from American Research Products (Belmont, MA). GST-tagged ubiquitin was from Boston Biochem (Cambridge, MA). The cDNA for rat nNOS was provided by Dr. Solomon Snyder (The Johns Hopkins Medical School, Baltimore, MD). Plasmid encoding AR112Q was provided by Dr. Kenneth Fishbeck (N.I.H.), and plasmids encoding amino-terminal truncated AR16Q and AR112Q were from Dr. Diane Merry (Thomas Jefferson University, Philadelphia, PA).

Expression and purification of nNOS, Hsp90, Hsp70, Hsp40, HOP and p23

Rat nNOS was expressed in Sf9 insect cells using a recombinant baculovirus and purified by 2′,5′-ADP Sepharose and gel-filtration chromatography as described previously [161]. Heme was added as an albumin conjugate during the expression to convert all of the nNOS to the holo-nNOS dimer [161]. Hsp90 and Hsp70 were purified from rabbit reticulocyte lysate by sequential chromatography on DE52, hydroxylapatite, and ATP-agarose as described previously [162]. YDJ-1, the yeast ortholog of Hsp40, was expressed in bacteria and purified by sequential chromatography on DE52 and hydroxylapatite as described previously [163]. Recombinant human Hop (Hsp organizing protein) and p23 were purified as described by Kanelakis and Pratt [164]. For over-expression of Hsp70, the

full-length human Hsp70 cDNA was amplified by PCR from clone pET23hsp70, kindly provided by Dr. David Toft (Mayo Clinic, Rochester, MN) using a 5' primer encoding a polyhistidine tag followed by an HA epitope. The 1.9-kb PCR fragment was digested with *EcoRI* and *XhoI* and cloned into pcDNA4/HisMax-C vector (Invitrogen). The entire coding region of Hsp70 was verified by sequencing.

GR•Hsp90 heterocomplex reconstitution

Mouse GR was expressed in Sf9 cells and cytosol was prepared as described previously [145]. Receptors were immunoadsorbed from aliquots of 50 µl (for measuring steroid binding) or 100 µl (for Western blotting) of Sf9 cell cytosol by rotation for 2 h at 4 ºC with 14 µl of protein A-Sepharose precoupled to 8 µl of FiGR ascites suspended in 300 µl TEG buffer (10 mM TES, pH 7.6, 50 mM NaCl, 4 mM EDTA, 10% glycerol). Immunoadsorbed GR was stripped of endogenously associated Hsp90 by incubating the immunopellet for an additional 2 h at 4 ºC with 350 µl of 0.5 M NaCl in TEG buffer. The pellets were then washed once with 1 ml of TEG buffer followed by a second wash with 1 ml of Hepes buffer (10 mM Hepes, pH 7.4). For GR•Hsp90 heterocomplex reconstitution by reticulocyte lysate, immunopellets containing GR stripped of chaperones were incubated with 50 µl of lysate and 5 µl of an ATP-regenerating system (50 mM ATP, 250 mM creatine phosphate, 20 mM magnesium acetate, and 100 units/ml creatine phosphokinase). For heterocomplex reconstitution with purified proteins, immunopellets containing stripped GR were incubated with 15 µg of purified Hsp90, the indicated µg of purified Hsp70, 0.6 µg of purified HOP, 6 µg of purified p23, 0.125 µg of purified YDJ-1 adjusted to 55 µl with HKD buffer (10 mM Hepes, pH 7.4, 100 mM KCl, 5 mM dithiothreitol) containing 20 mM sodium molybdate and 5 µl of the ATP-

regenerating system. The assay mixtures were incubated for 20 min at 30 ºC with suspension of the pellets by shaking the tubes every 2 min. At the end of the incubation, the pellets were washed twice with 1 ml of ice-cold TEGM buffer (TEG with 20 mM sodium molybdate) and assayed for steroid binding capacity and for GR-associated Hsp90.

Assay of steroid binding capacity

Washed immune pellets to be assayed for steroid binding were incubated overnight at 4 ºC in 50 µl HEM buffer (10 mM Hepes, pH 7.4, 1 mM EDTA, 20 mM molybdate) plus 50 nM [^{3}H]dexamethasone. Samples were then washed three times with 1 ml of TEGM buffer and counted by liquid scintillation spectrometry. Steroid binding is expressed as counts/min of [^{3}H]dexamethasone bound/FiGR immunopellet prepared from 50 µl of Sf9 cell cytosol.

Ubiquitination of nNOS by DE52-retained fraction of reticulocyte lysates

The DE52-retained fraction of rabbit reticulocyte lysate was prepared as described by Hershko et al. [52]. Purified nNOS (0.6 µg) was incubated for 1 h at 37 ºC with 4.5 µl of DE52-retained fraction of rabbit reticulocyte lysate (final concentration 7 mg protein/ml), 0.3 mg/ml bovine serum albumin, 8.3 µM GST-tagged ubiquitin, 1 mM dithiothreitol, 2 µl of the ATP-regenerating system, 1 µl of Complete Mini protease inhibitor cocktail, 0.6 mM N-Acetyl-Leu-Leu-Nle-CHO, and 0.8 µM ubiquitin aldehyde (deubiquitination inhibitor), adjusted to a final volume of 20 µl with 50 mM Tris, pH 7.5. Methylene blue was added to yield the indicated final concentration, with all samples containing a final concentration of 0.1% ethanol vehicle. Incubations were terminated by boiling with an equal volume of SDS-sample buffer containing 8 M urea and 2 M thiourea.

Gel electrophoresis and Western blotting

GR immune pellets were resolved on 12% SDS-polyacrylamide gels and transferred to Immobilon-P membranes. The membranes were probed with 0.25 µg/ml BuGR2 for GR, 1 µg/ml AC88 for Hsp90, or 1 µg/ml anti-Hsp70. The immunoblots were then incubated a second time with ^{125}I-conjugated counterantibody to visualize the immunoreactive bands. For experiments with nNOS, aliquots (25 µl) from the ubiquitination reactions boiled in SDS-sample buffer were resolved on 5% SDS-polyacrylamide gels, transferred to nitrocellulose membranes, and probed with anti-nNOS (1:8000), followed by horseradish peroxidase-conjugated counterantibody. Immunoreactive bands were visualized with the use of enhanced chemiluminescence reagent (Super Signal, Pierce) and X-Omat film (Eastman Kodak Co.). The monoubiquitinated nNOS bands were scanned and the relative densities were determined with ImageJ software (http://rsb.info.nih.gov/ij/). Relative densities for 3 experiments are presented in bar graphs as percent of control ± S.E. Statistical probability is expressed as $*p<0.05$, $**p<0.01$, $***p<0.0001$.

For analysis of AR protein expression, HeLa cells were grown in 6-well dishes in phenol red-free DMEM supplemented with 10% charcoal/dextran-stripped fetal calf serum. Cells were transfected with Fugene 6 transfection reagent using 3 µl Fugene 6 and 1µg DNA. Twenty four hours post-transfection, cells were pooled and replated, then treated as indicated starting 48 hours post-transfection. Following incubation, cells were washed with PBS, harvested and lysed by sonication in RIPA buffer containing phosphatase and proteinase inhibitors. Protein samples were electrophoresed through 4 – 20% SDS-polyacrylamide gradient gels and transferred to Immunobilon-P membranes

using a semi-dry transfer apparatus. Immunoreactive proteins were detected by chemiluminescence, and relative densities of bands were quantified as described above.

Assay of caspase activity

Caspase activity was determined by measuring cleavage of the fluorescent substrate DEVD-AFC using the ApoTarget caspase-3/CPP 32 fluorometric protease assay kit (Invitrogen) 48 hr post-transfection. Fluorescence intensity was measured using a Fluoroskan Ascent FL fluorometer (Thermo Electron Corp.).

Abbreviations used

CHIP, carboxy terminus of Hsc70-interacting protein; GR, glucocorticoid receptor; HSF1, heat shock factor 1; HD, Huntington disease; nNOS, neuronal nitric oxide synthase; polyQ AR, polyglutamine androgen receptor; PES, phenylethynesfulonamide; SBMA, spinal and bulbar muscular atrophy; SCA, spinocerebellar ataxia; TPR, tetratricopeptide repeat; trAR112Q, amino-terminal fragment of the androgen receptor with 12 glutamines.

Acknowledgements

We thank Drs. Solomon Snyder, Kenneth Fishbeck, Diane Merry, David Toft and Jack Bodwell for providing plasmids and antibodies used in this work. This work was supported by a McKnight Foundation Neuroscience of Brain Disorders Award (to A.P.L) and by National Institutes of Health grants GM77430 (to Y.O.) and NS055746 (to A.P.L).

This chapter was originally published as: Wang, A.M., Morishima, Y., Clapp, K.M., Peng, H.-M., Pratt, W.B., Gestwicki, J.E., Osawa, Y., Lieberman, A.P. **Inhibition of**

Hsp70 by Methylene Blue Affects Signaling Protein Function and Ubiquitination and Modulates Polyglutamine Protein Degradation. J Biol Chem. 2010 May 21; 285(21): 15714–15723 with AW and YM as co first authors. YM contributed figures 1-4, and AW contributed figures 5-8.

Chapter 4

Allosteric activators of Hsp70 promote polyglutamine androgen receptor clearance and rescue toxicity in a *Drosophila* model of spinal and bulbar muscular atrophy

Abstract

Pathways regulating degradation of unfolded proteins are prime therapeutic targets for protein aggregation neurodegenerative diseases, including those caused by CAG/polyglutamine tract expansions. We sought novel strategies to target the Hsp90/Hsp70-based chaperone machinery and increase degradation of the polyglutamine androgen receptor (polyQ AR) to achieve therapeutic benefits in models of spinal and bulbar muscular atrophy (SBMA). We demonstrate that over-expression of Hip, a co-chaperone that enhances Hsp70 substrate binding affinity, promotes client protein ubiquitination and polyQ AR clearance. Furthermore, we identify a small molecule allosteric activator of Hsp70 that acts similarly to Hip by promoting Hsp70 binding to unfolded substrates, enhancing client protein ubiquitination and stimulating polyQ AR clearance. Both genetic and pharmacologic approaches of targeting Hsp70 alleviate toxicity in a *Drosophila* model of SBMA. Our findings highlight the therapeutic potential

of Hsp70 allosteric activators, and provide new insights into the role of the chaperone machinery in protein quality control.

Introduction

The CAG/polyglutamine disorders are a family of nine neurodegenerative diseases caused by similar microsatellite expansions in coding regions of unrelated genes [1]. These disorders are currently untreatable, with symptom onset typically in midlife and death 15 – 20 years later. Among these diseases is spinal and bulbar muscular atrophy (SBMA), a progressive neuromuscular disorder that affects only men and is characterized by proximal limb and bulbar muscle weakness, atrophy and fasciculations [7]. The clinical features of SBMA correlate with a loss of lower motor neurons in the brainstem and spinal cord, and with marked myopathic and neurogenic changes in skeletal muscle [7,8]. The causative mutation in SBMA is a CAG repeat expansion in the first exon of the *Androgen Receptor (AR)* gene [13]. The expanded glutamine tract promotes hormone-dependent AR unfolding and oligomerization, steps that are critical to toxicity. In SBMA, as in other CAG/polyglutamine disorders, the mutant protein disrupts multiple downstream pathways, and toxicity likely results from the cumulative effects of altering a diverse array of cellular processes including transcription, RNA splicing, axonal transport and mitochondrial function [17-19,26,33,36,40,41,44,49,165]. The existence of divergent mechanisms of toxicity indicates that potential treatments targeting a single downstream pathway are likely to be unsuccessful.

These observations prompted us to focus instead on understanding the proximal mechanisms that regulate degradation of the polyglutamine AR (polyQ AR), with the goal of harnessing these pathways to diminish levels of the toxic protein and ameliorate

the disease phenotype. The cellular machinery that plays the dominant role in regulating proteostasis of the AR is the Hsp90/Hsp70-based chaperone machinery, in which Hsp90, Hsp70, and co-chaperones function together as a multiprotein complex [67,166]. In contrast to the classic model of chaperones interacting with unfolded proteins to facilitate their refolding, the Hsp90/Hsp70-based chaperone machinery instead acts on pre-folded proteins in their native conformations to assist in the opening and stabilization of ligand binding clefts, an action that forms the basis for the role of the chaperone machinery in the triage of damaged proteins for degradation [128,166]. Indeed, access of ligand to the steroid binding clefts of nuclear receptors, including the AR, is dependent upon the Hsp90/Hsp70 chaperone machinery [67,128]. Furthermore, as a client of the chaperone machinery, the polyQ AR is stabilized by its interaction with Hsp90. When Hsp90 is inhibited, the polyQ AR no longer associates with Hsp90 and is rapidly degraded [57,69]. Through this mechanism, Hsp90 inhibitors ameliorate the phenotype of SBMA transgenic mice [57,71]. Although Hsp90 inhibitors concurrently induce a stress response, their beneficial effects are independent of the stress response. AR112Q expressing mouse embryonic fibroblasts deficient in HSF-1, which cannot induce a stress response, still clear the polyQ AR after treatment with Hsp90 inhibitors [69]. The chaperone machinery plays a central role in the triage of unfolded proteins, but the mechanism by which this triage is accomplished is incompletely understood.

Genetic evidence indicates that Hsp70 plays a central role in promoting clearance of the polyQ AR. Over-expression of Hsp70 or its co-chaperone Hsp40, promotes polyQ AR degradation and diminishes toxicity in cellular models of SBMA [80,135]. Similarly, transgenic over-expression of Hsp70 [81] or the Hsp70-dependent E3 ubiquitin ligase CHIP

(C-terminus of Hsc70-interacting protein) [78] rescues the phenotype of SBMA mice. Here, we test an alternative approach to modulating chaperone machinery function by targeting Hsp70 with allosteric activators. Our strategy is based on the observation that over-expression of Hip (Hsp70 interacting protein), a co-chaperone that stabilizes Hsp/Hsc70 in its ADP-dependent conformation exhibiting high substrate affinity [86,167], prevents the accumulation of polyglutamine inclusions in a cellular model [90]. Although it was suggested that Hip acts by promoting the Hsp70 refolding cycle, we demonstrate that Hip facilitates the CHIP-mediated ubiquitination of an Hsp90 client and promotes proteasomal degradation of the polyQ AR. Furthermore, we identify a small molecule allosteric activator of Hsp70 that acts similarly to Hip by promoting Hsp70 binding to unfolding substrates to facilitate their CHIP-mediated ubiquitination. We show that both genetic and pharmacologic approaches of targeting Hsp70 promote polyQ AR clearance and alleviate toxicity in a *Drosophila* model of SBMA. Our findings highlight the therapeutic potential of this novel strategy to allosterically activate Hsp70 in a protein aggregation neurodegenerative disorder, and provide new insights into the role of the chaperone machinery in protein quality control.

Results

Hip increases client protein ubiquitination and degradation.

We reasoned that stabilizing Hsp70 in its high-affinity substrate binding state would increase CHIP-mediated ubiquitination and degradation of Hsp90-client proteins. Our approach was based on the observation that Hip, or Hsp70-interacting-protein, is a co-chaperone that stabilizes Hsp70 in its ADP-dependent confirmation [86]. As ADP-bound Hsp70 recognizes denatured or damaged substrates with high affinity [167], we

hypothesized that Hip over-expression would facilitate Hsp70-mediated degradation. To test this notion, we first studied a well-characterized Hsp90 client protein, neuronal nitric oxide synthase (nNOS). nNOS ubiquitination is dependent upon Hsp70 [85] and is mediated by CHIP [85,149,168]. Using an established system to study nNOS ubiquitination [147], we found that Hip over-expression yielded a significant, dose-dependent increase in the accumulation of ubiquitinated nNOS species in cells treated with the proteasome inhibitor lactacystin (**Fig. 4.1a**). This observation suggested that a similar strategy could also promote clearance of toxic proteins that are clients of the Hsp90/Hsp70 chaperone machinery. To test this notion, we over-expressed Hip with the polyQ AR. Hip over-expression promoted clearance of soluble and RIPA-insoluble AR112Q that formed after addition of the synthetic androgen ligand R1881 (**Fig. 4.1b**), and diminished the frequency of androgen-dependent intranuclear inclusions in cells stably expressing tetracycline (tet)-regulated AR112Q (**Fig. 4.1d**). As these effects were blocked by inhibition of protein degradation with MG132 (**Fig. 4.1c**), we conclude that Hip over-expression enhanced client protein ubiquitination and degradation.

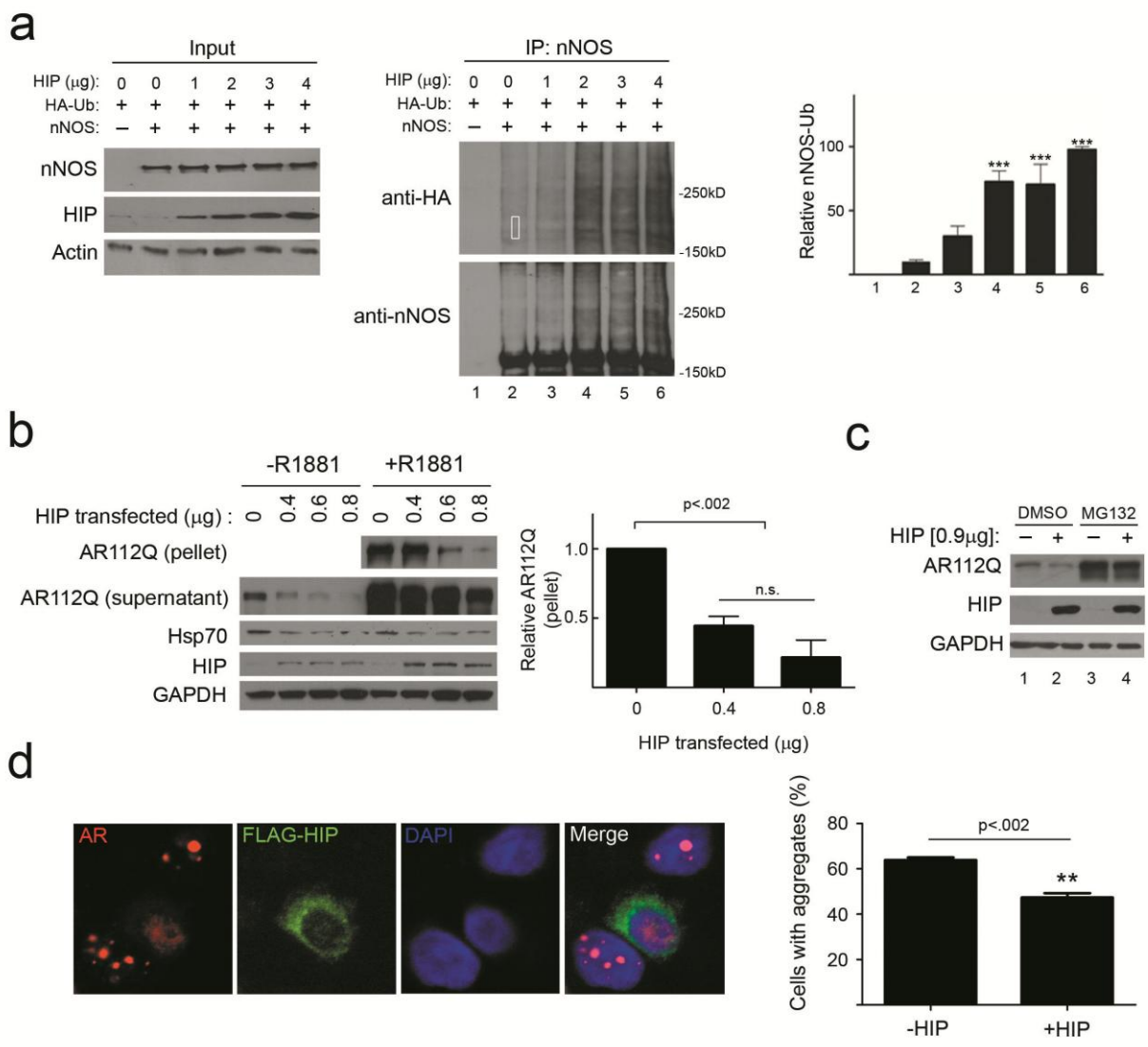

Figure 4.1 Hip increases client protein ubiquitination and promotes AR112Q clearance.

(a) Hip promotes nNOS ubiquitination. HEK293T cells transiently expressing nNOS, HA-ubiquitin (HA-Ub) and increasing amounts of Hip were treated with lactacystin (24hr). nNOS was immunoprecipitated (IP) from cytosolic lysates (input, on left; IP in middle), and western blots were probed as indicated. At right, Ub-nNOS signal (in area indicated by rectangle) from three separate experiments was quantified (mean ± SEM). ****P*<0.001. **(b)** Hip promotes AR112Q clearance. HeLa cells transiently expressing AR112Q and increasing amounts of Hip were treated with R1881 (10 nM) for 24 hr. Lysates were separated into supernatant and 15,000 *g* pellet fractions, then analyzed by western blot (left). At right, pelleted AR from three experiments was quantified. n.s. = not significant. **(c)** Hip promotes AR112Q degradation. HeLa cells were co-transfected with AR112Q and Hip, then treated with R1881 (10 nM) for 24 hrs prior to 8 hr treatment with MG132 (10 μM). **(d)** Hip diminishes AR112Q aggregates. PC12 cells expressing tet-regulated AR112Q were transfected with FLAG-Hip were visualized by confocal microscopy (left). The expression of Hip significantly decreased the frequenct of polyQ AR intranuclear inclusions (right, mean ± SEM).

YM-1 is a small molecule allosteric activator of Hsp70.

These observations prompted us to seek small molecules that increase the affinity of Hsp70 for denatured proteins, with the expectation that they could act like Hip to promote client protein ubiquitination and degradation. To accomplish this, we synthesized a limited set of compounds using MKT-077 as a chemical scaffold (**Fig. 4.2a**), as this compound was reported previously to bind Hsp70 [169]. NMR spectroscopy recently established that MKT-077 binds with low micromolar affinity to the nucleotide-binding domain of ADP- but not ATP-bound Hsp70 [170]. Furthermore, limited trypsin proteolysis confirmed that MKT-077 binding favors the ADP-bound conformation of Hsp70 [170]. Based on these observations, we screened MKT-077 derivatives for their ability to increase the affinity of Hsp70 binding to a denatured target protein. Using an ELISA-like assay, we identified YM-1 (**Fig. 4.2a**) as a potent activator of Hsp70 binding to denatured luciferase (**Fig. 4.2b**). Moreover, we found that biotin-labeled MKT-077, a probe for the YM-1 binding site, competes with Hip for binding to Hsp70 (**Fig. 4.2c**). Based on these data, we propose that YM-1 acts similarly to Hip to bind Hsp70 and favor accumulation of the ADP-bound form, which has tight affinity for its substrates.

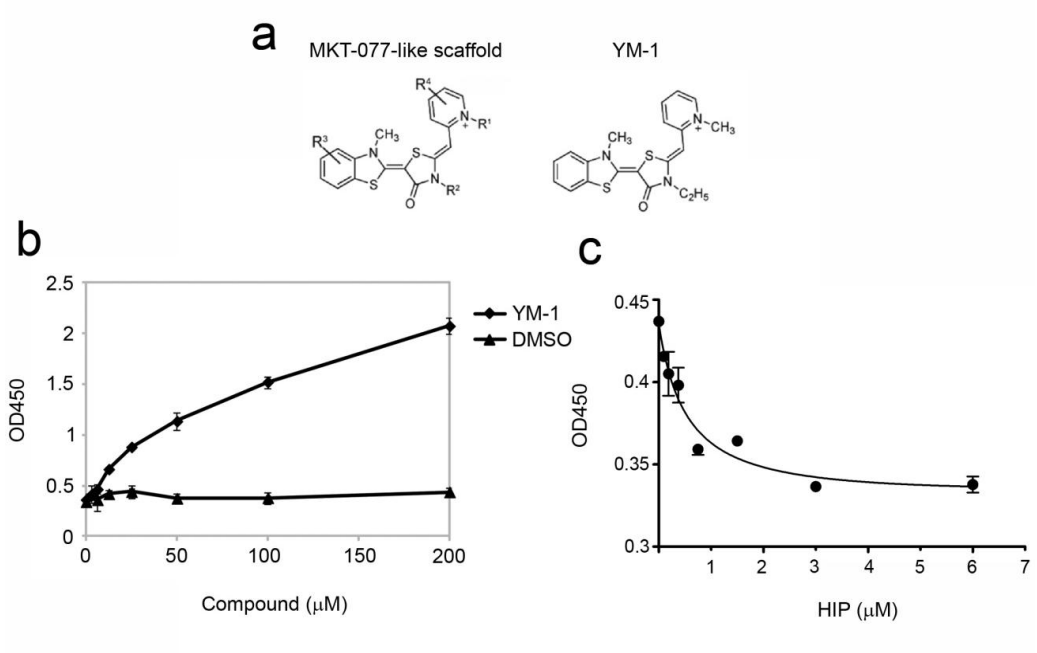

Figure 4.2 YM-1 increases Hsp70 binding to a denatured substrate.

(a) Chemical structures of a generic MKT-077-like scaffold (left) and YM-1 (right). **(b)** YM-1 promotes binding of Hsp70 to denatured luciferase. ELISA plates were coated with denatured luciferase, and binding of Hsp70 was measured using an HRP-coupled Hsp70 antibody. Data are mean ± SEM. **(c)** YM-1 and Hip bind competitively to Hsp70. Binding of biotin-labeled MKT-077 (a probe of the YM-1 binding site) to immobilized Hsp70 is diminished by pre-incubation with increasing amounts of Hip. Data are mean ± SEM. Experiments performed by Yoshi Miyata.

YM-1 increases client protein ubiquitination and degradation.

Given that YM-1 acts upon Hsp70 to increase its affinity for denatured substrates, we next sought to characterize its effects on the Hsp90 client proteins nNOS and AR112Q. To investigate the influence of YM-1 on ubiquitination, we treated cells stably expressing nNOS with increasing concentrations of YM-1 in the presence of lactacystin (**Fig. 4.3a**). Similar to the effects of Hip over-expression, YM-1 treatment led to a dose-dependent accumulation of high molecular weight, ubiquitinated nNOS species. Additionally, YM-1 diminished polyQ AR levels in tet-inducible PC12 cells in a manner similar to that mediated by Hip over-expression. YM-1 significantly decreased the

accumulation of RIPA-insoluble AR112Q (**Fig. 4.3b**) and diminished the occurrence of AR intranuclear inclusions in the presence of ligand (**Fig. 4.3c**). In contrast to this decrease of insoluble and aggregated polyQ AR species, treatment with YM-1 only slightly diminished levels of soluble AR112Q, suggesting that unfolded AR species were most sensitive to its action.

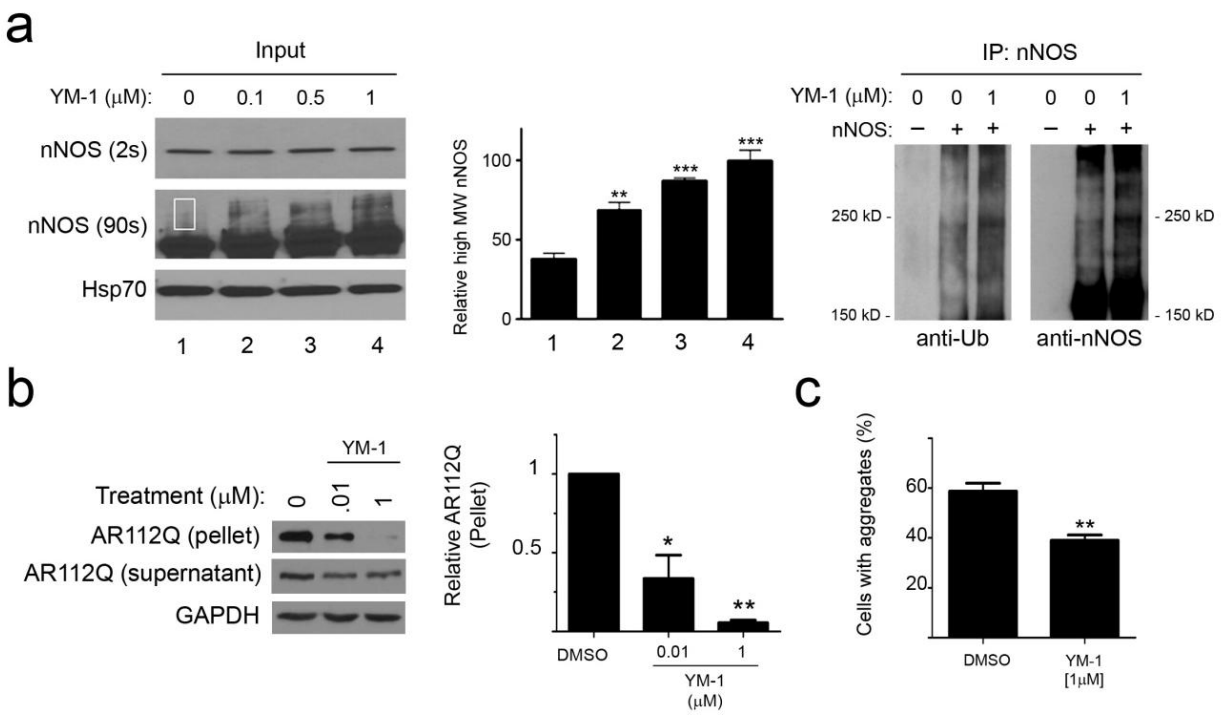

Figure 4.3 YM-1 increases client protein ubiquitination and diminishes AR112Q aggregation.

(a) YM-1 promotes nNOS ubiquitination. HEK293 cells stably expressing nNOS were treated with increasing amounts of YM-1 and lactacystin for 24 hrs. Short exposure of input (on left) shows unmodified nNOS, while longer exposure shows an accumulation of a higher molecular weight (MW) species representing mono-ubiquitinated nNOS [168] (highlighted in rectangle). Quantification of mono-ubiquitinated nNOS rom four separate experiments is shown in the middle, **P<0.01, ***P<0.001. Immunoprecipitation (on right) shows increased nNOS poly-ubiquitination in the presence of YM-1. **(b)** YM-1 decreases insoluble AR112Q. PC12 cells expressing tet-regulated AR112Q were treated with R1881 (10 nM) and YM-1 for 24 hrs. Immunoblot analysis shows soluble and pelleted (15,000 *g*) AR112Q. At right, pelleted AR112Q from three separate experiments was quantified. *P<0.05, **P<0.01. **(c)** PC12 cells were treated as in (**b**), AR was visualized by fluorescence microscopy and cells with nuclear inclusions quantified **P<0.01.

We postulated that YM-1 exerted these effects by increasing polyQ AR degradation. To test this notion, we induced AR112Q expression in tet-regulated PC12 cells in the presence of ligand for 48 hrs to allow for robust expression and ligand-dependent unfolding. Transgene expression was then shut off by washing out doxycycline, and cells were incubated for an additional 72 hrs with or without YM-1

(**Fig. 4.4a**). YM-1 significantly promoted the clearance of AR112Q as reflected by the loss of immunofluorescence staining (**Fig. 4.4b**). Immunoblot analysis revealed that YM-1 promoted the clearance of both RIPA-insoluble AR112Q and high molecular weight oligomers that remained in the soluble fraction after ultracentrifugation (**Fig. 4.4c**). These oligomers formed in a hormone-dependent manner and were detected only in cells expressing the polyQ AR (data not shown). The effects of YM-1 were blocked by inhibition of protein degradation with MG132 (**Fig. 4.4d**), supporting the interpretation that YM-1 enhanced polyQ AR degradation. Unlike previously described small molecule inhibitors of Hsp90, such as geldanamycin, YM-1 exerted these effects without increasing the expression of the stress-responsive molecular chaperones Hsp70, Hsp40 or Hsp25 (**Fig. 4e**). Notably, the activity of YM-1 was abrogated by siRNA knock-down of Hsp70, thus identifying Hsp70 as its critical cellular target (**Fig. 4.4f**).

Allosteric activators of Hsp70 rescue toxicity in a *Drosophila* model of SBMA.

The potency of YM-1 in promoting polyQ AR degradation in cells prompted us to test its efficacy in a *Drosophila* model of SBMA in which the UAS/Gal4 system drives expression of hAR52Q [171]. When hAR52Q was expressed by the eye-specific *GMR* promoter, flies exhibited a dihydrotestosterone-dependent (DHT-dependent) rough eye phenotype characterized by ommatidial degeneration and extranumerary inter-ommatidial bristles, particularly in the posterior aspects of the eye (**Fig. 4.5a, b**). We found that DHT-dependent eye degeneration in this line was relatively modest, and was partially rescued by rearing flies on YM-1 (**Fig. 4.5c**).

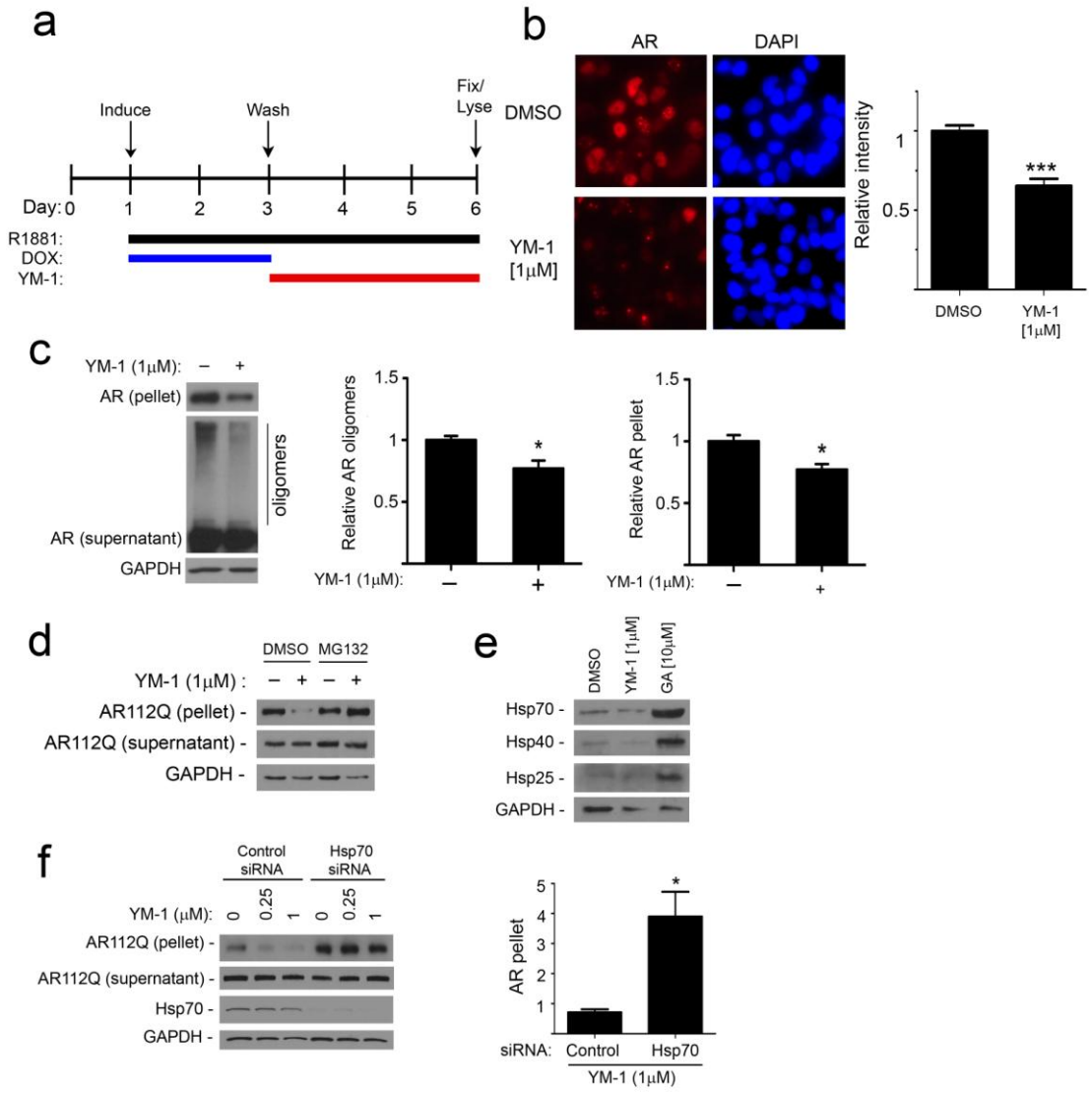

Figure 4.4 YM-1 increases Hsp70-dependent degradation of AR112Q.

(a) Experimental time-line for analysis of AR112Q degradation. PC12 cells were induced to express AR112Q in the presence of R1881 (10 nM) for 48 hr, then washed to remove doxycycline to turn off the transgene. Cells were incubated an additional 72 hrs in the presence or absence of YM-1, then stained for AR (b) or lysed for analysis of oligomeric species (c). **(b)** YM-1 promotes AR112Q clearance. Cells were treated as in (a) and stained for AR. Quantification of signal intensity at (right) shows a significant decrease in the presence of YM-1. ***P<0.001. **(c)** YM-1 promotes clearance of insoluble and oligomeric AR112Q. Lysates were prepared from cells treated as in (a). Immunoblot shows decreased AR112Q monomer in the 15,000 g pellet and diminished high MW oligomers in the soluble fraction after ultracentrifugation. Quantification of signal intensity at right (mean + SEM). *P<0.05. **(d)** YM-1 promotes AR112Q degradation. Immunoblot of AR112Q in supernatant and pellet shows that effects of YM-1 are blocked by 24 hr treatment with MG132 (10 μM). **(e)** YM-1 does not induce a stress response. HeLa cells treated with vehicle, YM-1, or geldanamycin (GA) for 24hr were probed for expression of inducible Hsp70, Hsp40, and Hsp25. **(f)** YM-1 effects are dependent upon Hsp70. PC12 cells expressing tet-regulated AR112Q were transfected with siRNAs targeted at inducible Hsp70 or non-targeted control. Effects of YM-1 on pelleted AR112Q are shown on left and quantified on right. *P<0.05.

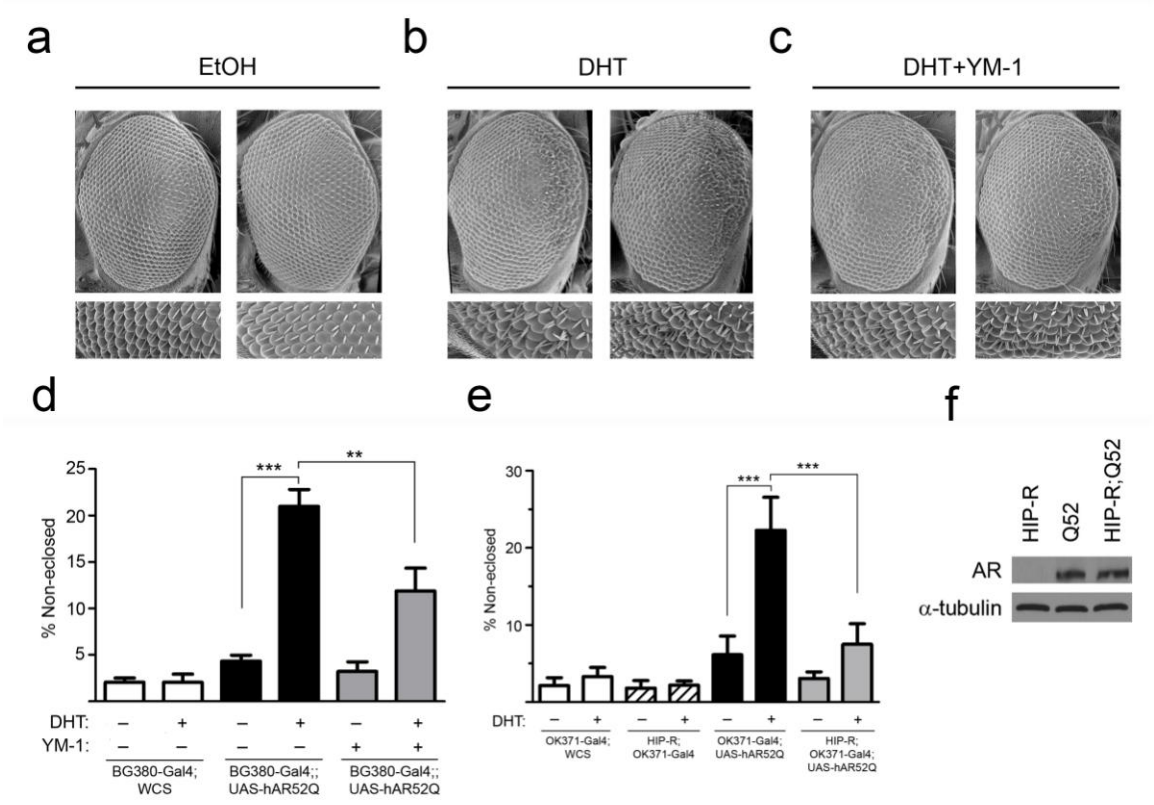

Figure 4.5 Hsp70 allosteric activators rescue toxicity in *Drosophila* expressing AR52Q.

(a - c) Representative scanning electron micrographs of eyes from GMR-Gal4;UAS-hAR52Q flies reared at 29° C. Lower panels show high magnification images from posterior aspects of eyes.**(a)** Normal eyes in flies reared on food supplemented with vehicle control. **(b)** Eye degeneration in flies reared on food containing dihydrotestosterone (1 mM DHT). **(c)** Suppression of degeneration in flies reared on food containing DHT plus YM-1 (1 mM). **(d)** DHT-dependent toxicity is rescued by YM-1. Reported are the percent of pupae that fail to eclose (mean ± SEM) when reared on DHT or vehicle. Flies compared are BG380-Gal4;;WCS (white bars), BG380-Gal4;;UAS-hAR52Q (black bars), and BG380-Gal4;;UAS-hAR52Q reared on YM-1 (gray bars). **P<0.01, ***P<0.001. **(e)** Over-expression of HIP-R suppresses toxicity. Reported are the percent of pupae that fail to eclose (mean ± SEM) when reared on DHT or vehicle. Flies compared are OK371-Gal4;WCS (white bars), HIP-R;OK371-Gal4 (striped bars), OK371-Gal4;UAS-hAR52Q (black bars), and HIP-R;OK371-Gal4;UAS-hAR52Q (gray bars). ***P<0.001. **(f)** Immunoblot analysis of AR52Q expression in adult fly heads under control of the OK371-Gal4 driver. Expression of AR52Q (middle lane) is not diminished when expressed in conjunction with HIP-R (far right lane) in flies reared on food supplemented with vehicle control.

We sought a more readily quantifiable and robust phenotype that was mediated by polyQ AR expression in motor neurons to test the effects of targeting Hsp70. Eclosion is the final stage of *Drosophila* development in which adult flies escape from their pupal

case. When hAR52Q was expressed in motor neurons by the *BG380* or *OK371* promoters, a significant percentage of flies failed to eclose in a DHT-dependent manner (**Fig. 4.5d, e**). In contrast, flies expressing the wild type AR in motor neurons exhibited no hormone-dependent toxicity in this assay ($P>0.05$, not shown). Strikingly, DHT-dependent toxicity of the polyQ AR was significantly rescued by rearing flies on YM-1 (**Fig. 4.5d**). Similarly, polyQ AR toxicity was rescued by the presence of a UAS-responsive enhancer element just upstream of the coding sequence of HIP-R (**Fig. 4.5e**), a *Drosophila* ortholog of Hip. Although we considered the possibility that a second UAS might confound this analysis by diminishing polyQ AR expression in these double transgenics, we found that this was not the case (**Fig. 4.5f**). We conclude that allosteric activation of Hsp70 by a small molecule or genetic manipulation rescued toxicity in a *Drosophila* model of SBMA.

Discussion

We sought to manipulate endogenous cellular systems that regulate polyQ AR protein degradation to alleviate the toxicity that underlies a protein aggregation neurodegenerative disorder. For the AR, the major chaperones involved in protein quality control decisions are Hsp90 and Hsp70, which act together in a multichaperone machinery to regulate its function, trafficking and turnover [67,128]. Prior attempts at identifying small molecules to target this pathway focused primarily on inhibitors of Hsp90 ATPase activity, such as geldanamycin and its derivatives. We describe an alternative approach using allosteric activators of Hsp70. This strategy is based on the observation that Hip, an Hsp70 co-chaperone, interacts with the ATPase domain of

Hsp70 and stabilizes it in its ADP-bound state [86] to promote binding to unfolded substrates [167]. The therapeutic potential of targeting Hip was suggested by prior studies showing that its over-expression in cell culture diminishes aggregation of a long glutamine tract [90]. Hip over-expression also decreases the formation of fibrils by another Hsp90 client protein, α–synuclein, and its knock-down in *C. elegans* increases α–synuclein aggregation [91]. Here we extend these observations to SBMA models and characterize a novel small molecule that acts similarly to Hip to allosterically modulate Hsp70. We show that YM-1, which binds and stabilizes Hsp70 in its ADP-bound state [170], promotes Hsp70 affinity for denatured proteins, enhances client protein ubiquitination, stimulates clearance of the polyQ AR, and rescues toxicity in a *Drosophila* model of SBMA.

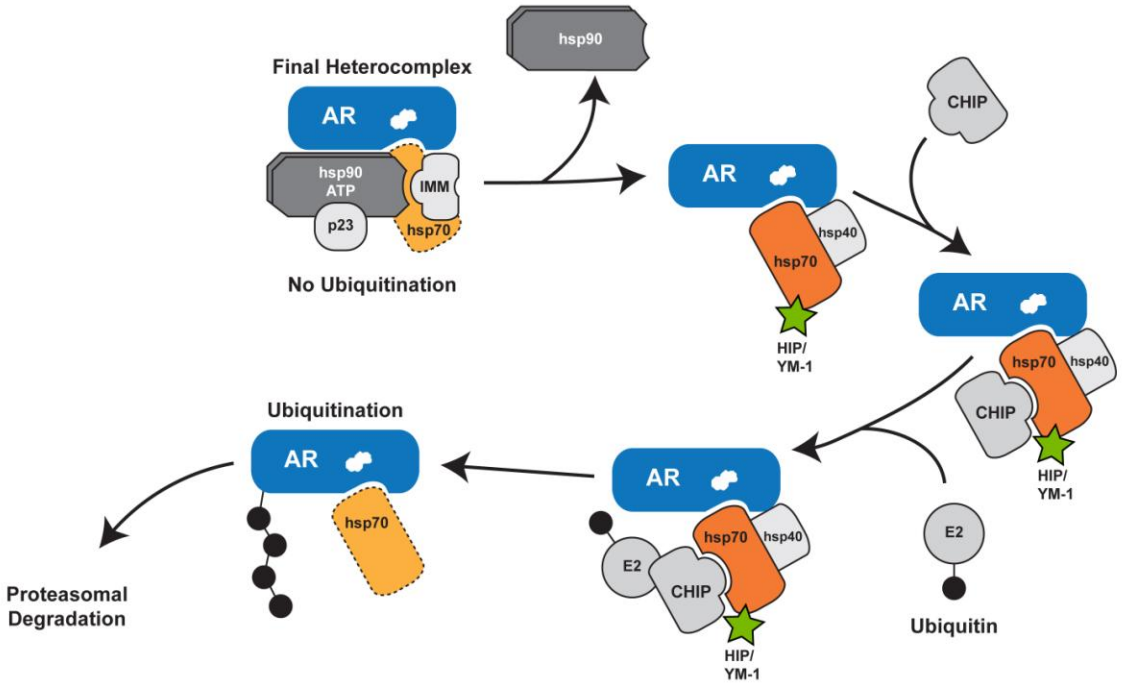

Figure 4.6 Model of the Hsp90/Hsp70-based chaperone machinery and regulation of polyQ AR degradation.

Hsp90 and Hsp70 form a heterocomplex to stabilize the polyQ AR, enable ligand binding and guide intracellular localization (top left). Dissociation of Hsp90, such as following the addition of small molecule inhibitors or due to ligand-dependent conformation change of the polyQ AR, permits unfolding of the mutant protein. Substrate-bound Hsp70 then recruits chaperone dependent ubiquitin ligases such as CHIP to promote degradation through the proteasome. We demonstrate here that allosteric activators of Hsp70, including Hip and YM-1 (in green), increase substrate binding affinity, facilitate client protein ubiquitination and promote polyQ AR clearance by the proteasome. This strategy alleviates polyglutamine toxicity by facilitating degradation of the mutant protein. IMM, immunophilin.

Our findings support a model of chaperone machinery function whereby Hsp90 and Hsp70 have essentially opposing roles in the triage of unfolded proteins [150,166], in that Hsp70 promotes substrate ubiquitination whereas Hsp90 inhibits ubiquitination (**Figure 4.6**). We envision that as the mutant AR undergoes ligand- and polyQ length-dependent conformational change, Hsp90 can no longer interact with it to inhibit ubiquitination. E3 ligases interacting with substrate-bound Hsp70 then target ubiquitin-charged E2 enzymes to the nascently unfolding substrate. In this way the Hsp90/Hsp70-based chaperone machinery can function as a comprehensive protein management system for quality

control of damaged proteins. Support for this model is provided by the observation that stabilizing the Hsp90 chaperone complex with the polyQ AR by over-expressing the co-chaperone p23 decreases ligand-dependent unfolding and aggregation [69]. This model predicts that in the absence of Hsp90, AR-associated Hsp70 recruits chaperone-dependent E3 ubiquitin ligases, such as CHIP, to promote degradation [76]. Consistent with this notion, we found previously that a small molecule inhibitor of Hsp70, methylene blue, impairs polyQ AR degradation [85]. Here we show that genetic or pharmacologic allosteric activators of Hsp70 promote client protein ubiquitination, enhance clearance of the polyQ AR and alleviate toxicity in a SBMA flies.

In addition to the polyQ AR, other proteins that unfold and aggregate in age-dependent neurodegenerative disorders are clients of the Hsp90 chaperone machinery. In addition to α–synuclein, evidence indicates that huntingtin and tau are also Hsp90 clients [129,172,173]. Accumulation of these unfolded proteins causes a variety of disorders, for which available treatment options are largely supportive. Our model of chaperone machinery function suggests that the strategies identified here for SBMA may have more far-reaching applicability. We suggest that, like the use of Hsp90 inactivators, targeting Hsp70 with allosteric activators may lead to new therapeutic approaches for many of the protein aggregation disorders that occur in the aging population by increasing degradation of the mutant protein.

Materials and Methods

Materials

HeLa cells were from the American Type Culture Collection. PC12 cells expressing tet-inducible forms of the AR were characterized previously [174]. Phenol red-free Dulbecco's modified Eagle's medium (DMEM) was from Invitrogen (Carlsbad, CA), charcoal-stripped calf serum was from Thermo Scientific Hyclone Products (Waltham, MA) and horse serum was from Invitrogen. Fugene 6 was from Roche (Indianapolis, IN), and DHT and MG132 were from Sigma (St. Louis, MO). Geldanamycin and the anti-72/73-kDa Hsp70 (N27F3-4), stress-inducible Hsp70, Hsp40, Hsp25 and Hip antibodies were from Enzo Life Sciences (Plymouth Meeting, PA). The AR (N-20), FLAG, and GAPDH antibodies were from Santa Cruz Biotechnology (Santa Cruz, CA), Sigma, and Abcam (Cambridge, MA) respectively. The HRP-tagged secondary antibodies were from Biorad, and the Alexa Flour 594 and 488 conjugated secondary antibodies were from Invitrogen. Plasmid encoding Hip was from GeneCopoeia and modified by the addition of a triple FLAG tag. Hsp70 siRNAs were ON-TARGET*plus* SMART pool rat HSPA1A or non-targeting control (Dharmacon).

Cell culture and transfection

HeLa cells were grown in phenol red-free DMEM supplemented with 10% charcoal/dextran-stripped fetal calf serum. Cells were transfected with 3 μl Fugene 6 and 1 μg DNA. Twenty-four hours post-transfection, cells were pooled and replated, then treated as indicated. PC12 cells were grown in phenol red-free DMEM supplemented with 5% charcoal/dextran-stripped fetal calf serum, 10% charcoal-stripped horse serum, G418 (Gibco) and hygromycin B (Invitrogen). AR expression was induced with 0.5

μg/mL doxycycline (Clontech). PC12 cells were transfected by electroporation with the Lonza Nucleofector kit. HEK293T cells were grown in DMEM and transfected using Ca^{2+}-phosphate.

Analysis of protein expression

Cells were washed with PBS, harvested, and lysed by sonication in RIPA buffer containing phosphatase and proteinase inhibitors. For analysis of oligomers, cells were lysed in high salt lysis buffer (20 mM HEPES, pH 7.5, 400mM NaCl, 5 mM EDTA, 1 mM EGTA, 1% NP-40). Lysates were centrifuged at 4°C for 15 min at 15,000 *g* and protein concentration was determined by a BCA protein assay. Samples for oligomer analysis were subjected to ultracentrifugation at 100,000 *g* for 30 min at 4°C. Protein samples were electrophoresed through 10% SDS-polyacrylamide or 4%-20% gradient gels and transferred to nitrocellulose membranes using a semi-dry transfer apparatus. Immunoreactive proteins were detected by chemiluminescence. Signal intensity was normalized to GAPDH, and densitometric analysis was performed using ImageJ (NIH).

nNOS ubiquitination

HEK293T cells were transfected with cDNAs for HA-ubiquitin, nNOS, Hip or vector plasmid. Lysates were collected after 48 hrs for western blot and immunoprecipitation. HEK293 cells stably expressing nNOS were treated with increasing amounts of YM-1 for 24 hrs in the presence of 10 μM lactacystin prior to western blot and immunoprecipitation. Immunoblots were probed as indicated and densitometric analysis was performed using ImageJ.

Immunofluorescence

PC12 cells were transfected with 3xFLAG-Hip as indicated. Following induction and small molecule treatment, cells were fixed, stained and mounted using Vectashield mounting medium with DAPI (Burlingame, CA). Fluorescence images were captured using a Zeiss Axio Imager.Z1 microscope, and nuclear signal intensity was quantified by ImageJ (NIH). Data are from at least 3 fields per condition in 3 experiments. Confocal microscopy was performed using a Zeiss LSM 510-META Laser Scanning Confocal Microscopy system.

Luciferase Binding Assay

Binding of Hsp70 to immobilized firefly luciferase was performed as previously described [175]. YM-1 was added from a stock solution of 2.5 mM and diluted to a final DMSO concentration of 4%. All results were compared to an appropriate solvent control. Experiments were performed in triplicate.

Hip and MKT-077 scaffold binding assay

Human Hsp72 and Hip were purified as previously described [176,177] and the Hsp70-binding assay was carried out using an adaptation of a previously described assay [178]. Briefly, Hsp72 (2.3 μM) was immobilized on ELISA plates (ThermoFisher brand, clear, non-sterile, flat bottom). The treated wells were pre-incubated with Hip (0 – 6 μM) for 5 min prior to addition of biotin-labeled MKT, a probe of the YM-1 binding site [170]. The labeled probe was incubated in the wells for 2 hrs at room temperature, followed by three washes with 150 μL tris-buffered saline with Tween 20 (TBST) and incubation with 100 mL 3% bovine serum albumin (BSA) in TBST for 5 min. The BSA solution was discarded and the wells were incubated with streptavidin-horseradish peroxidase for 1 hr.

Following three additional washes with TBST, the wells were incubated with 100 μL 3,3′,5,5′-tetramethylbenzidine substrate (Cell Signaling Technology, Danvers, MA) for 30 min. After addition of stop solution, the absorbance was read in a SpectraMax M5 plate reader at 450 nm. Results were compared to control wells lacking Hsp70. Experiments were performed in triplicate and at least two independent trials were performed for each condition.

Drosophila stocks and phenotypes

The following strains were used in this study: White Canton-S (wild type), BG380-Gal4 [179], GMR-Gal4 [180], OK371-Gal4 [181], HIP^{EY14563} (Bloomington), HIP-R^{EY01382} (Bloomington). UAS-hAR52Q flies were provided by Ken-ichi Takeyama [171].

Drosophila stocks were maintained on yeast glucose media at 25°C and experimental flies were kept on Jazz-Mix food at 29°C. Food was cooled to <50°C, then supplemented with 1 mM DHT, 1 mM YM-1, or vehicle (ethanol) control. The eclosion phenotype was scored by marking existing pupal cases at 10 days post addition of parents. Following 7 days at 29°C, the percentage of marked pupal cases that failed to eclose was determined for 200-800 flies of each condition. Scanning electron micrographs were captured by the University of Michigan Microscopy & Image Analysis Core on 1 - 2 day old GMR-Gal4;UAS-hAR52Q adult female flies reared on food supplemented as indicated.

Statistics

Statistical significance was assessed by ANOVA with Newman-Keuls multiple comparison test, or unpaired Student's *t*- test using the software package Prism 5 (GraphPad Software). *P* values less than 0.05 were considered significant.

Acknowledgments

We thank Satya Reddy, Jennifer Diep and Travis Washington for technical assistance, and Ken-ichi Takeyama and the Bloomington Stock Center for fly strains. This work was supported by the N.I.H. (NS055746, NS055746-04S1 to APL; GM077430 to YO; NS069844 to CAC) and the National Science Foundation (IOS-0842701 to CAC).

Chapter 5

Conclusion

In this dissertation, I discuss the roles of two different protein degradation pathways in modulating disease pathogenesis in SBMA. We established that activation of autophagy in SBMA accentuates muscle wasting and that limiting activity of the autophagic process by genetically decreasing Beclin-1 expression decreases the observed muscular atrophy, while extending lifespan in our mouse model. In addition to investigating the role of autophagy on disease pathogenesis, we also probed our model of chaperone machinery activity in protein quality control, wherein Hsp90 binds client proteins, stabilizing them against ubiquitination. In contrast, inhibition of Hsp90 or activation of Hsp70 allows E3 ligases to interact with Hsp70 and ubiquitinate the unstable client protein. We focused on the effects of modulating Hsp70's substrate affinity, targeting in particular its nucleotide binding state both genetically and pharmacologically, to control degradation of unfolded substrate. Our results demonstrated that the expanded polyQ AR undergoes Hsp70 dependent degradation, and that pharmacologically inhibiting Hsp70's intrinsic ATPase activity led to accumulation of the polyQ AR, and inhibition of CHIP mediated ubiquitination. The remainder of this Discussion will address remaining questions and future directions.

Autophagy inhibitors in muscle wasting

Loss of muscle mass can exacerbate some neurodegenerative and age-related diseases, and several studies indicate that muscle pathology contributes to disease pathology [98,182,183]. Myopathic changes in muscle, as well as changes in protein expression reflective of denervation, manifest early in disease progression in AR113Q knock-in mice, prior to detectable loss of motor neurons [98]. Lending more support to a non-cell autonomous disease process, overexpression of wild-type AR in skeletal muscle mimicks the hormone dependent myopathy and motor axon loss seen in SBMA knock-in mice [100]. Further, overexpression of IGF-1 in skeletal muscle alone rescues disease phenotype in SBMA transgenic mice [101], highlighting the importance of muscle health in disease progression.

Denervation atrophy is characterized by an increase of protein degradation with a concomitant decrease in protein synthesis[184]. Autophagy is activated in muscle following denervation, and has been shown to contribute to the process of protein degradation in atrophying muscle [185]. Additionally, gene expression changes in atrophying muscle include several autophagy related genes, consistent with the observation that lysosomal proteases are upregulated following denervation [186,187]. Together these studies indicate a potential role of autophagy in maintaining muscle mass. In Chapter 2, we probe the role of autophagy in SBMA, and help to further establish a link between atrophy and autophagy. Our results demonstrate that activation of autophagy leads to increased atrophy, while limiting activation of autophagy leads to a significant increase in lifespan, with a concurrent increase in muscle fiber size. Though we establish an important link between autophagy and muscle wasting, the effects of inhibiting Beclin-1 expression

upon muscle fiber size are modest. However, the lifespan extension is striking, and is likely reflective of the benefits of limiting autophagy in other cell types as well as muscle. An important direction for future work will be the identification of the cellular targets through which Beclin-1 haploinsufficiency exerts its lifespan extending effects.

The results in Chapter 2 contrast with findings in other neurodegenerative models that activation of autophagy can be beneficial. Many age-related neurodegenerative diseases are characterized by the accumulation and aggregation of misfolded proteins, several of which appear to be targets of the autophagic pathway [188]. For example, in some familial forms of amyotrophic lateral sclerosis (ALS), mutant superoxide dismutase-1 (SOD1) aggregates and leads to motor neuron degeneration [189], and activation of autophagy in this disease context ameliorates the disease phenotype in SOD1 mutant mice [111]. The difference in the effects of increased autophagy on these two different disease models is likely reflective of differences in the pathways used to degrade the individual mutant proteins. SOD1 is largely degraded through autophagy [111] while the AR is a proteasomal substrate [57,85]. Subcellular localization of the protein is also important; while SOD1 is cytosolic and accessible to the autophagic machinery, the disease causing AR translocates to the nucleus, where it escapes autophagic degradation [30]. Similarly, in Huntington disease, where aggregates are largely cytoplasmic, increased autophagy has been shown to be beneficial in both cell and fly models of the disease [122]. This difference in localization and degradation further highlights the importance of disease context in the search for therapeutics in protein aggregation diseases. It is possible that inducing autophagy in patients, while increasing degradation of the disease causing protein, may accelerate degeneration of muscle and exacerbate devastating

aspects of the disease phenotype. Taken together, our data indicate that targeting protein degradation through other components of the protein quality control machinery, such as the Hsp90-based chaperone machinery may be a more beneficial therapeutic target than autophagy in SBMA and in other diseases caused by misfolded substrates of the Hsp90 machinery.

Activation of Hsp70

The results of chapter 3, in which we established that inhibiting the ATPase activity of Hsp70 increased aggregation of the polyQ AR, led us to investigate the effects of activating Hsp70 through pharmacological and genetic means. While our results in Chapter 4 establish that enhancing Hsp70's affinity for substrate increases degradation of the polyQ AR and decreases toxicity in a *Drosophila* model of SBMA, there are many questions left to be answered. Will activation of Hsp70 ameliorate disease phenotype in SBMA mice? What is the mechanism by which Hip and YM-1 increase degradation of the polyQ AR? Is it the same Hsp70-specific mechanism for both described in our model?

Furthering our understanding of Hsp90 chaperone machinery

Mechanistically, our model predicts that association of the polyQ AR with Hsp90 stabilizes the receptor, while increased association of the mutant AR with Hsp70 allows for increased ubiquitination and degradation in the absence of Hsp90 (**Figures 1.3** and **4.6**). We have shown that inhibitors of Hsp90 lead to increased degradation of the mutant receptor that can be monitored by western blot [69], and several Hsp90 inhibitors are currently in late-phase clinical trials for the treatment of cancer [11,190]. According to our model, Hsp90 inhibition would act synergistically with Hsp70 activation, destabilizing

the AR further, and increasing degradation. We hypothesize that activating Hsp70 degradation through treatment with YM-1, or over-expression of Hip, would sensitize cells and animal models to Hsp90 inhibition. This line of investigation into a synergistic effect of targeting the two arms of the chaperone machinery would reinforce our model of protein triage and perhaps provide two targets for a more efficacious therapy.

Although our data imply that Hip and YM-1 are acting similarly to bind Hsp70 and increase its activity, the mechanism by which they increase degradation of client proteins remains to be defined. One possible mechanism could be that keeping Hsp70 in its ADP-bound, high-substrate-affinity state increases the dwell time of substrate within the binding cleft of Hsp70, favoring increased ubiquitination and subsequent degradation, but this remains to be tested. While our results establish the effects of Hip and YM-1 on ubiquitination of a more manageable Hsp90 client, nNOS, confirmation of a similar increase in polyQ AR ubiquitination would support our model of protein triage. This question can be addressed by overexpression and knock down studies of Hip, or treatment with YM-1in cell culture, assaying for ubiquitin, analogous to the nNOS immunoprecipitation experiments performed in Chapters 3 and 4. Additionally, confirmation that other Hsp90 client proteins are triaged in the same manner as nNOS and AR would bolster our model, and increase the impact of these findings across several other neurodegenerative diseases.

Our preliminary data indicate that YM-1 and Hip compete for the same binding domain on Hsp70, but the specificity of action by each on Hsp70 needs to be confirmed. In chapter 4, we show that knockdown of Hsp70 abrogates the effects of YM-1 on insoluble AR112Q in PC12 cells, but this knockdown also has several off-target effects.

A more physiologically relevant study of whether Hsp70 is the biological target of YM-1 would require single amino acid substitutions in the YM-1/Hip binding domain of Hsp70. This would allow for knock down of endogenous Hsp70 in tet-inducible PC12 cells while simultaneously expressing the Hsp70 mutant that should have all other physiological activity except Hip or YM-1 binding. Specificity of YM-1in vivo could be assayed in *Drosophila* through use of existing Hsp70 dominant negative or RNAi expressing flies crossed to the SBMA model flies. Our expectation is that flies expressing downregulated or dominant negative Hsp70 with AR52Q in motorneurons would not respond to YM-1 treatment as seen by the eclosion rescue shown in Chapter 4. However, this particular set of experiments could prove to be technically challenging, as noted, knock down of Hsp70 leads to several adverse effects upon both *Drosophila* and cellular models [191,192], and could result in toxicity too severe to be able to rescue or assay.

Testing the validity of Hsp70 as a therapeutic target

Our results in cell and *Drosophila* models of SBMA indicate that modulating the activity of Hsp70 is a promising therapeutic target in SBMA. Our laboratory has generated a knock-in mouse model of SBMA in which much of the mouse AR gene was swapped with human sequence, including 113 CAG repeats in the first exon of the androgen receptor gene. This insertion resulted in an expanded glutamine tract AR under control of endogenous mouse regulatory elements, and the mouse model reproduces the neuromuscular and systemic manifestations of Kennedy disease [98]. These mice exhibit androgen dependent muscle weakness, weight loss and early death, display neurogenic muscle atrophy and myopathy, and develop AR immunoreactive intranuclear inclusions in spinal cord and skeletal muscle. This phenotype allows for ready analysis of the effects

of activating Hsp70 in a mammalian model system. Overexpressing Hip or dosage of YM-1 in this model should rescue our well-characterized disease phenotype, as measured by survival, weight, grip strength, muscle fiber size, and occurrence of intranuclear inclusions in muscle and spinal cord. Of immediate interest would be the pharmacokinetics of YM-1, with assays to measure its permeability of the blood-brain barrier, half-life, and toxicity to determine the appropriate dosage.

In addition to polyQ AR, other disease causing proteins that unfold and aggregate are also Hsp90 clients. Our work was initially based on the observation that Hip over expression in cell culture decreased aggregation of an expanded glutamine tract [90], and the aggregation of another Hsp90 client, the disease-causing protein in familial Parkinson disease, α-synuclein [91]. Conversely, knockdown of Hip in *C. elegans* increased α-synuclein aggregation [91]. In addition to α-synuclein in familial Parkinson disease, there is evidence that huntingtin, the mutant protein that causes Huntington disease, and tau, a disease causing protein in Alzheimer disease and some frontotemporal lobe dementias, are also clients of the Hsp90 chaperone machinery [129,172,173]. Our model of chaperone machinery function would predict that the strategies identified in this dissertation may be beneficial in a wide range of protein aggregation diseases caused by Hsp90 clients, like Huntington or Parkinson disease, for which therapeutic options are limited.

In conclusion, my graduate work has made a number of important contributions towards the understanding of protein degradation pathways in SBMA. These projects identified novel therapeutic targets which promise to bring us closer to directed therapies for a number of diseases for which current treatments are largely supportive. In addition to the potential clinical applications identified here, our results have furthered our

knowledge of the Hsp90 based chaperone machinery, establishing a more unified theory of protein triage for Hsp90 client proteins.

References

1. Zoghbi, H.Y. & Orr, H.T. Glutamine repeats and neurodegeneration. *Annu Rev Neurosci* **23**, 217-247 (2000).
2. Li, M., *et al.* Nuclear inclusions of the androgen receptor protein in spinal and bulbar muscular atrophy. *Ann Neurol* **44**, 249-254 (1998).
3. Miller, J., *et al.* Identifying polyglutamine protein species in situ that best predict neurodegeneration. *Nat Chem Biol* **7**, 925-934 (2011).
4. Adachi, H., *et al.* Widespread nuclear and cytoplasmic accumulation of mutant androgen receptor in SBMA patients. *Brain* **128**, 659-670 (2005).
5. Saudou, F., Finkbeiner, S., Devys, D. & Greenberg, M.E. Huntingtin acts in the nucleus to induce apoptosis but death does not correlate with the formation of intranuclear inclusions. *Cell* **95**, 55-66 (1998).
6. Arrasate, M., Mitra, S., Schweitzer, E.S., Segal, M.R. & Finkbeiner, S. Inclusion body formation reduces levels of mutant huntingtin and the risk of neuronal death. *Nature* **431**, 805-810 (2004).
7. Kennedy, W.R., Alter, M. & Sung, J.H. Progressive proximal spinal and bulbar muscular atrophy of late onset. A sex-linked recessive trait. *Neurology* **18**, 671-680 (1968).
8. Sobue, G., *et al.* X-linked recessive bulbospinal neuronopathy. A clinicopathological study. *Brain* **112 (Pt 1)**, 209-232 (1989).
9. Dejager, S., *et al.* A comprehensive endocrine description of Kennedy's disease revealing androgen insensitivity linked to CAG repeat length. *J Clin Endocrinol Metab* **87**, 3893-3901 (2002).
10. Katsuno, M., *et al.* Pathogenesis, animal models and therapeutics in Spinal and bulbar muscular atrophy (SBMA). *Exp Neurol* (2006).
11. Banno, H., *et al.* Phase 2 trial of leuprorelin in patients with spinal and bulbar muscular atrophy. *Ann Neurol* **65**, 140-150 (2009).
12. Fernandez-Rhodes, L.E., *et al.* Efficacy and safety of dutasteride in patients with spinal and bulbar muscular atrophy: a randomised placebo-controlled trial. *Lancet Neurol* **10**, 140-147 (2011).
13. La Spada, A.R., Wilson, E.M., Lubahn, D.B., Harding, A.E. & Fischbeck, K.H. Androgen receptor gene mutations in X-linked spinal and bulbar muscular atrophy. *Nature* **352**, 77-79 (1991).
14. Cutress, M.L., Whitaker, H.C., Mills, I.G., Stewart, M. & Neal, D.E. Structural basis for the nuclear import of the human androgen receptor. *J Cell Sci* **121**, 957-968 (2008).
15. He, B., Lee, L.W., Minges, J.T. & Wilson, E.M. Dependence of selective gene activation on the androgen receptor NH2- and COOH-terminal interaction. *J Biol Chem* **277**, 25631-25639 (2002).

16. Wong, C.I., Zhou, Z.X., Sar, M. & Wilson, E.M. Steroid requirement for androgen receptor dimerization and DNA binding. Modulation by intramolecular interactions between the NH2-terminal and steroid-binding domains. *J Biol Chem* **268**, 19004-19012 (1993).
17. Chamberlain, N.L., Driver, E.D. & Miesfeld, R.L. The length and location of CAG trinucleotide repeats in the androgen receptor N-terminal domain affect transactivation function. *Nucleic Acids Res* **22**, 3181-3186 (1994).
18. Lieberman, A.P., Harmison, G., Strand, A.D., Olson, J.M. & Fischbeck, K.H. Altered transcriptional regulation in cells expressing the expanded polyglutamine androgen receptor. *Hum Mol Genet* **11**, 1967-1976 (2002).
19. Kazemi-Esfarjani, P., Trifiro, M.A. & Pinsky, L. Evidence for a repressive function of the long polyglutamine tract in the human androgen receptor: possible pathogenetic relevance for the (CAG)n-expanded neuronopathies. *Hum Mol Genet* **4**, 523-527 (1995).
20. Sato, T., *et al.* Late onset of obesity in male androgen receptor-deficient (AR KO) mice. *Biochem Biophys Res Commun* **300**, 167-171 (2003).
21. Sopher, B.L., *et al.* Androgen receptor YAC transgenic mice recapitulate SBMA motor neuronopathy and implicate VEGF164 in the motor neuron degeneration. *Neuron* **41**, 687-699 (2004).
22. Katsuno, M., *et al.* Testosterone reduction prevents phenotypic expression in a transgenic mouse model of spinal and bulbar muscular atrophy. *Neuron* **35**, 843-854 (2002).
23. Abel, A., Walcott, J., Woods, J., Duda, J. & Merry, D.E. Expression of expanded repeat androgen receptor produces neurologic disease in transgenic mice. *Hum Mol Genet* **10**, 107-116 (2001).
24. McManamny, P., *et al.* A mouse model of spinal and bulbar muscular atrophy. *Hum Mol Genet* **11**, 2103-2111 (2002).
25. Merry, D.E., Kobayashi, Y., Bailey, C.K., Taye, A.A. & Fischbeck, K.H. Cleavage, aggregation and toxicity of the expanded androgen receptor in spinal and bulbar muscular atrophy. *Hum Mol Genet* **7**, 693-701 (1998).
26. Mhatre, A.N., *et al.* Reduced transcriptional regulatory competence of the androgen receptor in X-linked spinal and bulbar muscular atrophy. *Nat Genet* **5**, 184-188 (1993).
27. Lin, X., Antalffy, B., Kang, D., Orr, H.T. & Zoghbi, H.Y. Polyglutamine expansion down-regulates specific neuronal genes before pathologic changes in SCA1. *Nat Neurosci* **3**, 157-163 (2000).
28. Wyttenbach, A., *et al.* Polyglutamine expansions cause decreased CRE-mediated transcription and early gene expression changes prior to cell death in an inducible cell model of Huntington's disease. *Hum Mol Genet* **10**, 1829-1845 (2001).
29. Klement, I.A., *et al.* Ataxin-1 nuclear localization and aggregation: role in polyglutamine-induced disease in SCA1 transgenic mice. *Cell* **95**, 41-53 (1998).
30. Montie, H.L., *et al.* Cytoplasmic retention of polyglutamine-expanded androgen receptor ameliorates disease via autophagy in a mouse model of spinal and bulbar muscular atrophy. *Hum Mol Genet* **18**, 1937-1950 (2009).

31. Nedelsky, N.B., *et al.* Native functions of the androgen receptor are essential to pathogenesis in a Drosophila model of spinobulbar muscular atrophy. *Neuron* **67**, 936-952 (2010).
32. Chevalier-Larsen, E.S., *et al.* Castration restores function and neurofilament alterations of aged symptomatic males in a transgenic mouse model of spinal and bulbar muscular atrophy. *J Neurosci* **24**, 4778-4786 (2004).
33. Irvine, R.A., *et al.* Inhibition of p160-mediated coactivation with increasing androgen receptor polyglutamine length. *Hum Mol Genet* **9**, 267-274 (2000).
34. Thomas, M., *et al.* Androgen receptor acetylation site mutations cause trafficking defects, misfolding, and aggregation similar to expanded glutamine tracts. *J Biol Chem* **279**, 8389-8395 (2004).
35. Fu, M., *et al.* Androgen receptor acetylation governs trans activation and MEKK1-induced apoptosis without affecting in vitro sumoylation and trans-repression function. *Mol Cell Biol* **22**, 3373-3388 (2002).
36. McCampbell, A., *et al.* CREB-binding protein sequestration by expanded polyglutamine. *Hum Mol Genet* **9**, 2197-2202 (2000).
37. Taylor, J.P., *et al.* Aberrant histone acetylation, altered transcription, and retinal degeneration in a Drosophila model of polyglutamine disease are rescued by CREB-binding protein. *Genes Dev* **17**, 1463-1468 (2003).
38. McCampbell, A., *et al.* Histone deacetylase inhibitors reduce polyglutamine toxicity. *Proc Natl Acad Sci U S A* **98**, 15179-15184 (2001).
39. Ranum, L.P. & Day, J.W. Myotonic dystrophy: RNA pathogenesis comes into focus. *Am J Hum Genet* **74**, 793-804 (2004).
40. Yu, Z., Wang, A.M., Robins, D.M. & Lieberman, A.P. Altered RNA splicing contributes to skeletal muscle pathology in Kennedy disease knock-in mice. *Dis Model Mech* **2**, 500-507 (2009).
41. Ranganathan, S., *et al.* Mitochondrial abnormalities in spinal and bulbar muscular atrophy. *Hum Mol Genet* **18**, 27-42 (2009).
42. Su, S., *et al.* Mitochondrial DNA damage in spinal and bulbar muscular atrophy patients and carriers. *Clin Chim Acta* **411**, 626-630 (2010).
43. Piccioni, F., *et al.* Androgen receptor with elongated polyglutamine tract forms aggregates that alter axonal trafficking and mitochondrial distribution in motor neuronal processes. *Faseb J* **16**, 1418-1420 (2002).
44. Szebenyi, G., *et al.* Neuropathogenic forms of huntingtin and androgen receptor inhibit fast axonal transport. *Neuron* **40**, 41-52 (2003).
45. Gunawardena, S., *et al.* Disruption of axonal transport by loss of huntingtin or expression of pathogenic polyQ proteins in Drosophila. *Neuron* **40**, 25-40 (2003).
46. Puls, I., *et al.* Mutant dynactin in motor neuron disease. *Nat Genet* **33**, 455-456 (2003).
47. Morfini, G.A., *et al.* Pathogenic huntingtin inhibits fast axonal transport by activating JNK3 and phosphorylating kinesin. *Nat Neurosci* **12**, 864-871 (2009).
48. Katsuno, M., *et al.* Reversible disruption of dynactin 1-mediated retrograde axonal transport in polyglutamine-induced motor neuron degeneration. *J Neurosci* **26**, 12106-12117 (2006).
49. Kemp, M.Q., *et al.* Impaired motoneuronal retrograde transport in two models of SBMA implicates two sites of androgen action. *Hum Mol Genet* (2011).

50. Malik, B., *et al.* Absence of disturbed axonal transport in spinal and bulbar muscular atrophy. *Hum Mol Genet* **20**, 1776-1786 (2011).
51. Hershko, A. & Ciechanover, A. The ubiquitin system. *Annu Rev Biochem* **67**, 425-479 (1998).
52. Hershko, A., Heller, H., Elias, S. & Ciechanover, A. Components of ubiquitin-protein ligase system. Resolution, affinity purification, and role in protein breakdown. *J Biol Chem* **258**, 8206-8214 (1983).
53. Chau, V., *et al.* A multiubiquitin chain is confined to specific lysine in a targeted short-lived protein. *Science* **243**, 1576-1583 (1989).
54. Voges, D., Zwickl, P. & Baumeister, W. The 26S proteasome: a molecular machine designed for controlled proteolysis. *Annu Rev Biochem* **68**, 1015-1068 (1999).
55. Adachi, H., *et al.* Transgenic mice with an expanded CAG repeat controlled by the human AR promoter show polyglutamine nuclear inclusions and neuronal dysfunction without neuronal cell death. *Hum Mol Genet* **10**, 1039-1048 (2001).
56. Bence, N.F., Sampat, R.M. & Kopito, R.R. Impairment of the ubiquitin-proteasome system by protein aggregation. *Science* **292**, 1552-1555 (2001).
57. Tokui, K., *et al.* 17-DMAG ameliorates polyglutamine-mediated motor neuron degeneration through well-preserved proteasome function in a SBMA model mouse. *Hum Mol Genet* (2008).
58. Klionsky, D.J. & Emr, S.D. Autophagy as a regulated pathway of cellular degradation. *Science* **290**, 1717-1721 (2000).
59. Kunz, J.B., Schwarz, H. & Mayer, A. Determination of four sequential stages during microautophagy in vitro. *J Biol Chem* **279**, 9987-9996 (2004).
60. Orenstein, S.J. & Cuervo, A.M. Chaperone-mediated autophagy: molecular mechanisms and physiological relevance. *Semin Cell Dev Biol* **21**, 719-726 (2010).
61. Ravikumar, B., *et al.* Regulation of mammalian autophagy in physiology and pathophysiology. *Physiol Rev* **90**, 1383-1435 (2010).
62. Liang, C., *et al.* Autophagic and tumour suppressor activity of a novel Beclin1-binding protein UVRAG. *Nat Cell Biol* **8**, 688-699 (2006).
63. Kihara, A., Noda, T., Ishihara, N. & Ohsumi, Y. Two distinct Vps34 phosphatidylinositol 3-kinase complexes function in autophagy and carboxypeptidase Y sorting in Saccharomyces cerevisiae. *J Cell Biol* **152**, 519-530 (2001).
64. Pattingre, S., *et al.* Bcl-2 antiapoptotic proteins inhibit Beclin 1-dependent autophagy. *Cell* **122**, 927-939 (2005).
65. Pratt, W.B. & Toft, D.O. Steroid receptor interactions with heat shock protein and immunophilin chaperones. *Endocr Rev* **18**, 306-360 (1997).
66. Fang, Y., Fliss, A.E., Robins, D.M. & Caplan, A.J. Hsp90 regulates androgen receptor hormone binding affinity in vivo. *J Biol Chem* **271**, 28697-28702 (1996).
67. Pratt, W.B. & Toft, D.O. Regulation of signaling protein function and trafficking by the hsp90/hsp70-based chaperone machinery. *Exp Biol Med (Maywood)* **228**, 111-133 (2003).
68. Brehmer, D., *et al.* Tuning of chaperone activity of Hsp70 proteins by modulation of nucleotide exchange. *Nat Struct Biol* **8**, 427-432 (2001).

69. Thomas, M., *et al.* Pharmacologic and genetic inhibition of hsp90-dependent trafficking reduces aggregation and promotes degradation of the expanded glutamine androgen receptor without stress protein induction. *Hum Mol Genet* **15**, 1876-1883 (2006).
70. Pratt, W.B., Galigniana, M.D., Harrell, J.M. & DeFranco, D.B. Role of hsp90 and the hsp90-binding immunophilins in signalling protein movement. *Cell Signal* **16**, 857-872 (2004).
71. Waza, M., *et al.* 17-AAG, an Hsp90 inhibitor, ameliorates polyglutamine-mediated motor neuron degeneration. *Nat Med* **11**, 1088-1095 (2005).
72. Waza, M., *et al.* Modulation of Hsp90 function in neurodegenerative disorders: a molecular-targeted therapy against disease-causing protein. *J Mol Med (Berl)* **84**, 635-646 (2006).
73. Sittler, A., *et al.* Geldanamycin activates a heat shock response and inhibits huntingtin aggregation in a cell culture model of Huntington's disease. *Hum Mol Genet* **10**, 1307-1315 (2001).
74. Bercovich, B., *et al.* Ubiquitin-dependent degradation of certain protein substrates in vitro requires the molecular chaperone Hsc70. *J Biol Chem* **272**, 9002-9010 (1997).
75. Ballinger, C.A., *et al.* Identification of CHIP, a novel tetratricopeptide repeat-containing protein that interacts with heat shock proteins and negatively regulates chaperone functions. *Mol Cell Biol* **19**, 4535-4545 (1999).
76. Morishima, Y., *et al.* CHIP deletion reveals functional redundancy of E3 ligases in promoting degradation of both signaling proteins and expanded glutamine proteins. *Hum Mol Genet* **17**, 3942-3952 (2008).
77. Al-Ramahi, I., *et al.* CHIP protects from the neurotoxicity of expanded and wild-type ataxin-1 and promotes their ubiquitination and degradation. *J Biol Chem* **281**, 26714-26724 (2006).
78. Adachi, H., *et al.* CHIP overexpression reduces mutant androgen receptor protein and ameliorates phenotypes of the spinal and bulbar muscular atrophy transgenic mouse model. *J Neurosci* **27**, 5115-5126 (2007).
79. Muchowski, P.J., *et al.* Hsp70 and hsp40 chaperones can inhibit self-assembly of polyglutamine proteins into amyloid-like fibrils. *Proc Natl Acad Sci U S A* **97**, 7841-7846 (2000).
80. Kobayashi, Y., *et al.* Chaperones Hsp70 and Hsp40 suppress aggregate formation and apoptosis in cultured neuronal cells expressing truncated androgen receptor protein with expanded polyglutamine tract. *J Biol Chem* **275**, 8772-8778 (2000).
81. Adachi, H., *et al.* Heat shock protein 70 chaperone overexpression ameliorates phenotypes of the spinal and bulbar muscular atrophy transgenic mouse model by reducing nuclear-localized mutant androgen receptor protein. *J Neurosci* **23**, 2203-2211 (2003).
82. Freeman, B.C., Myers, M.P., Schumacher, R. & Morimoto, R.I. Identification of a regulatory motif in Hsp70 that affects ATPase activity, substrate binding and interaction with HDJ-1. *EMBO J* **14**, 2281-2292 (1995).
83. Leu, J.I., Pimkina, J., Frank, A., Murphy, M.E. & George, D.L. A small molecule inhibitor of inducible heat shock protein 70. *Mol Cell* **36**, 15-27 (2009).

84. Jinwal, U.K., *et al.* Chemical manipulation of hsp70 ATPase activity regulates tau stability. *J Neurosci* **29**, 12079-12088 (2009).
85. Wang, A.M., *et al.* Inhibition of hsp70 by methylene blue affects signaling protein function and ubiquitination and modulates polyglutamine protein degradation. *J Biol Chem* **285**, 15714-15723 (2010).
86. Hohfeld, J., Minami, Y. & Hartl, F.U. Hip, a novel cochaperone involved in the eukaryotic Hsc70/Hsp40 reaction cycle. *Cell* **83**, 589-598 (1995).
87. Kanelakis, K.C., *et al.* Differential effects of the hsp70-binding protein BAG-1 on glucocorticoid receptor folding by the hsp90-based chaperone machinery. *J Biol Chem* **274**, 34134-34140 (1999).
88. Nollen, E.A., *et al.* Modulation of in vivo HSP70 chaperone activity by Hip and Bag-1. *J Biol Chem* **276**, 4677-4682 (2001).
89. Nelson, G.M., *et al.* The heat shock protein 70 cochaperone hip enhances functional maturation of glucocorticoid receptor. *Mol Endocrinol* **18**, 1620-1630 (2004).
90. Howarth, J.L., Glover, C.P. & Uney, J.B. HSP70 interacting protein prevents the accumulation of inclusions in polyglutamine disease. *J Neurochem* **108**, 945-951 (2009).
91. Roodveldt, C., *et al.* Chaperone proteostasis in Parkinson's disease: stabilization of the Hsp70/alpha-synuclein complex by Hip. *EMBO J* **28**, 3758-3770 (2009).
92. Scherzer, C.R., *et al.* Molecular markers of early Parkinson's disease based on gene expression in blood. *Proc Natl Acad Sci U S A* **104**, 955-960 (2007).
93. Orr, H.T. & Zoghbi, H.Y. Trinucleotide repeat disorders. *Annu Rev Neurosci* **30**, 575-621 (2007).
94. Lieberman, A.P. & Fischbeck, K.H. Triplet repeat expansion in neuromuscular disease. *Muscle Nerve* **23**, 843-850 (2000).
95. Sperfeld, A.D., *et al.* X-linked bulbospinal neuronopathy: Kennedy disease. *Arch Neurol* **59**, 1921-1926 (2002).
96. Katsuno, M., *et al.* Efficacy and safety of leuprorelin in patients with spinal and bulbar muscular atrophy (JASMITT study): a multicentre, randomised, double-blind, placebo-controlled trial. *Lancet Neurol* (2010).
97. Albertelli, M.A., Scheller, A., Brogley, M. & Robins, D.M. Replacing the mouse androgen receptor with human alleles demonstrates glutamine tract length-dependent effects on physiology and tumorigenesis in mice. *Mol Endocrinol* **20**, 1248-1260 (2006).
98. Yu, Z., *et al.* Androgen-dependent pathology demonstrates myopathic contribution to the Kennedy disease phenotype in a mouse knock-in model. *J Clin Invest* **116**, 2663-2672 (2006).
99. Yu, Z., *et al.* Abnormalities of Germ Cell Maturation and Sertoli Cell Cytoskeleton in Androgen Receptor 113 CAG Knock-In Mice Reveal Toxic Effects of the Mutant Protein. *Am J Pathol* **168**, 195-204 (2006).
100. Monks, D.A., *et al.* Overexpressioin of wild-type androgen receptor in muscle recapitulates polyglutamine disease. *Proc Natl Acad Sci U S A* (2007).
101. Palazzolo, I., *et al.* Overexpression of IGF-1 in muscle attenuates disease in a mouse model of spinal and bulbar muscular atrophy. *Neuron* **63**, 316-328 (2009).

102. Ron, D. Translational control in the endoplasmic reticulum stress response. *J Clin Invest* **110**, 1383-1388 (2002).
103. Ron, D. & Walter, P. Signal integration in the endoplasmic reticulum unfolded protein response. *Nat Rev Mol Cell Biol* **8**, 519-529 (2007).
104. Thomas, M., *et al.* The unfolded protein response modulates toxicity of the expanded glutamine androgen receptor. *J Biol Chem* **280**, 21264-21271 (2005).
105. Zinszner, H., *et al.* CHOP is implicated in programmed cell death in response to impaired function of the endoplasmic reticulum. *Genes Dev* **12**, 982-995 (1998).
106. Southwood, C.M., Garbern, J., Jiang, W. & Gow, A. The unfolded protein response modulates disease severity in Pelizaeus-Merzbacher disease. *Neuron* **36**, 585-596 (2002).
107. Pennuto, M., *et al.* Ablation of the UPR-mediator CHOP restores motor function and reduces demyelination in Charcot-Marie-Tooth 1B mice. *Neuron* **57**, 393-405 (2008).
108. Kostrominova, T.Y., Dow, D.E., Dennis, R.G., Miller, R.A. & Faulkner, J.A. Comparison of gene expression of 2-mo denervated, 2-mo stimulated-denervated, and control rat skeletal muscles. *Physiol Genomics* **22**, 227-243 (2005).
109. Glass, D.J. Signalling pathways that mediate skeletal muscle hypertrophy and atrophy. *Nat Cell Biol* **5**, 87-90 (2003).
110. Mammucari, C., *et al.* FoxO3 controls autophagy in skeletal muscle in vivo. *Cell Metab* **6**, 458-471 (2007).
111. Hetz, C., *et al.* XBP-1 deficiency in the nervous system protects against amyotrophic lateral sclerosis by increasing autophagy. *Genes Dev* **23**, 2294-2306 (2009).
112. Kouroku, Y., *et al.* ER stress (PERK/eIF2alpha phosphorylation) mediates the polyglutamine-induced LC3 conversion, an essential step for autophagy formation. *Cell Death Differ* **14**, 230-239 (2007).
113. Ogata, M., *et al.* Autophagy is activated for cell survival after endoplasmic reticulum stress. *Mol Cell Biol* **26**, 9220-9231 (2006).
114. Yue, Z., Jin, S., Yang, C., Levine, A.J. & Heintz, N. Beclin 1, an autophagy gene essential for early embryonic development, is a haploinsufficient tumor suppressor. *Proc Natl Acad Sci U S A* **100**, 15077-15082 (2003).
115. Zhong, Y., *et al.* Distinct regulation of autophagic activity by Atg14L and Rubicon associated with Beclin 1-phosphatidylinositol-3-kinase complex. *Nat Cell Biol* **11**, 468-476 (2009).
116. Qu, X., *et al.* Promotion of tumorigenesis by heterozygous disruption of the beclin 1 autophagy gene. *J Clin Invest* **112**, 1809-1820 (2003).
117. Kouroku, Y., *et al.* Polyglutamine aggregates stimulate ER stress signals and caspase-12 activation. *Hum Mol Genet* **11**, 1505-1515 (2002).
118. Nishitoh, H., *et al.* ASK1 is essential for endoplasmic reticulum stress-induced neuronal cell death triggered by expanded polyglutamine repeats. *Genes Dev* **16**, 1345-1355 (2002).
119. Carnemolla, A., *et al.* Rrs1 is involved in endoplasmic reticulum stress response in Huntington disease. *J Biol Chem* **284**, 18167-18173 (2009).
120. Urano, F., *et al.* Coupling of stress in the ER to activation of JNK protein kinases by transmembrane protein kinase IRE1. *Science* **287**, 664-666 (2000).

121. Pandey, U.B., *et al.* HDAC6 rescues neurodegeneration and provides an essential link between autophagy and the UPS. *Nature* **447**, 859-863 (2007).
122. Ravikumar, B., *et al.* Inhibition of mTOR induces autophagy and reduces toxicity of polyglutamine expansions in fly and mouse models of Huntington disease. *Nat Genet* **36**, 585-595 (2004).
123. Williams, A., *et al.* Novel targets for Huntington's disease in an mTOR-independent autophagy pathway. *Nat Chem Biol* **4**, 295-305 (2008).
124. Renna, M., Jimenez-Sanchez, M., Sarkar, S. & Rubinsztein, D.C. Chemical inducers of autophagy that enhance the clearance of mutant proteins in neurodegenerative diseases. *J Biol Chem* **285**, 11061-11067 (2010).
125. Sherman, M.Y. & Goldberg, A.L. Cellular defenses against unfolded proteins: a cell biologist thinks about neurodegenerative diseases. *Neuron* **29**, 15-32 (2001).
126. Isaacs, J.S., Xu, W. & Neckers, L. Heat shock protein 90 as a molecular target for cancer therapeutics. *Cancer Cell* **3**, 213-217 (2003).
127. Lee, D.H., Sherman, M.Y. & Goldberg, A.L. Involvement of the molecular chaperone Ydj1 in the ubiquitin-dependent degradation of short-lived and abnormal proteins in Saccharomyces cerevisiae. *Mol Cell Biol* **16**, 4773-4781 (1996).
128. Pratt, W.B., Morishima, Y. & Osawa, Y. The Hsp90 chaperone machinery regulates signaling by modulating ligand binding clefts. *J Biol Chem* **283**, 22885-22889 (2008).
129. Mitsui, K., *et al.* Purification of polyglutamine aggregates and identification of elongation factor-1alpha and heat shock protein 84 as aggregate-interacting proteins. *J Neurosci* **22**, 9267-9277 (2002).
130. Hay, D.G., *et al.* Progressive decrease in chaperone protein levels in a mouse model of Huntington's disease and induction of stress proteins as a therapeutic approach. *Hum Mol Genet* **13**, 1389-1405 (2004).
131. Zou, J., Guo, Y., Guettouche, T., Smith, D.F. & Voellmy, R. Repression of heat shock transcription factor HSF1 activation by HSP90 (HSP90 complex) that forms a stress-sensitive complex with HSF1. *Cell* **94**, 471-480 (1998).
132. Bagatell, R., *et al.* Induction of a heat shock factor 1-dependent stress response alters the cytotoxic activity of hsp90-binding agents. *Clin Cancer Res* **6**, 3312-3318 (2000).
133. Muchowski, P.J. & Wacker, J.L. Modulation of neurodegeneration by molecular chaperones. *Nat Rev Neurosci* **6**, 11-22 (2005).
134. Jana, N.R., *et al.* Co-chaperone CHIP associates with expanded polyglutamine protein and promotes their degradation by proteasomes. *J Biol Chem* **280**, 11635-11640 (2005).
135. Bailey, C.K., Andriola, I.F., Kampinga, H.H. & Merry, D.E. Molecular chaperones enhance the degradation of expanded polyglutamine repeat androgen receptor in a cellular model of spinal and bulbar muscular atrophy. *Hum Mol Genet* **11**, 515-523 (2002).
136. Warrick, J.M., *et al.* Suppression of polyglutamine-mediated neurodegeneration in Drosophila by the molecular chaperone HSP70. *Nat Genet* **23**, 425-428 (1999).
137. Chan, H.Y., Warrick, J.M., Gray-Board, G.L., Paulson, H.L. & Bonini, N.M. Mechanisms of chaperone suppression of polyglutamine disease: selectivity,

synergy and modulation of protein solubility in Drosophila. *Hum Mol Genet* **9**, 2811-2820 (2000).
138. Cyr, D.M., Hohfeld, J. & Patterson, C. Protein quality control: U-box-containing E3 ubiquitin ligases join the fold. *Trends Biochem Sci* **27**, 368-375 (2002).
139. Connell, P., *et al.* The co-chaperone CHIP regulates protein triage decisions mediated by heat-shock proteins. *Nat Cell Biol* **3**, 93-96 (2001).
140. Jiang, J., *et al.* CHIP is a U-box-dependent E3 ubiquitin ligase: identification of Hsc70 as a target for ubiquitylation. *J Biol Chem* **276**, 42938-42944 (2001).
141. Zhang, Y., *et al.* Parkin functions as an E2-dependent ubiquitin- protein ligase and promotes the degradation of the synaptic vesicle-associated protein, CDCrel-1. *Proc Natl Acad Sci U S A* **97**, 13354-13359 (2000).
142. Tsai, Y.C., Fishman, P.S., Thakor, N.V. & Oyler, G.A. Parkin facilitates the elimination of expanded polyglutamine proteins and leads to preservation of proteasome function. *J Biol Chem* **278**, 22044-22055 (2003).
143. Miller, V.M., *et al.* CHIP suppresses polyglutamine aggregation and toxicity in vitro and in vivo. *J Neurosci* **25**, 9152-9161 (2005).
144. Morishima, Y., *et al.* The Hsp organizer protein hop enhances the rate of but is not essential for glucocorticoid receptor folding by the multiprotein Hsp90-based chaperone system. *J Biol Chem* **275**, 6894-6900 (2000).
145. Morishima, Y., Murphy, P.J., Li, D.P., Sanchez, E.R. & Pratt, W.B. Stepwise assembly of a glucocorticoid receptor.hsp90 heterocomplex resolves two sequential ATP-dependent events involving first hsp70 and then hsp90 in opening of the steroid binding pocket. *J Biol Chem* **275**, 18054-18060 (2000).
146. Chen, S., Prapapanich, V., Rimerman, R.A., Honore, B. & Smith, D.F. Interactions of p60, a mediator of progesterone receptor assembly, with heat shock proteins hsp90 and hsp70. *Mol Endocrinol* **10**, 682-693 (1996).
147. Bender, A.T., Demady, D.R. & Osawa, Y. Ubiquitination of neuronal nitric-oxide synthase in vitro and in vivo. *J Biol Chem* **275**, 17407-17411 (2000).
148. Noguchi, S., *et al.* Guanabenz-mediated inactivation and enhanced proteolytic degradation of neuronal nitric-oxide synthase. *J Biol Chem* **275**, 2376-2380 (2000).
149. Peng, H.M., *et al.* Ubiquitylation of neuronal nitric-oxide synthase by CHIP, a chaperone-dependent E3 ligase. *J Biol Chem* **279**, 52970-52977 (2004).
150. Peng, H.M., *et al.* Dynamic cycling with Hsp90 stabilizes neuronal nitric oxide synthase through calmodulin-dependent inhibition of ubiquitination. *Biochemistry* **48**, 8483-8490 (2009).
151. Fewell, S.W., Day, B.W. & Brodsky, J.L. Identification of an inhibitor of hsc70-mediated protein translocation and ATP hydrolysis. *J Biol Chem* **276**, 910-914 (2001).
152. Fewell, S.W., *et al.* Small molecule modulators of endogenous and co-chaperone-stimulated Hsp70 ATPase activity. *J Biol Chem* **279**, 51131-51140 (2004).
153. Brodsky, J.L. & Chiosis, G. Hsp70 molecular chaperones: emerging roles in human disease and identification of small molecule modulators. *Curr Top Med Chem* **6**, 1215-1225 (2006).

154. Wisen, S. & Gestwicki, J.E. Identification of small molecules that modify the protein folding activity of heat shock protein 70. *Anal Biochem* **374**, 371-377 (2008).
155. Williamson, D.S., *et al.* Novel adenosine-derived inhibitors of 70 kDa heat shock protein, discovered through structure-based design. *J Med Chem* **52**, 1510-1513 (2009).
156. Oz, M., Lorke, D.E., Hasan, M. & Petroianu, G.A. Cellular and molecular actions of methylene blue in the nervous system. *Med Res Rev* (2009).
157. Morishima, Y., Kanelakis, K.C., Murphy, P.J., Shewach, D.S. & Pratt, W.B. Evidence for iterative ratcheting of receptor-bound hsp70 between its ATP and ADP conformations during assembly of glucocorticoid receptor.hsp90 heterocomplexes. *Biochemistry* **40**, 1109-1116 (2001).
158. Mayer, B., Brunner, F. & Schmidt, K. Inhibition of nitric oxide synthesis by methylene blue. *Biochem Pharmacol* **45**, 367-374 (1993).
159. Luo, D., Das, S. & Vincent, S.R. Effects of methylene blue and LY83583 on neuronal nitric oxide synthase and NADPH-diaphorase. *Eur J Pharmacol* **290**, 247-251 (1995).
160. Ravikumar, B., *et al.* Dynein mutations impair autophagic clearance of aggregate-prone proteins. *Nat Genet* **37**, 771-776 (2005).
161. Bender, A.T., *et al.* Neuronal nitric-oxide synthase is regulated by the Hsp90-based chaperone system in vivo. *J Biol Chem* **274**, 1472-1478 (1999).
162. Dittmar, K.D., Hutchison, K.A., Owens-Grillo, J.K. & Pratt, W.B. Reconstitution of the steroid receptor.hsp90 heterocomplex assembly system of rabbit reticulocyte lysate. *J Biol Chem* **271**, 12833-12839 (1996).
163. Dittmar, K.D., Banach, M., Galigniana, M.D. & Pratt, W.B. The role of DnaJ-like proteins in glucocorticoid receptor.hsp90 heterocomplex assembly by the reconstituted hsp90.p60.hsp70 foldosome complex. *J Biol Chem* **273**, 7358-7366 (1998).
164. Kanelakis, K.C. & Pratt, W.B. Regulation of glucocorticoid receptor ligand-binding activity by the hsp90/hsp70-based chaperone machinery. *Methods Enzymol* **364**, 159-173 (2003).
165. Morfini, G., *et al.* JNK mediates pathogenic effects of polyglutamine-expanded androgen receptor on fast axonal transport. *Nat Neurosci* (2006).
166. Pratt, W.B., Morishima, Y., Peng, H.M. & Osawa, Y. Proposal for a role of the Hsp90/Hsp70-based chaperone machinery in making triage decisions when proteins undergo oxidative and toxic damage. *Exp Biol Med (Maywood)* **235**, 278-289 (2010).
167. Mayer, M.P., Brehmer, D., Gassler, C.S. & Bukau, B. Hsp70 chaperone machines. *Adv Protein Chem* **59**, 1-44 (2001).
168. Clapp, K.M., *et al.* C331A mutant of neuronal nitric-oxide synthase is labilized for Hsp70/CHIP (C terminus of HSC70-interacting protein)-dependent ubiquitination. *J Biol Chem* **285**, 33642-33651 (2010).
169. Wadhwa, R., *et al.* Selective toxicity of MKT-077 to cancer cells is mediated by its binding to the hsp70 family protein mot-2 and reactivation of p53 function. *Cancer Res* **60**, 6818-6821 (2000).

170. Rousaki, A., *et al.* Allosteric drugs: the interaction of antitumor compound MKT-077 with human Hsp70 chaperones. *J Mol Biol* **411**, 614-632 (2011).
171. Takeyama, K., *et al.* Androgen-dependent neurodegeneration by polyglutamine-expanded human androgen receptor in Drosophila. *Neuron* **35**, 855-864 (2002).
172. Petrucelli, L., *et al.* CHIP and Hsp70 regulate tau ubiquitination, degradation and aggregation. *Hum Mol Genet* **13**, 703-714 (2004).
173. Dou, F., *et al.* Chaperones increase association of tau protein with microtubules. *Proc Natl Acad Sci U S A* **100**, 721-726 (2003).
174. Walcott, J.L. & Merry, D.E. Ligand promotes intranuclear inclusions in a novel cell model of spinal and bulbar muscular atrophy. *J Biol Chem* **277**, 50855-50859 (2002).
175. Chang, L., *et al.* Chemical screens against a reconstituted multiprotein complex: myricetin blocks DnaJ regulation of DnaK through an allosteric mechanism. *Chem Biol* **18**, 210-221 (2011).
176. Chang, L., Thompson, A.D., Ung, P., Carlson, H.A. & Gestwicki, J.E. Mutagenesis reveals the complex relationships between ATPase rate and the chaperone activities of Escherichia coli heat shock protein 70 (Hsp70/DnaK). *J Biol Chem* **285**, 21282-21291 (2010).
177. Kanelakis, K.C., *et al.* hsp70 interacting protein Hip does not affect glucocorticoid receptor folding by the hsp90-based chaperone machinery except to oppose the effect of BAG-1. *Biochemistry* **39**, 14314-14321 (2000).
178. Miyata, Y., *et al.* High-throughput screen for Escherichia coli heat shock protein 70 (Hsp70/DnaK): ATPase assay in low volume by exploiting energy transfer. *J Biomol Screen* **15**, 1211-1219 (2010).
179. Budnik, V., *et al.* Regulation of synapse structure and function by the Drosophila tumor suppressor gene dlg. *Neuron* **17**, 627-640 (1996).
180. Freeman, M. Reiterative use of the EGF receptor triggers differentiation of all cell types in the Drosophila eye. *Cell* **87**, 651-660 (1996).
181. Mahr, A. & Aberle, H. The expression pattern of the Drosophila vesicular glutamate transporter: a marker protein for motoneurons and glutamatergic centers in the brain. *Gene Expr Patterns* **6**, 299-309 (2006).
182. Marcuzzo, S., *et al.* Hind limb muscle atrophy precedes cerebral neuronal degeneration in G93A-SOD1 mouse model of amyotrophic lateral sclerosis: a longitudinal MRI study. *Exp Neurol* **231**, 30-37 (2011).
183. Sambataro, F. & Pennuto, M. Cell-autonomous and non-cell-autonomous toxicity in polyglutamine diseases. *Prog Neurobiol* (2011).
184. Goldberg, A.L. Protein turnover in skeletal muscle. II. Effects of denervation and cortisone on protein catabolism in skeletal muscle. *J Biol Chem* **244**, 3223-3229 (1969).
185. Schiaffino, S. & Hanzlikova, V. Studies on the effect of denervation in developing muscle. II. The lysosomal system. *J Ultrastruct Res* **39**, 1-14 (1972).
186. Lecker, S.H., *et al.* Multiple types of skeletal muscle atrophy involve a common program of changes in gene expression. *FASEB J* **18**, 39-51 (2004).
187. Sacheck, J.M., *et al.* Rapid disuse and denervation atrophy involve transcriptional changes similar to those of muscle wasting during systemic diseases. *FASEB J* **21**, 140-155 (2007).

188. Berger, Z., *et al.* Rapamycin alleviates toxicity of different aggregate-prone proteins. *Hum Mol Genet* **15**, 433-442 (2006).
189. Pasinelli, P. & Brown, R.H. Molecular biology of amyotrophic lateral sclerosis: insights from genetics. *Nat Rev Neurosci* **7**, 710-723 (2006).
190. Trepel, J., Mollapour, M., Giaccone, G. & Neckers, L. Targeting the dynamic HSP90 complex in cancer. *Nat Rev Cancer* **10**, 537-549 (2010).
191. Elefant, F. & Palter, K.B. Tissue-specific expression of dominant negative mutant Drosophila HSC70 causes developmental defects and lethality. *Mol Biol Cell* **10**, 2101-2117 (1999).
192. Wild, J., *et al.* Partial loss of function mutations in DnaK, the Escherichia coli homologue of the 70-kDa heat shock proteins, affect highly conserved amino acids implicated in ATP binding and hydrolysis. *Proc Natl Acad Sci U S A* **89**, 7139-7143 (1992).